ENGINEERING RESEARCH INSTITUTE
UNIVERSITY OF MICHIGAN
ANN ARBOR

THEORETICAL STUDY, DESIGN, AND CONSTRUCTION OF C-W MAGNETRONS FOR FREQUENCY MODULATION

FINAL REPORT

Technical Report No. 7
Electron Tube Laboratory
Department of Electrical Engineering

By: J. R. BLACK
H. W. WELCH, Jr.
G. R. BREWER
J. S. NEEDLE
W. PETERSON

Approved by: G. HOK
W. G. DOW

PROJECT M762, CONTRACT NO. W-36-039 sc-35561, SIGNAL CORPS, DEPARTMENT OF THE ARMY, DEPARTMENT OF ARMY PROJECT NO. 3-99-13-022, SIGNAL CORPS PROJECT NO. 27-112B-0.

FEBRUARY, 1951

LIST OF FIGURES

LIST OF FIGURES (Cont'd.)

SECTION IV

LIST OF FIGURES (Cont'd.)

PERSONNEL

Scientific and Engineering Personnel		Time Worked in Man Months*
W. G. Dow	Professor of Electrical Engineering	Supervisor
H. W. Welch, Jr.	Research Physicist	7.65
J. R. Black	Research Engineers	10.78
G. Hok		1.87
H. A. Martens		1.95
J. S. Needle	Instructor of Electrical Engineering	2.04
G. R. Brewer	Research Associates	9.51
S. Ruthberg		3.90
H. W. Batten	Research Assistant	1.99
W. W. Peterson	Student Assistant	4.81
Service Personnel		
V. R. Burris	Machine Shop Foreman	5.81
R. F. Steiner	Assembly Technicians	11.04
J. W. Van Natter		9.76
A. Town	Technicians	6.73
J. Mossar		
C. Pratt		
C. A. Jaycox		
R. F. Denning	Laboratory Machinists	18.71
D. L. McCormick		
T. G. Keith		
E. A. Kayser		
N. Navarre	Draftsmen	6.37
J. Merithew		
S. Spiegelman	Stenographers	5.68
M. J. Walker		

* Time worked is figured on the basis of 172 hours per month.

MAJOR REPORTS ISSUED TO DATE

Contract No. W-36-039 sc-32245. Subject: Theoretical Study, Design and Construction of C-W Magnetrons for Frequency Modulation.

Technical Report No. 1 --

H. W. Welch, Jr. "Space-Charge Effects and Frequency Characteristics of C-W Magnetrons Relative to the Problem of Frequency Modulation", November 15, 1948.

Technical Report No. 2 --

H. W. Welch, Jr., G. R. Brewer. "Operation of Interdigital Magnetrons in the Zero-Order Mode", May 23, 1949.

Technical Report No. 3 --

H. W. Welch, Jr., J. R. Black, G. R. Brewer, G. Hok. "Final Report", May 27, 1949.

Contract No. W-36-039 sc-35561. Subject: Theoretical Study, Design and Construction of C-W Magnetrons for Frequency Modulation.

Interim Report --

H. W. Welch, Jr., J. R. Black, G. R. Brewer. December 15, 1949.

Quarterly Report No. 1 --

H. W. Welch, Jr., J. R. Black, G. R. Brewer, G. Hok. April, 1950.

Quarterly Report No. 2 --

H. W. Welch, Jr., J. R. Black, G. R. Brewer, J. S. Needle, W. Peterson. July, 1950.

Quarterly Report No. 3 --

H. W. Welch, Jr., J. R. Black, J. S. Needle, H. W. Batten, G. R. Brewer, W. Peterson, S. Ruthberg. September, 1950.

Technical Report No. 4 --

H. W. Welch, Jr. "Effects of Space Charge on Frequency Characteristics of Magnetrons", Proc. IRE, 38, 1434-1449, December, 1950.

MAJOR REPORTS ISSUED TO DATE (Cont'd.)

Technical Report No. 5 --

H. W. Welch, Jr., S. Ruthberg, H. W. Batten, W. Peterson. "Analysis of Dynamic Characteristics of the Magnetron Space, Preliminary Results", January, 1951.

Technical Report No. 6 --

J. S. Needle, G. Hok. "A New Single-Cavity Resonator for a Multianode Magnetron", January 8, 1951.

ABSTRACT

Two methods for frequency modulating magnetrons have been investigated. One method employs the use of voltage tuning or "frequency pushing" while the other utilizes a magnetron-type space charge to produce a variable reactance.

Basic theory concerning the dynamic characteristics of a magnetron space charge and the propagation of electromagnetic waves in a magnetron space charge has been developed in order to give a more complete understanding of the problem. Also the theory of a new type single-cavity resonator has been developed. This type of resonator geometry is extremely flexible from the standpoint of inserting more than one set of anodes and also for tuning and loading.

The design factors and operating characteristics of five different types of tubes are presented as well as a brief summary of the tube-construction techniques employed at this laboratory. Progress made towards the development of a new type of tube to be used as a tool for the study of the magnetron-type space charge is briefly given.

A general outline of the laboratory facilities of this laboratory is discussed. Suggestions are offered for the direction to be taken in future research in this field. Assembly drawings for all tubes designed and built in this laboratory in the period covered by this report are given.

THEORETICAL STUDY, DESIGN, AND CONSTRUCTION OF C-W MAGNETRONS FOR FREQUENCY MODULATION

FINAL REPORT

I. INTRODUCTION

1. Purpose

The purpose of this report is to summarize the progress in the University of Michigan Electron Tube Laboratory during the period from December 1, 1949, through November 30, 1950, on Contract No. W-36-039 sc-35561 for the Signal Corps. Work done on this contract in the period May 1 to November 30, 1949, has been covered in a previous report,"Theoretical Study, Design and Construction of C-W Magnetrons for Frequency Modulation", Interim Report issued December 1, 1949.

The general objectives of the program under this contract are to increase the knowledge of space-charge effects and frequency characteristics in C-W magnetrons and to apply this knowledge to the development of magnetrons which can be frequency modulated. Prior to March 1, 1950, the emphasis had been in the 2000 to 2400 megacycle range. The general technique adapted was to employ a magnetron-type space charge as a variable reactance element in a reactance tube within the same vacuum envelope as the oscillator magnetron. Three models of f-m tubes were under development using this principle.

The study of a new method of frequency modulation was initiated on this contract March 1, 1950.

Early in 1949, Wilbur of General Electric Laboratories discovered that under certain conditions very wide frequency pushing at uniform power levels is obtainable. Frequency shifts have been observed between 1.5 to 1 and 15 to 1, depending upon loading, efficiency, and cathode temperature. The above phenomena have been observed at frequencies below 1000 megacycles. Loading conditions of the tubes have been quite restrictive, consisting of a load attached directly to the terminals of the anode structure. The Q's are in the order of 10 or less. With a transmission line between the load and the tube it is possible to obtain Q's of the same order; however, problems involving the long-line effect immediately arise. Since March 1, 1950, the objectives on this phase of the program have been to obtain sufficient understanding of the above type of operation so that it may be extended to microwave frequencies of 3000 to 4000 megacycles.

2. Outline of Procedure

Results accomplished prior to the period covered by this report at the University of Michigan Vacuum Tube Laboratory were presented in the Technical Reports Nos. 1, 2, and 3 and in the Interim Report. (See list of publications at the front of this report.)

The status quo at the beginning of December 1, 1949, was as follows:

a. The understanding of the magnetron-type space charge insofar as effects on frequency were concerned was fairly complete, based on experimental and theoretical observations presented in Technical Report No. 1.

b. Factors influencing the design of interdigital magnetrons for operation in the zero-order mode had been evaluated, several tubes constructed, and results presented in Technical Report No. 2.

c. Three designs for frequency-modulated magnetrons employing a magnetron-type space charge for a variable reactance had been developed. Construction had been started on six tubes of one of these designs (Model 6), and four had operated in the desired mode. Sketchy modulation data were obtained in one. A second-type tube (Model 5) was under construction. Cold tests had been made on a third type to obtain data necessary to complete its design.

d. A program to supplement previously obtained experimental data on the characteristics of the space charge had been initiated with the purpose of checking unexplored regions of magnetic field, thus providing further check on theoretical analysis.

In order to fulfill the aims of this contract three methods of attack were undertaken:

A. Low-Q Operation of Magnetrons. The most apparent features of the operation obtained at the General Electric laboratories are the following:

a. The Q is extremely low, probably in the order of 10 or less.

b. The voltage-tuning phenomenon is similar to the usual frequency pushing, but is much more pronounced due to the low Q.

c. The low current drop-out usually experienced when a magnetron is heavily loaded is conspicuously absent.

d. The cathode temperature must be limited to achieve satisfactory operation. A tungsten cathode giving a definite emission boundary is required. This limitation of emission seems to be intimately related to the maximum-current boundary and a required criterion for operation.

e. Efficiency is reduced as band width is increased. This must be due to decreased electronic efficiency since circuit efficiency is obviously very high.

f. Loading is accomplished directly at the tube anode terminals (i.e., almost directly across the capacitive portion of the resonant circuit). Loads farther from the tube may cause trouble with long-line effect.

The program of study of low-Q operation at the Michigan Laboratory includes the following:

a. Development of a theory of frequency pushing which will permit quantitative, or at least semi-quantitative, predictions to be made about particular designs.

b. Determination of the causes of current drop-out as they are related to loading.

c. Investigation of the effect of temperature-limited cathode operation on the fundamentals of space-charge behavior in an oscillating magnetron.

d. Experimental study of tubes especially built for low-Q operation with emphasis on the above three points and a study of long-line effects.

The experimental work of part d is just being started as this report is written.

B. Construction of F-M Magnetrons. Three different f-m structures employing the magnetron-type space charge as a variable reactance were to be constructed and studied experimentally with the objective to develop an operating f-m tube. The three structures have been designated Models 5, 6, and 8, the basic geometries of which are shown in Fig. 2.1.

Model 5: Fig. 2.1a depicts the geometry of the Model 5 f-m magnetron, and Dwg. No. B10,005 in Appendix A shows the assembly drawing of the tube. Model 5 is a nontunable interdigital tube utilizing coupling to the cathode line to introduce the effect of the modulating space charge supplied by a second cathode.

Model 6: At the beginning of this period four Model 6 tubes had been constructed which operated in the desired mode; however, difficulty was experienced due to power being coupled out of the modulator cathode stem. The geometry of Model 6 is depicted in Fig. 2.1b; it consists essentially of a full-wave capacity-loaded coaxial cavity having two sets of

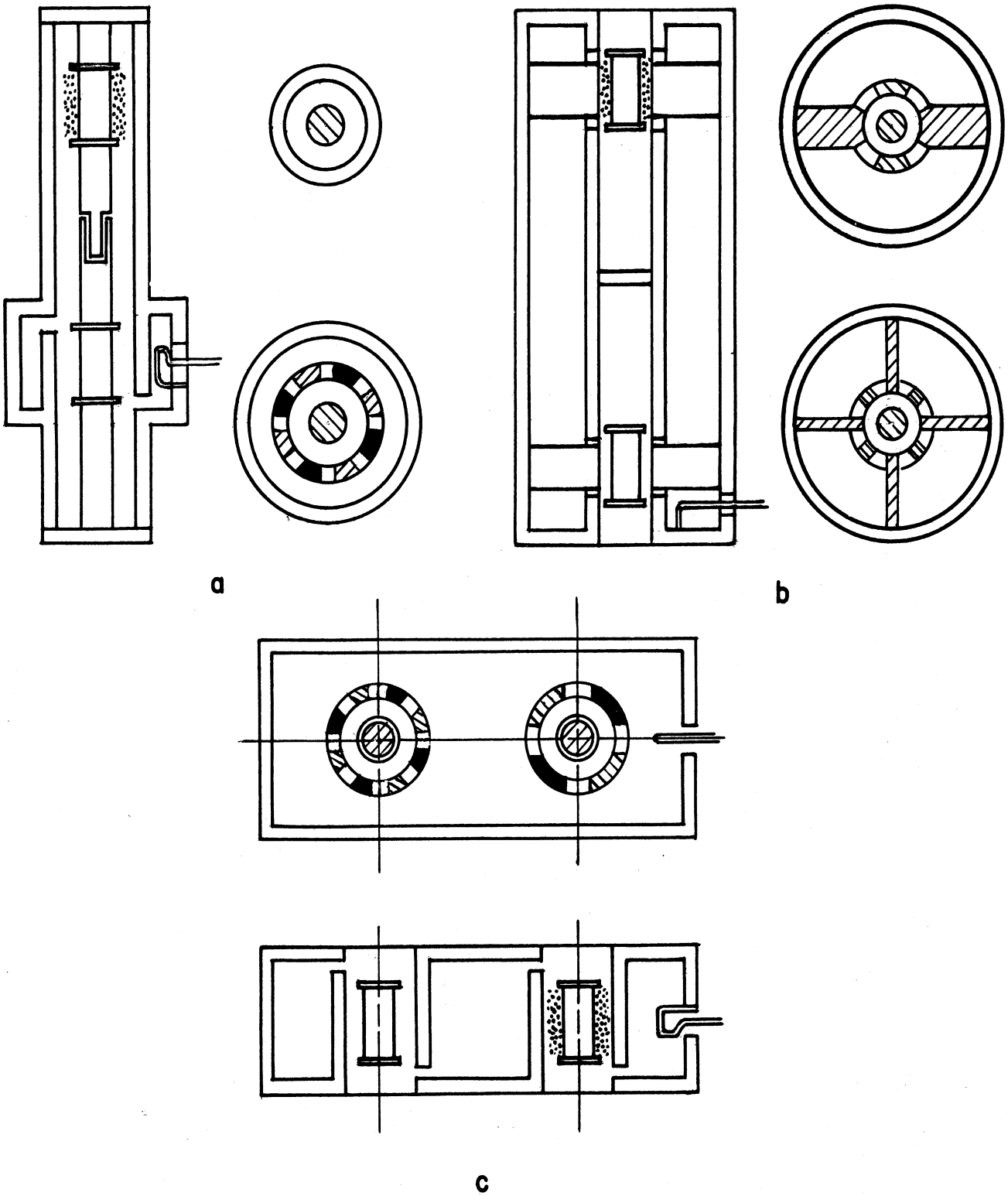

FIG. 2.1 BASIC GEOMETRIES FOR FREQUENCY MODULATION MAGNETRONS DEVELOPED IN THE UNIVERSITY OF MICHIGAN ELECTRON TUBE LABORATORY.

NOTE: MODULATING SPACE CHARGE INDICATED BY DOTS.

anodes, each placed at voltage maxima points. The anodes consist of vanes extending from the outer conductor and protruding through slots in the inner conductor. An assembly drawing of Model 6 is shown in Dwg. No. B10,006A in Appendix A. Sixteen anodes are employed in the oscillator section while four anodes are used in the modulator portion of this tube.

Model 8: The Model 8 f-m magnetron geometry is shown in Fig. 2.1c; it consists of a capacity-loaded full-wavelength rectangular cavity employing interdigital anodes at each voltage maximum in the cavity. One anode acts as an oscillator while the other is used as a variable reactance tube. Dwg. No. B10,008 in Appendix A shows an assembly drawing of Model 8. The initial Model 8 was designed with two identical sets of anodes in order to investigate the possibility of this structure operating as a high-power C-W magnetron with both sets of anodes operating as oscillators. Frequency-modulation data could also be obtained from this structure.

C. Study of Magnetron Space Charge. The study of magnetron space charge was more or less deemphasized during 1949, under the pressure of developing interdigital tubes and f-m magnetrons. However, it was resumed in the period covered by this report for the following reasons:

a. During the development of more or less unconventional f-m magnetrons and the study of voltage tuning, problems involving the space charge have been continuously recurrent, i.e., mode-jump current, optimum loading conditions, symmetry of fields in the interaction space, etc. These problems arise due to inadequate knowledge of dynamic characteristics of magnetron space charge.

b. No analyses on extensive experimental data exist which give an understanding of losses in the magnetron space-charge swarm. This is

a rather serious problem and in the use of such a swarm for modulation may be the limiting feature. Knowledge of the magnitude of this loss, the relative importance of cathode back bombardment and collection of current by the anode, and a theoretical understanding of basic phenomena could be very useful in devising methods for minimizing or eliminating the loss.

c. Experimental data supporting the general theory presented in Technical Report No. 1 were inadequate, although important reactive properties of the space charge which are usable in the production of frequency modulation were conclusively verified. Also some restrictive approximations were made on development of the theory. In order to complete the picture, a detailed survey of space-charge swarm properties insofar as they affect wave propagation would be necessary for wide ranges of magnetic field and for various orientations of direction of propagation and polarization of the wave with respect to magnetic field.

One of the attractive features in the study of space charge is that positive results obtained in any part of the program will be helpful in understanding all three of the phenomena mentioned above and the results will contribute to the knowledge of both frequency modulation and magnetron oscillation.

The following steps were taken to carry out this program:

A study of dynamic characteristics of the magnetron space charge was undertaken with the specific objective of increasing the understanding of voltage tuning and factors affecting maximum-current boundary.

A theoretical study of the propagation of electromagnetic waves in a magnetron space charge was started and was to be backed experimentally by measurement to be taken on specially designed tubes.

A detailed study of the r-f properties of a magnetron space charge by hot impedance tests was undertaken to supplement the experimental data presented in Technical Report No. 1.

Work was also started on the design and development of a smooth-bore magnetron for experimentally verifying theories on the magnetron space charge. It was hoped to serve in integrating the various theories andin making the understanding of magnetron space charge more vivid. This tube is called the "trajectron" and is discussed in Section 15 of this report.

3. Tubes Planned for Construction

The following tube models were planned for construction during this period:

Model 5	f-m structure
Model 6	f-m structure
Model 8	f-m structure
Model 7	magnetron oscillator to study the operation of a new type of single-cavity resonator for a magnetron (This resonant system is employed in Model 6 and Model 9 and will be used in the study of low-Q operation.)
Model 9	low-power magnetron having an external resonant cavity for studying low-Q operation
Models 11001, 11002, 11003	this series of magnetron diodes was to be built to study the propagation of electromagnetic waves in a magnetron space charge
Model 11004	trajectron for studying the space charge in a smooth d-c magnetron

Tubes constructed in the period covered in this report are given in Table 3.1. Assembly drawings of these tubes are presented in Appendix A of this report.

TABLE 3.1

Tube No.	Model No.	Date Assembled	History	Operated	Present Condition
26	6A	12-49	1. removed modulator cathode, Model 7 2. inserted modulator cathode, Model 9 3. removed modulator cathode	yes	operable
27	5	2-50	1. realigned cathodes 2. changed choke design	yes	operable
28	11.001A	1-50	lost in brazing	no	inoperable
29	6A	2-50	lost in H_2 furnace due to miscalibrated thermocouple	no	inoperable
30	11.001A	2-50	lost in H_2 furnace due to miscalibrated thermocouple	no	inoperable
31	6A	2-50	1. removed modulator cathode, Model 7 2. inserted Model 9 modulator cathode 3. inserted Model 10 modulator cathode 4. removed Model 10 modulator cathode 5. replaced burned-out oscillator cathode with Model 6 cathode with $\lambda/4$ bypass	yes	operable
32	11.001B	5-50	1. replaced filament 2. replaced sagged filament 3. opened for inspection	yes	inoperable
33	7A	4-50	1. replaced burned-out cathode with Model 6 having $\lambda/4$ bypass 2. replaced cathode with modified Model 6 having $\lambda/4$ bypass 3. replaced cathode with Model 12 4. replaced burned-out Model 12 cathode	yes	operable
34	11.003	7-50	1. replaced sagged cathode	yes	inoperable
35	9.0	7-50	1. glass seals could not be annealed with this design	no	inoperable

TABLE 3.1 (Cont'd.)

Tube No.	Model No.	Date Assembled	History	Operated	Present Condition
36	8.0	9-50	1. removed cathodes for cold test	yes	inoperable
37	11.004	8-50	1. rebuilt due to cathode failure	yes	operable
38	9A	9-50	1. jig sintered to tube	no	inoperable
39	9A	9-50		yes	operable
40	7B	9-50	1. replaced Mod. 12 cathode with Mod. 16 2. replaced Mod. 16 cathode with .260-in. dia. cathode similar in construction to Mod. 12	yes	operable
41	7C	10-50		yes	operable
42	7D	10-50		yes	operable
43	9B	11-50		yes	operable
44			construction not started to date		
45	7E	11-50		yes	inoperable

During the period covered by this report, construction was started on nineteen different tube structures. Fourteen tubes were operated hot on the test bench and of these fourteen, ten are still operable. Five tubes were lost at assembly due to the following causes: One was lost due to solder flowing to the wrong place. Two were lost at the same time in the hydrogen furnace due to a miscalibrated thermocouple. One had a jig sintered to it while being brazed, and one could not be constructed due to the fact that the glass seals could not be properly annealed.

A number of these fourteen tubes were pumped down and operated several times with differently designed cathodes inserted in them. This is indicated in the "history" column of Table 3.1. A total of eighteen changes and pump-downs were made after these tubes were built.

II. BASIC THEORY

4. Dynamic Characteristics of the Magnetron Space Charge, Low-Q Operation (H. W. Welch, Jr.)

The major emphasis in theoretical effort during the period covered by this report has been on acquiring better understanding of the space charge in the oscillating magnetron. The purpose of this emphasis was to make possible the better understanding of low-Q operation so that this operation might be obtained at shorter wavelengths. The results of this study have been presented in detail in Technical Report No. 5 entitled "Dynamic Characteristics of the Magnetron Space Charge". The following is a brief summary of the important results of this report.

Operation at very low circuit Q's was first obtained by Wilbur and Peters at General Electric Research Laboratories[1] at frequencies under 1000 megacycles. This operation was described in Section 2 of this report.

One well-known property of conventional magnetrons operating in the vicinity of 10 cm is that very heavy loading will cause low maximum-current boundary and may even cause operation to cease altogether. The causes of this current limitation are, therefore, immediately important to a study of low-Q operation. Also, a clearer understanding of voltage tuning, or frequency pushing, is needed. Finally, it is desirable that power output should be relatively constant, independent of frequency.

The possible causes of current drop-out which are suggested are the following:

a. cathode limitation of available current,

b. space charge limitation of available current,

---

[1] Final Report, C-W Magnetron Research, Contract No. W-36-039 sc-32279, Report No. RL 341, General Electric Company, April 1, 1950.

c. limitation of current due to transit-time effects,

d. induced-current limitation placed by maximum possible density and extent of space charge in the bunches, or spokes, of space charge,

e. mode competition causing current drop-out in one mode when another mode is more favorable to magnetron oscillation, and

f. debunching or overbunching due to inadequate focussing by the r-f field as the spoke changes in position and the current increases.

Power-supply regulation is also a factor in determining current drop-out which has been considered in some detail by Raytheon engineers. (Mr. E. Dench and Mr. W. C. Brown have supplied information on this point.) This was not considered in the study at Michigan since it is more of a circuit problem than a tube problem.

The space-charge distribution used in this study is shown in Fig. 4.1. The hub of the space-charge "wheel" is assumed to extend to the radius at which outermost electrons become synchronous with the travelling r-f wave in the interaction space between anode and cathode. All the space charge outside of this radius is assumed to be synchronous. This assumption with the force-balance equation is sufficient to define the anode voltage for which the synchronous electrons reach the anode, and the constant synchronous space-charge density, which is independent of radius. Conversely the anode voltage defines the synchronous velocity. This velocity determines the frequency of oscillation of the magnetron. As long as the space charge is capable of supplying the r-f current to the circuit, the magnetron will operate at the frequency determined by the synchronous velocity. If circuit conductance is relatively independent of frequency, this current is a minimum near resonance because the shunt susceptance becomes zero in this region. One criterion for getting voltage tuning over

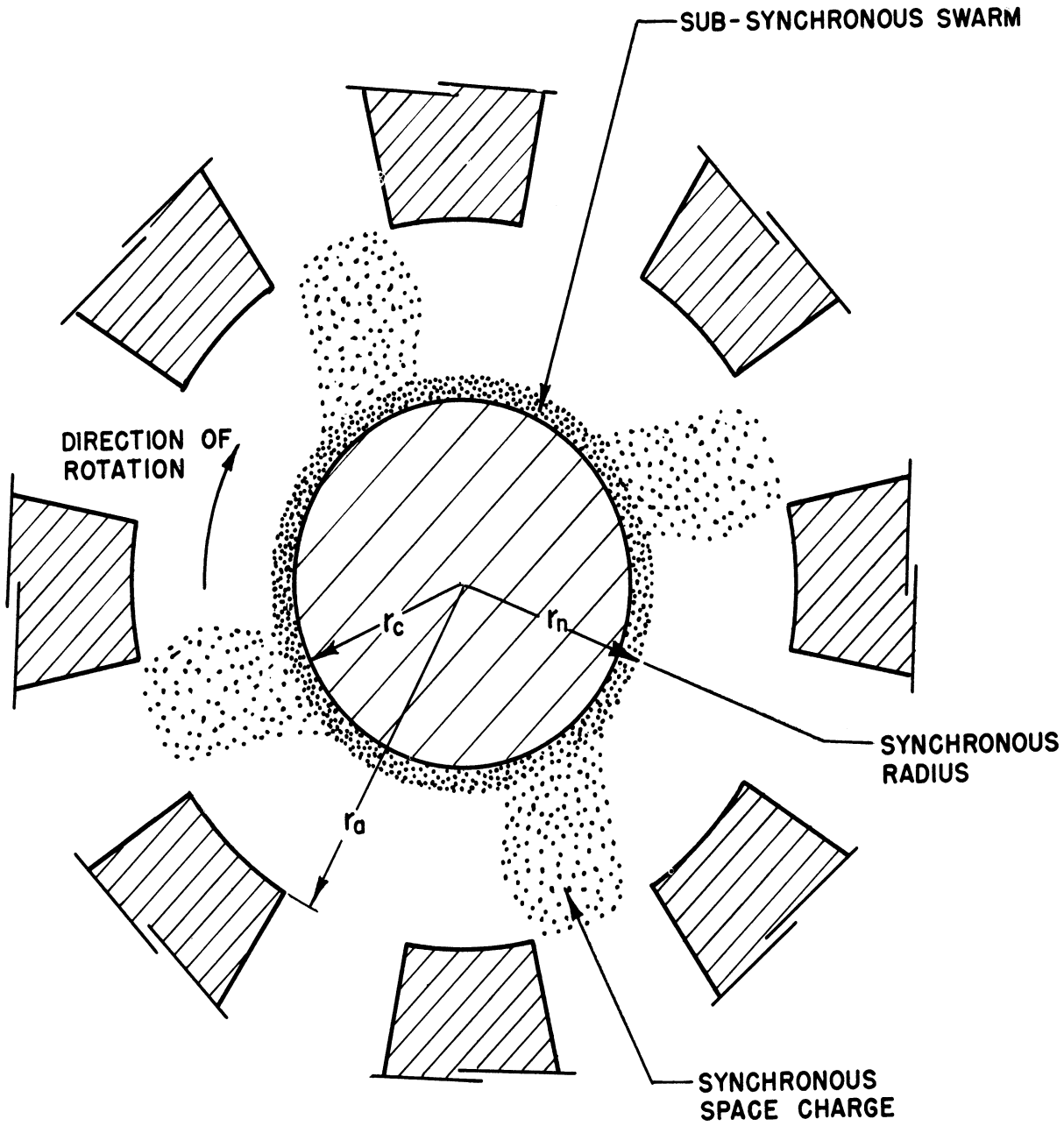

FIG. 4.1

BASIC PHYSICAL PICTURE OF THE MAGNETRON SPACE CHARGE DESCRIBED IN SECTION 4

a wide range is, therefore, to make the circuit admittance small enough over a large frequency range that the magnetron space-charge swarm is capable of supplying the required current. Thus a low-Q circuit is required, and if the conductance value is fixed, the low Q must result from low energy storage, or low circuit capacitance.

Methods for estimating the amount of r-f current available in a given interaction-space design are presented in detail in Report No. 5. It is assumed that the most important contribution is that of the induced current due to the rotating spokes of space charge. The exact form of the spokes is not calculable. Quantitative results obtained by different assumptions of the spoke shape compare favorably with experimental observations. Regardless of what the exact spoke shape may be, it is possible to estimate the maximum induced current for a given interaction space by assuming well-defined rectangular spokes having a width equal to the anode-segment width.

The effect of radial velocities and collection current on the r-f current has not been considered as yet. However, the amount of power input is limited by the collection current. This point is quite important to the low-Q operation. If tuning is to be obtained by changing anode voltage without changing power output and without reaching excessive r-f voltages, some mechanism must be provided to limit power input or change electronic efficiency or both. The collection current can be limited by operating the cathode temperature-limited. In order to get a well-defined current limitation by temperature a pure-metal cathode must be used, such as tungsten. This procedure was used by the G. E. group. Under these conditions, the d-c plate current remains relatively constant while the anode voltage and frequency increase. The voltage for a given frequency is given approximately by the Hartree voltage as would be expected from the statements

made above. The quantitative expression for the Hartree voltage is determined by the choice of a synchronous velocity of the electrons in the spokes and the assumption that electrons in the hub are behaving as they would in the static magnetron. With these assumptions the Hartree voltage is

$$E_h = \pi r_a^2 \frac{f}{n} B\left(1 - \frac{r_c^2}{r_a^2}\right) - 2\pi^2 \frac{m}{e} \frac{f^2}{n^2} r_a^2 \qquad (4.1)^1$$

For large B the f^2 term can be neglected and f is proportional to E_h. (See Fig. 8.8, Technical Report No. 5.) As the voltage increases, since the maximum available number of electrons per second is being utilized (under temperature-limited conditions), the energy of the increased voltage goes into increase in velocity of the electrons. Thus, electrons strike the anode at higher energies and electronic efficiency is decreased. This is desirable if power output is to be kept constant. The r-f voltage and current do not continually build up, and the maximum-current boundary which may be caused by overbunching and the induced-current limitation is not reached.

The space-charge-limited current in the magnetron is calculated assuming that it is controlled by the potential at the radius of the hub in the space-charge swarm (Fig. 4.1). The values given by this calculation are less than the 1/2 Allis current used by Slater[2] by a factor of 2 or more.

The results of calculation of induced current from the assumed space-charge distribution in some particular geometries show that, in these

---

1 See Technical Report No. 1 for a discussion of the derivation of this equation.

2 Slater, J. C., Microwave Electronics, Van Nostrand, 1950.

particular cases at least, the induced-current limitation is much more severe than the space-charge-current limitation. A factor of 5 or 10 to 1 is calculated for the ratio of space-charge-limited current to induced current. This is also observed in the operation of the tube.

Calculation of transit times indicates that space-charge distribution may be upset due to insufficient recovery time during an r-f cycle. These calculations are approximate, however, and should be considered more carefully before drawing conclusions.

Effects of mode separation have not been considered in any detail, since a recent doctoral thesis at M.I.T. is using this as a subject.[1]

5. Propagation of Electromagnetic Waves in the Magnetron Space Charge (G. R. Brewer)

In order to provide information on the properties of a magnetron space-charge cloud as it affects the magnetron resonant circuit, an analysis was carried out concerned with the propagation of electromagnetic waves in the magnetron space charge. This first work was reported in Technical Report No. 1. During the period of work covered by this report, this analysis has been extended to include the effects of the variation with position of the electron velocities, and other effects in the space charge. This work will be discussed completely in a forthcoming technical report but will be described here briefly in order to illustrate the scope of the work done.

The complete solution of the interaction of the waves in a multicavity magnetron and the space charge was considered too complicated to

---

[1] Moats, R. R., M.I.T.; this work will be presented at the 1951 IRE National Convention.

yield results with any degree of generality. Therefore, the radial and tangential components of the actual fields in the magnetron were used separately in the analysis, each compoent giving rise to a different direction of propagation, tangential or radial. In the use of space-charge clouds for frequency modulation, the characteristics for propagation in the direction parallel to the magnetic field were desired so that this problem was also solved. Using these simplified types of fields, solutions were obtained for both the plane and cylindrical magnetron structures.

The Euler hydrodynamical equation,

$$\frac{\partial v}{\partial t} + (v \cdot v)\, v = -\frac{e}{m}\left[E + v \times B\right] - \frac{\nabla p}{nm} \quad ,$$

which is derivable[1] directly from the Boltzmann transport equation, will be used to find the equations of motion for this problem of electron-wave interaction.

In this equation,

v = electron velocity

E = total electric field

B = steady magnetic field (effect of r-f magnetic field can be neglected)

n = number of electrons per unit volume

p = electron gas pressure.

A term was introduced into this equation, in the form of a frictional force proportional to the electron velocity, which includes the effect of collisions between the electrons and gas particles in the space charge. It will be shown in the forthcoming report that the pressure gradient (∇p) term does not affect the final result, so that this may be ignored. The equation

---

[1] Chapman and Cowling, The Mathematical Theory of Nonuniform Gases, Cambridge, 1939, Chapter 3.

of motion of the electrons in the space charge subject to the electric field of the propagating wave and the applied magnetic field is then

$$\frac{\partial v}{\partial t} + (v \cdot v)\, v + gv = -\frac{e}{m}\left[E + v \times B\right] .$$

From this equation the electron velocity, and therefore the current, are obtained in terms of the applied fields. Substitution of the current relations into the Maxwell field equations enables the determination of the complex index of refraction of the space-charge medium. It can be shown that the effect of the electron motion is equivalent to an electric energy storage in the medium in addition to the usual energy storage in free space, given by $E^2 \epsilon_o/2$. Thus, the space charge can be considered, insofar as wave propagation is concerned, as a dielectric whose relative dielectric constant is a function of the ratio ω/ω_c between the wave frequency (ω) and the magnetic field $B = (m/e)\,\omega_c$.

It is found that the effective dielectric constant of the space charge can assume values which are positive and greater or less than unity, and also negative values. The interpretation of the latter value involves an analogy to a conducting material in which a wave is attenuated upon entering.

The results of this analysis are expressed in the following equations for the effective dielectric constant and conductivity of the space charge. The Hull-Brillouin equation for space-charge density has been used in the following:

a. Propagation of a plane wave in the direction of the applied magnetic field.

$$\text{Plane Magnetron:} \quad \epsilon_{eff} = 1 - \frac{1}{(\omega/\omega_c)^2}$$

Cylindrical Magnetron: (r_c = cathode radius)

$$\epsilon_{eff} = 1 + \frac{(1 + r_c^4/r^4)\left[1 \pm (1/\sqrt{2})(\omega/\omega_c)\sqrt{1 - r_c^2/r^2}\right]}{1 - r_c^2/r^2 - 2(\omega/\omega_c)^2}$$

$$\sigma \cong g\epsilon_o \frac{(\omega_c^2/2)\left[(\omega_c^2/2)(1 - r_c^2/r^2) + \omega^2\right] \pm (\omega\omega_c^3/\sqrt{2})\sqrt{1 - r_c^2/r^2}}{\left[(\omega_c^2/2)(1 - r_c^2/r^2) - \omega^2\right]^2}$$

These relations are plotted in Figs. 5.1 and 5.2 for $r_c/r \ll 1$.

b. Propagation of a plane or cylindrical wave in the direction normal to anode and cathode.

Plane Magnetron: $$\epsilon_{eff} = 1 - \frac{1}{(\omega/\omega_c)^2}$$

$$\sigma = \frac{g\epsilon_o}{(\omega/\omega_c)^2}$$

These equations are seen to be the same as those for the plane magnetron in case a, above.

Cylindrical Magnetron:

$$\epsilon_{eff} \cong 1 - \frac{\omega_c^2}{2\omega^2}\left(1 + \frac{r_c^4}{r^4}\right)\left[\frac{\omega^2 - (\omega_c^2/2)(1 + r_c^4/r^4)}{\omega^2 - (\omega_c^2/2)(2 + r_c^4/r^4 - r_c^2/r^2)}\right]$$

$$\sigma \cong g\omega\epsilon_o\left[\frac{1 + 2(\omega/\omega_c)^2}{1 - 2(\omega/\omega_c)^2} - \frac{7 - 8(\omega/\omega_c)^2 - \omega_c^2/2\omega^2}{4\left[1 - 2(\omega^2/\omega_c^2)\right](1 - \omega^2/\omega_c^2)^2}\right]$$

These relations are plotted in Fig. 5.3 for $r_c/r \ll 1$.

To provide a verification of the above outlined theory, one tube for investigation of space-charge properties has been constructed and

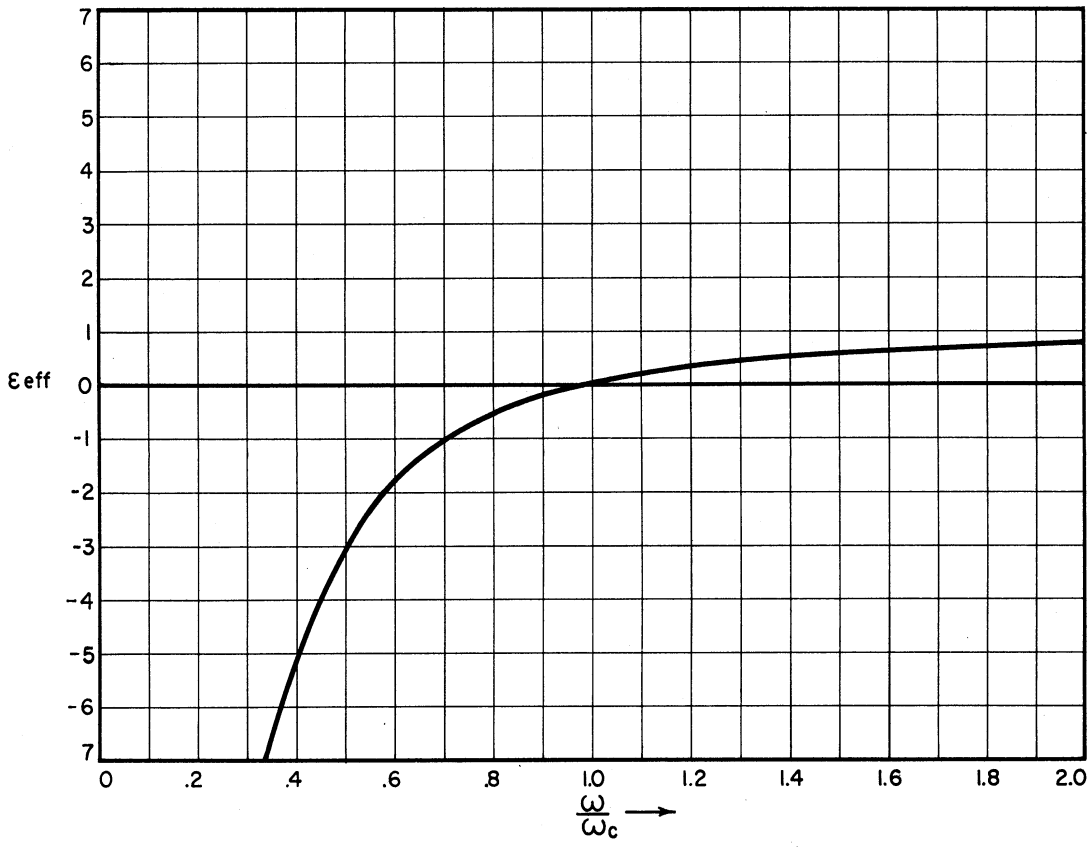

FIG. 5.1 ε_{eff} FOR PLANE MAGNETRON
PROPAGATION NORMAL TO MAGNETIC FIELD

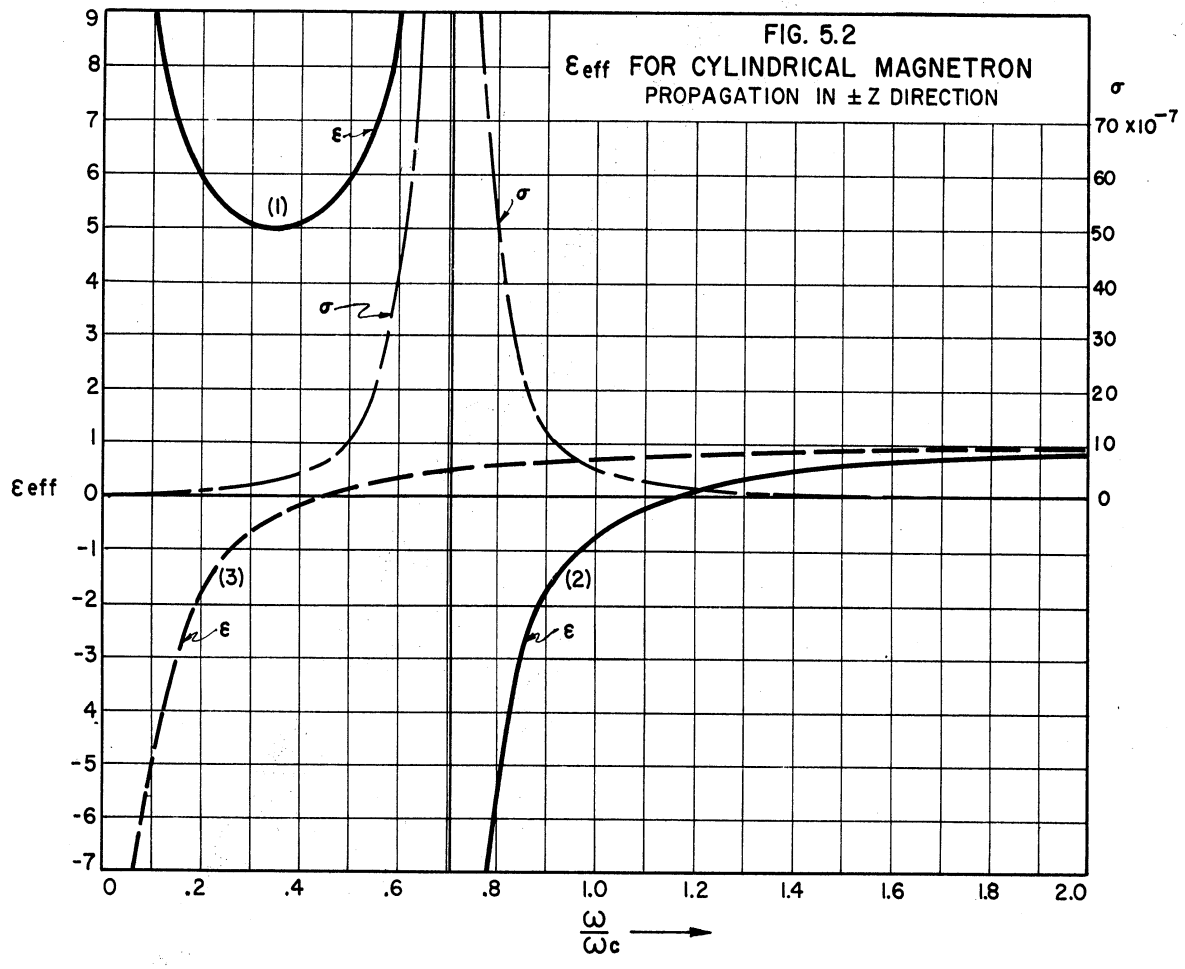

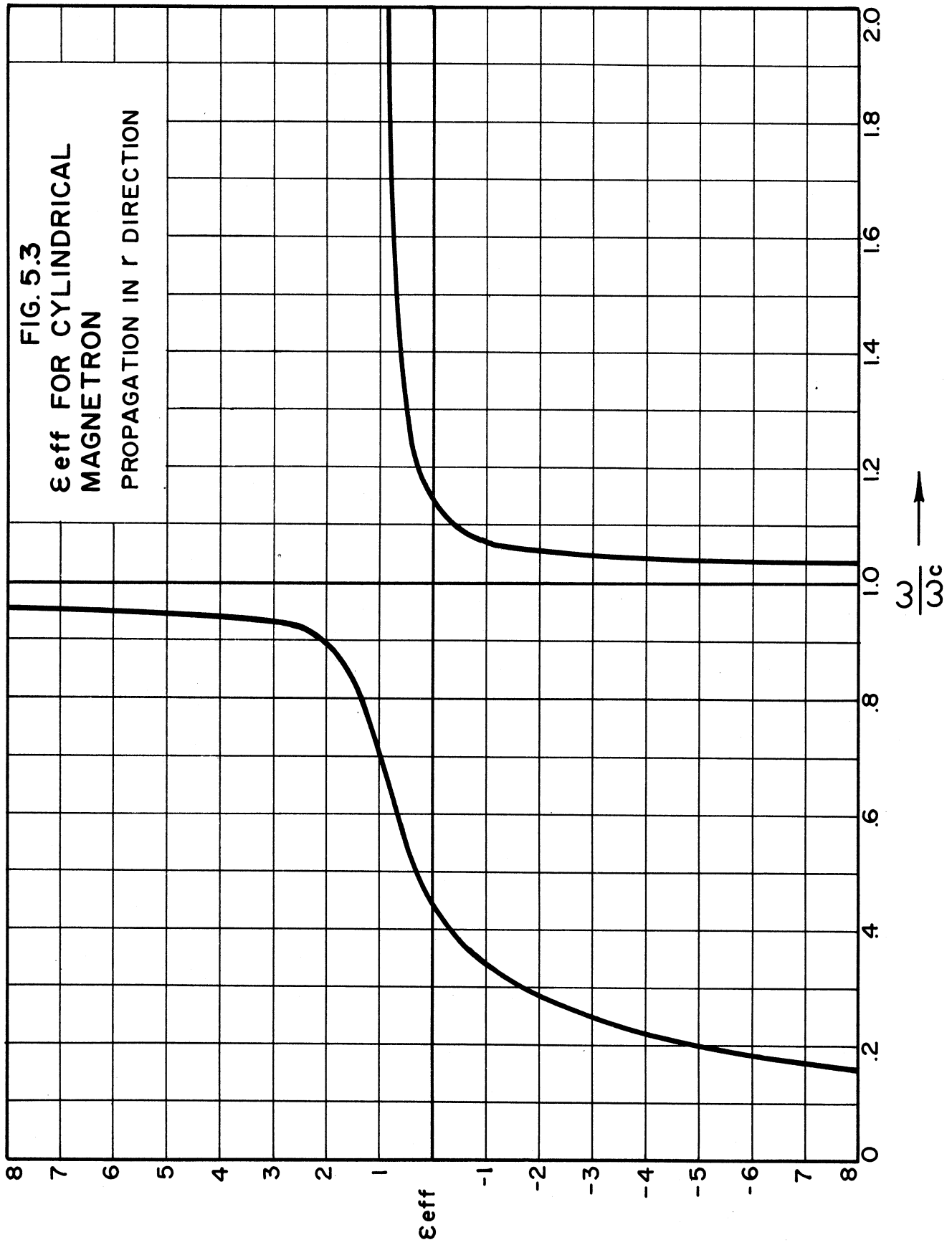
FIG. 5.3
εeff FOR CYLINDRICAL MAGNETRON
PROPAGATION IN r DIRECTION
εeff
8 7 6 5 4 3 2 1 -1 -2 -3 -4 -5 -6 7 8
0 .2 .4 .6 .8 1.0 1.2 1.4 1.6 1.8 2.0
ω/ωc

tested, and another is under construction at the present time. In both of these tubes the cylindrical space charge is placed in a resonant cavity so that it can interact with the electric fields of the particular mode which possesses field configurations duplicating those used in the analysis.

In the case of propagation along the direction of the applied magnetic field, the tube consisted of a $\lambda/2$ coaxial cavity with the filament and surrounding space charge as part of the center conductor. A drawing of this tube is shown in Dwg. No. B11,003, Appendix A. The change in resonant wavelength of the tube was noted as a function of the applied magnetic field. The data so obtained are shown in Fig. 5.4. Examination of Fig. 5.2 shows that when ω/ω_c is decreased to 1.17 the effective dielectric constant becomes negative and the cloud begins to behave as a conducting material, which should increase the capacitance across the coaxial line of the cavity, thus increasing its resonant wavelength. This resonant wavelength should remain above the "cold" resonant wavelength (B = 0) as ω/ω_c is decreased further to about 0.6, when it will decrease to the "cold" value. The experimental curve seems to confirm this latter point of wavelength shift, but the lower value of ω/ω_c at which λ_o changes is seen to be 1.4 instead of the expected 1.17. This may be due to a space-charge density on the boundary of the cloud different from the Hull-Brillouin value used in calculating Fig. 5.2, or to some irregularities in the tube itself. This point is being investigated further.

It is believed that these experimental data confirm at least qualitatively the predictions made on the basis of the theory developed.

A second tube is being constructed for investigation of the case of wave propagation in the radial direction. This tube is to be placed in

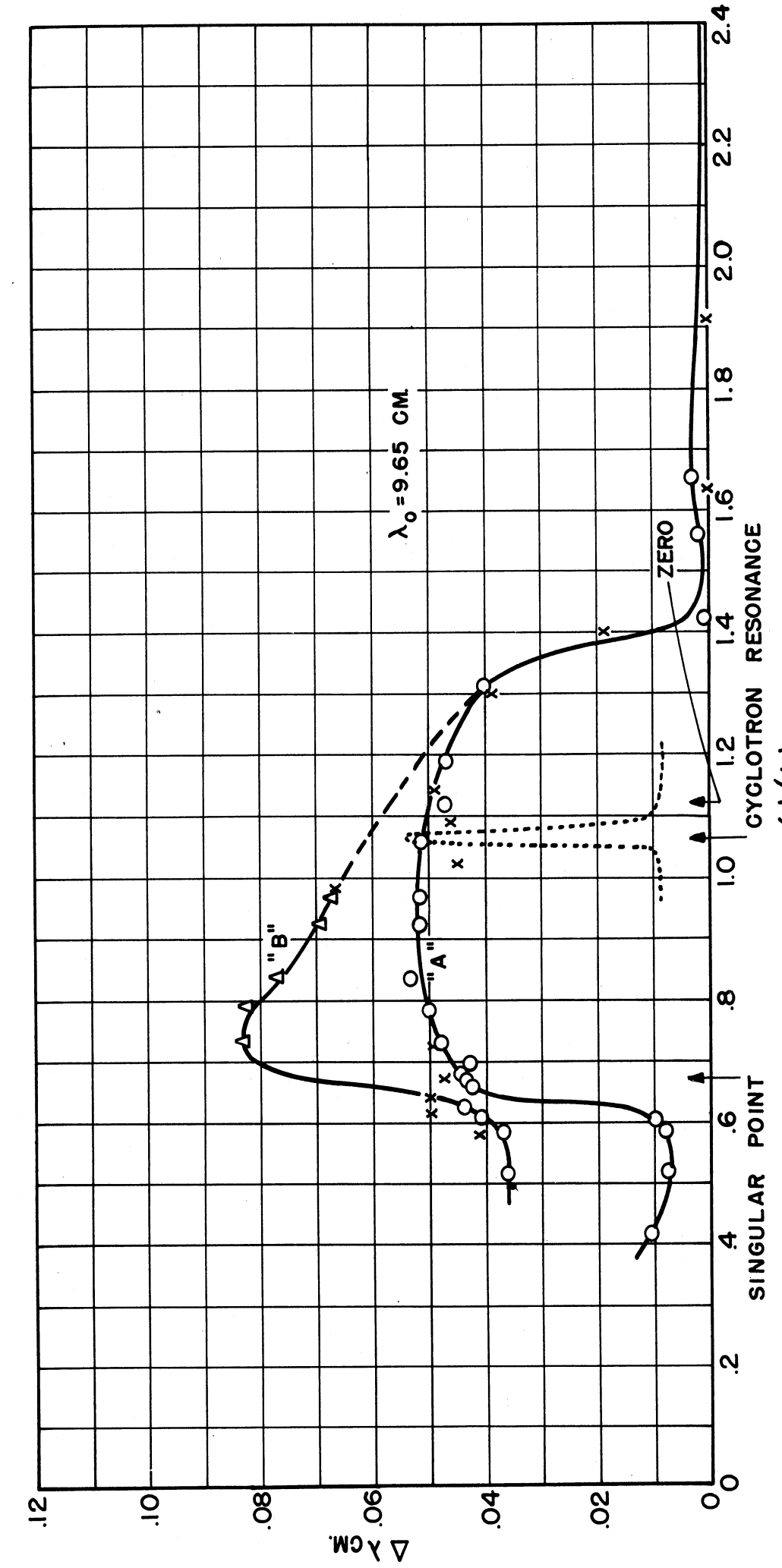

FIG. 5.4
CHANGE IN RESONANT WAVELENGTH OF 10 CM.
CAVITY vs ω/ω_c

PG. 89
BK. 6
G.R.B

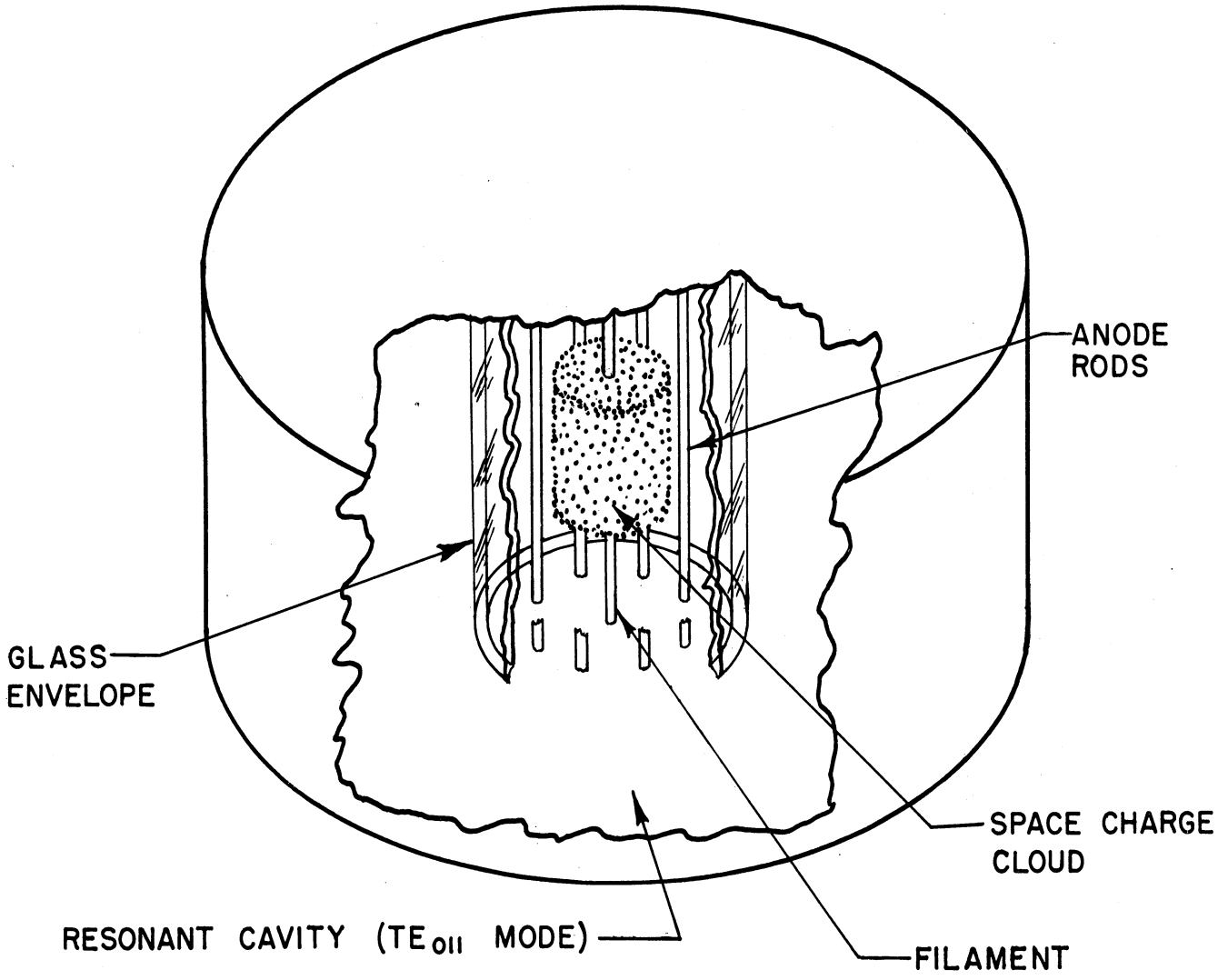

FIG. 5.5 TE_{011} RESONANT CAVITY FOR SPACE CHARGE STUDY

a cylindrical cavity resonating in the TE_{011} mode. The effect of the space charge on resonant wavelength and Q of the cavity will be measured and used as indications of the properties of the space-charge cloud. A drawing of this tube and cavity is shown in Fig. 5.5.

6. Theory of a New Single-Cavity Resonator for Multi-Anode Magnetron (J. S. Needle)

The analysis[1] presented in this section is applicable to a single-cavity resonator magnetron which consists of a section of coaxial transmission line excited at its center by an r-f voltage produced between a system of radial-vane anodes and longitudinal-bar anodes. The radial-vane anodes extend inward from the outer conductor of the coaxial line and protrude through slots bounded by longitudinal-bar anodes in the center conductor of the coaxial line.

The essential features of the resonator geometry are illustrated in the sketch of Fig. 6.1. This basic geometry is utilized in the Model 6, 7, and 9 magnetrons which are discussed elsewhere in this report.

The analysis was developed in order to determine the equations for the resonance frequency of the cavity, the external Q, and the impedance between the bars and vanes (see Section AA of Fig. 6.1), as seen by the electrons. The development is restricted to a lossless cavity resonator in the absence of the cathode.

We shall assume that the actual resonator may be represented by a lossless transmission line with lumped-constant admittances, as shown in Fig. 6.2.

Here $Y_L = G_L + jB_L$ is the load admittance transferred into the coaxial cavity; ℓ_1, ℓ_2, ℓ_3, are, respectively, the distance of the "T"

---

1 See Technical Report No. 6 for a more detailed presentation of this analysis.

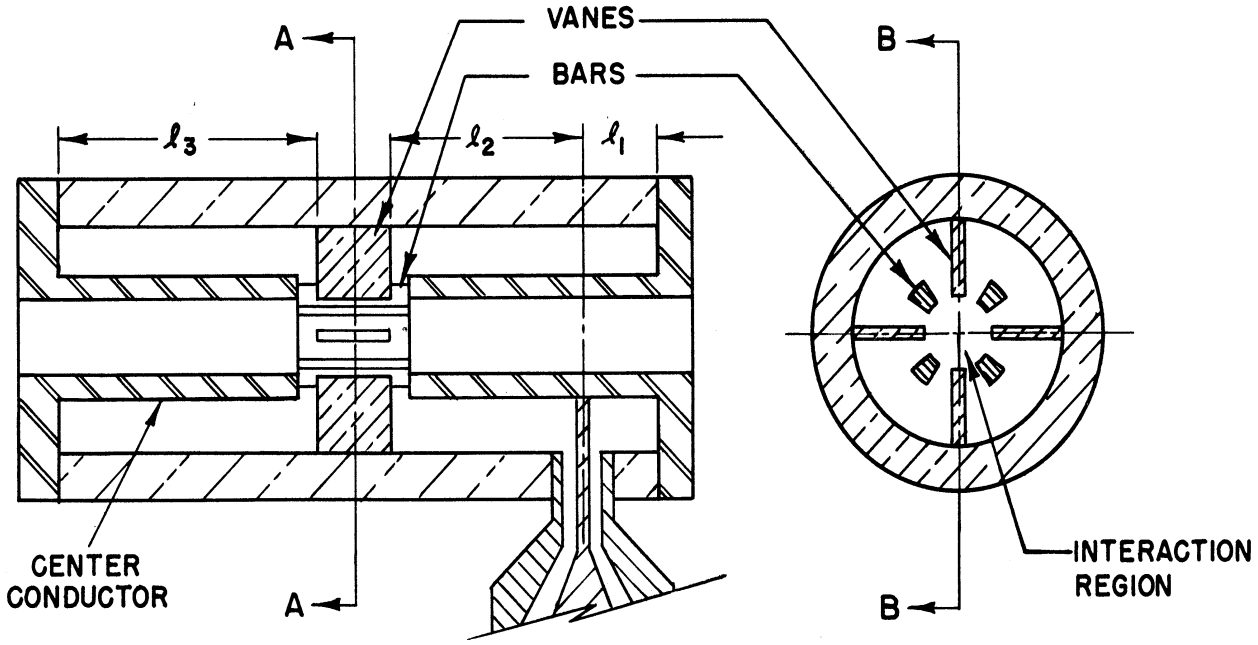

FIG. 6.1 SKETCH OF MODEL 7 GEOMETRY

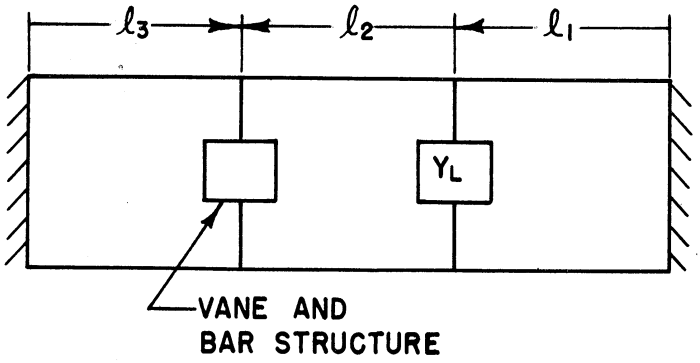

FIG. 6.2
TRANSMISSION LINE EQUIVALENT CIRCUIT

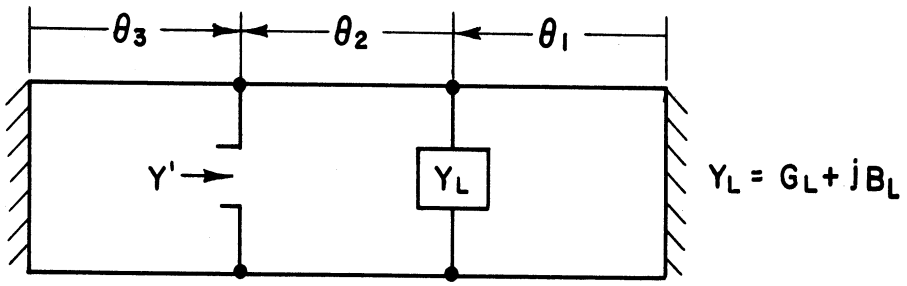

FIG. 6.3
EQUIVALENT CIRCUIT OF COAXIAL RESONATOR MAGNETRON

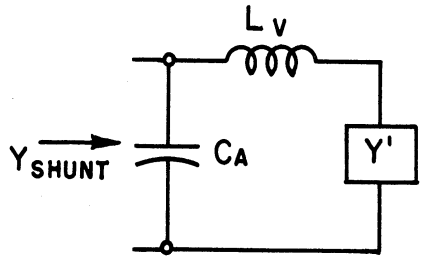

FIG. 6.4
EQUIVALENT CIRCUIT USED IN CALCULATION OF SHUNT ADMITTANCE

coupling connection from one shorted end of the coaxial cavity, the distance measured from the "T" to the right edge of the vanes, and the distance from the remaining short-circuited end of the coaxial line to the left edge of the vanes. Figs. 6.3 and 6.4 complete the equivalent circuit representation of the actual cavity. In Fig. 6.3, Y' is the admittance of the coaxial cavity plus load at the position of the bar-and-vane structure, and the θ quantities defined by the relation

$$\theta_i = \frac{2\pi \ell_i}{\lambda} \quad . \tag{6.1}$$

Fig. 6.4 indicates the lumped-constant representation employed to obtain the shunt admittance, Y shunt, between the bars and the vanes. Here L_V represents the total inductance of all the vanes in parallel, and C_A is the total capacitance between the vanes and bars.

Algebraic and trigonometric operations result in two rather complicated expressions,[1] one for the shunt conductance and one for the shunt susceptance looking into the spaces between the vanes and bars. These expressions are given a simpler approximate form by making use of certain inequalities which were determined numerically from the more general relations. The final approximate Eqs 6.2 and 6.3 are for the special case where $\theta_1 + \theta_2 = \theta_3$, and operation is into a matched load.

$$G_{shunt} \cong G_L Z_o^2 \frac{\sin^2 \theta_1}{4 \cos^2 \theta_3} \frac{1}{\left[\omega L_V + \frac{Z_o}{2} \tan \theta_3\right]^2} \tag{6.2}$$

$$B_{shunt} \cong \omega C_A - \frac{1}{\omega L_V + \frac{Z_o}{2} \tan \theta_3} \quad . \tag{6.3}$$

---

[1] See Eqs 4.8 and 4.9 of Technical Report No. 6.

Eq 6.3, when set equal to zero, gives the condition for resonance, i.e., resonance of the cavity in the absence of the cathode.

To obtain an expression for Q_e we assume B_{shunt} varies linearly with frequency in the region $\omega = \omega_o$; then,

$$\left(\frac{d\ B_{sh}}{d\omega}\right)_{\omega=\omega_o} (\omega_1 - \omega_o) = G_{shunt} \tag{6.4}$$

where ω_1 is the frequency deviation at the half-power points, or,

$$\frac{1}{G_{shunt}}\left(\frac{d\ B_{sh}}{d\omega}\right)_{\omega=\omega_o} = \frac{1}{\omega_1 - \omega_o} \ ; \tag{6.5}$$

multiplying both sides of Eq 6.5 by $\omega_o/2$ yields

$$\frac{\omega_o}{2\ G_{shunt}}\left(\frac{d\ B_{sh}}{d\omega}\right)_{\omega=\omega_o} = \frac{\omega_o}{2(\omega_1 - \omega_o)} = Q_e \ . \tag{6.6}$$

Carrying out the indicated differentiation, we obtain:

$$Q_e = \left[C_A + \frac{L_V + \frac{\theta_3\ Z_o}{2\omega_o}\sec^2\theta_3}{\left(\omega_o L_V + \frac{Z_o}{2}\tan\theta_3\right)^2}\right]\frac{\omega_o}{2\ G_{shunt}} \ . \tag{6.7}$$

III. EXPERIMENTAL RESULTS

7. Model 7, Single-Coaxial-Cavity Design Parameters (J. S. Needle, H. W. Welch, Jr.)

The equations necessary for the design of the Model 7 single-coaxial-cavity resonator magnetron are given in the previous section of this report. Design parameters used in the Model 7 tube are listed below. Reference should be made to Fig. 6.1 for a more complete understanding of the quantities given herein. Dwg. Nos. B10,007A, B10,007B, and B10,007C in Appendix A show various forms of the Model 7 structure.

N = 16 anodes

C_A = 4.88$\mu\mu$f (total bar-to-vane capacitance)

L_V = 122.9$\mu\mu$henries (vane inductance — 8 vanes in parallel)

ℓ_1 = 0.3175 cm

ℓ_2 = 1.530 cm

ℓ_3 = 1.848 cm

Z_o = 24.4 ohms (characteristic impedance of the coaxial-line segments)

r_1 = .953 cm (outer radius of inner coaxial-line conductor)

r_2 = 1.428 cm (inner radius of outer coaxial-line conductor)

ℓ_{vane} = 0.762 cm (axial vane dimension)

ℓ_{slot} = 1.021 cm (axial slot dimension)

t_{vane} = 0.1295 cm (vane thickness)

w_{slot} = 0.389 cm (slot width)

ω_o = 13.45 x 10^9 radians/sec (14 cm)

Circuit efficiencies of the order of 90 per cent were predicted on the basis of cold tests made on brass models. Actual tube-circuit efficiencies are listed in Table 8.1 of the next section. The discrepancy between the predicted efficiency and actual circuit efficiencies is attributed to the effects of the cathode circuit on the resonator.

The region of interaction between the electrons and the r-f field is located within the center conductor at its midpoint. For π mode-operation, the bars of the center conductor form one set of anodes and the vanes the other. The design of the interaction space is based on conventional procedures. For the Model 7 tubes the interaction-space parameters are as follows:

λ = 14 cm

N = 16 anodes

r_a = .665 cm = anode radius

r_c = .381 cm = cathode radius

L = .763 cm = length of cathode

r_a/r_c = 1.75 (1.50 has also been used)

E_o = 355 volts

B_o = 286 gauss

where:

$$E_o = \frac{m}{2e}\left(\frac{2\pi c}{n\lambda}\right)^2 r_a^2 \text{ volts} \qquad \left(n = \frac{N}{2}\right) \tag{7.1}$$

$$B_o = \frac{2m}{e}\left(\frac{2\pi c}{n\lambda}\right)\frac{1}{1 - \left(\frac{r_c}{r_a}\right)^2} \text{ webers/meter}^2 . \tag{7.2}$$

Typical operation

E = 3000 volts I = 100 ma

B = 900 gauss P_o = 100 to 150 w

The electronic efficiency, using the values for E and E_o given above, turns out to 88 per cent. The difference between this theoretical electronic efficiency and the electronic efficiencies listed in Table 8.1 is thought to be caused by the effects of cathode unbalance.[1]

Maximum electronic efficiency is given by

$$\eta_e = 1 - \frac{E_o}{E} .$$

8. Performance of the Model 7 (G. R. Brewer, H. W. Welch, Jr.)

The coaxial single-cavity magnetron, designated as the Model 7, utilizes as the resonant circuit a $\lambda/2$ coaxial cavity, with vanes from the outer conductor protruding through slots in the inner conductor (see Section 6).

During the period covered by this report, five tubes, each of different design, have been constructed and tested. One of these tubes was tested twice, using cathodes of two different diameters. Three of these tubes yielded output power in excess of 140 watts, one giving 260 watts.

Table 8.1 summarizes the performance data obtained from the Model 7 tubes to date. Each of these tubes will be discussed briefly.

The Model 7A No. 33, shown in Dwg. No. B10,007A in Appendix A, was constructed with an additional output, coupling to the vane mode. This was for the purpose of studying the effect, on the 14-cm mode, of changes

---

[1] See Section 7 of Technical Report No. 6.

TABLE 8.1

SUMMARY OF MODEL 7 TUBE PERFORMANCE

Tube	Description*	Q_L	Q_o	Q_{ext}	λ_o	B(gauss)	E_b(volts)	I_b(amps)	Max. Mode-Jump Current	P_o Watts	η %	η_c %	η_e %
7A-33	Two output loops. Thoriated tungs. cathode with $\lambda/4$ bypass.	200	460	354	14.05	1390	3100	0.100		105	34	57	60
						1550	3530	0.092	0.100	150	46	57	81
						1940	4780	0.090	0.110	260	60	57	
7B-40	One output. Thoriated tungs. cathode with $\lambda/4$ bypass. r_a/r_c = 1.5 r_a/r_c = 2.1	211	1625	243	13.91	1390	2890	0.070	0.080	15	7.4	87	8.5
		Note: cold-test data taken with a dummy cathode made of solid nickel				1390	3500	0.030	0.030				
7C-41	One output. Oxide-coated cathode with $\lambda/4$ choke and $\lambda/4$ bypass	176	790	226	13.77	1290			0.180				
								Operated pulsed only.					
7D-42	One output. Thoriated tungs. cathode with $\lambda/4$ bypass. Size of coupling loop is double that of all other models.	64.5	658	72	14.59	1390	3400	0.055		102	55	90	61
						1690	4300	0.070		165	55	90	61
						1690	4230	0.060	0.072	146	58	90	65
7E-45	One output. Oxide-coated cathode with small diameter stem. Modified bar-and-vane structure.					1390			0.050				
								Operated pulsed only.					

* All tubes except the Model 7B-No. 40 have an anode-to-cathode ratio of 1.75.

in impedance coupled into the vane mode. The tube used a thoriated tungsten cathode with quarter-wave bypass sleeve on the cathode-support stem. It operated quite satisfactorily, giving up to 260 watts of output power at 60 per cent efficiency, as seen from the performance chart of Fig. 8.1.

Changes in mode-jump current of the 14-cm mode were observed as the impedance presented at the output coupling to the vane mode was changed. It was observed that the mode-jump current was affected when the applied magnetic field was small, i.e., when the mode separation is relatively small; but no effect could be observed for large magnetic fields in which the mode-voltage separation is larger. This tube gave the most satisfactory performance as far as power output and efficiency are concerned. In this tube, $r_a/r_c = 1.75$.

The Model 7B No. 40 yielded up to 146 watts of output power at 58 per cent efficiency, being almost equal to the Model 7A No. 33 at the same magnetic field. This tube was made with a backing ring in the vanes to reduce the vane-mode resonant wavelength, thus increasing mode separation. Two cathodes of different emitting-section diameter were tried in this tube. The performance characteristics are shown in Figs. 8.2 and 8.3, where it is seen that the change in r_a/r_c from 2.1 to 1.5 had very little effect on the operation. It is seen from the two performance charts that mode-jump current is not as high as in the No. 33; the reasons for this reduction are being investigated.

Tubes 7C No. 41 and 7E No. 45 were made with oxide-coated cathodes. It was found that these tubes would not operate satisfactorily under d-c conditions, due to back heating of the cathode and resultant sparking. Pulsed data were taken, however, and the observed mode-jump currents will

FIG. 8.1

PERFORMANCE CHART- COAXIAL SINGLE CAVITY MAGNETRON

FUNDAMENTAL CAVITY MODE $\lambda \approx 14.10$ CM

MODEL 7A NO. 33

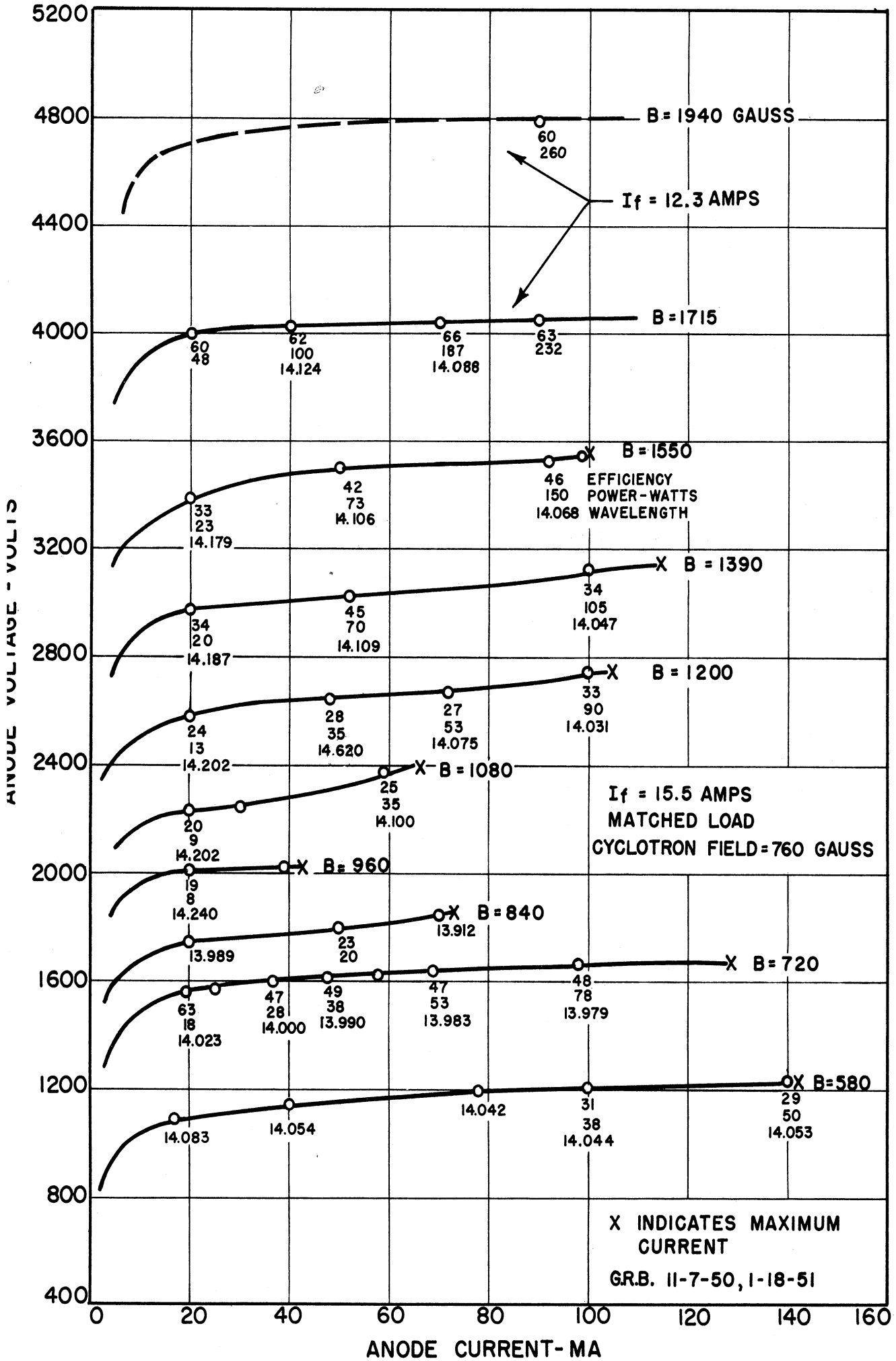

FIG. 8.2

PERFORMANCE CHART - COAXIAL SINGLE-CAVITY MAGNETRON

FUNDAMENTAL CAVITY MODE λ = 14.10 CM

MODEL 7BC18 NO. 40

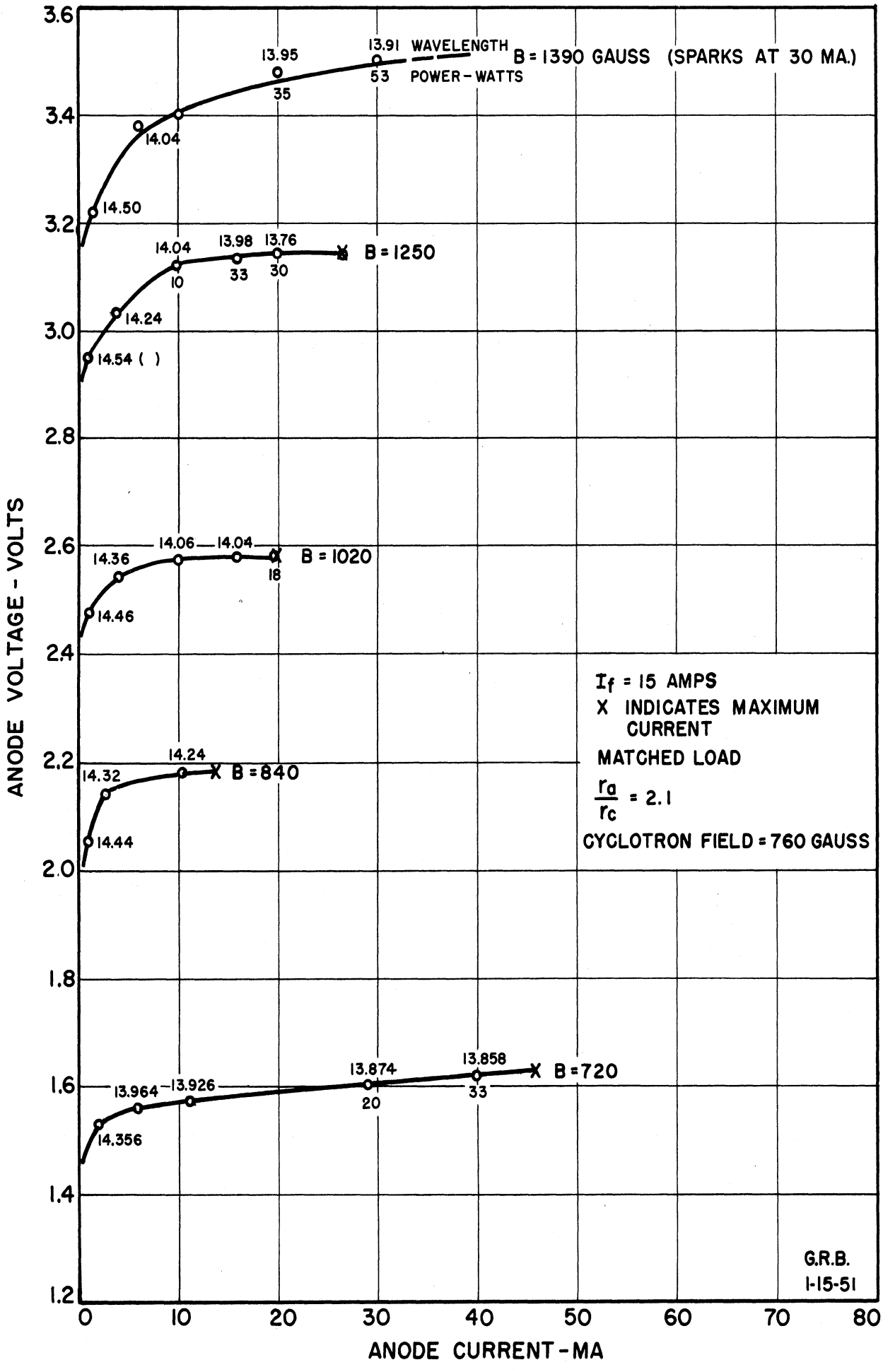

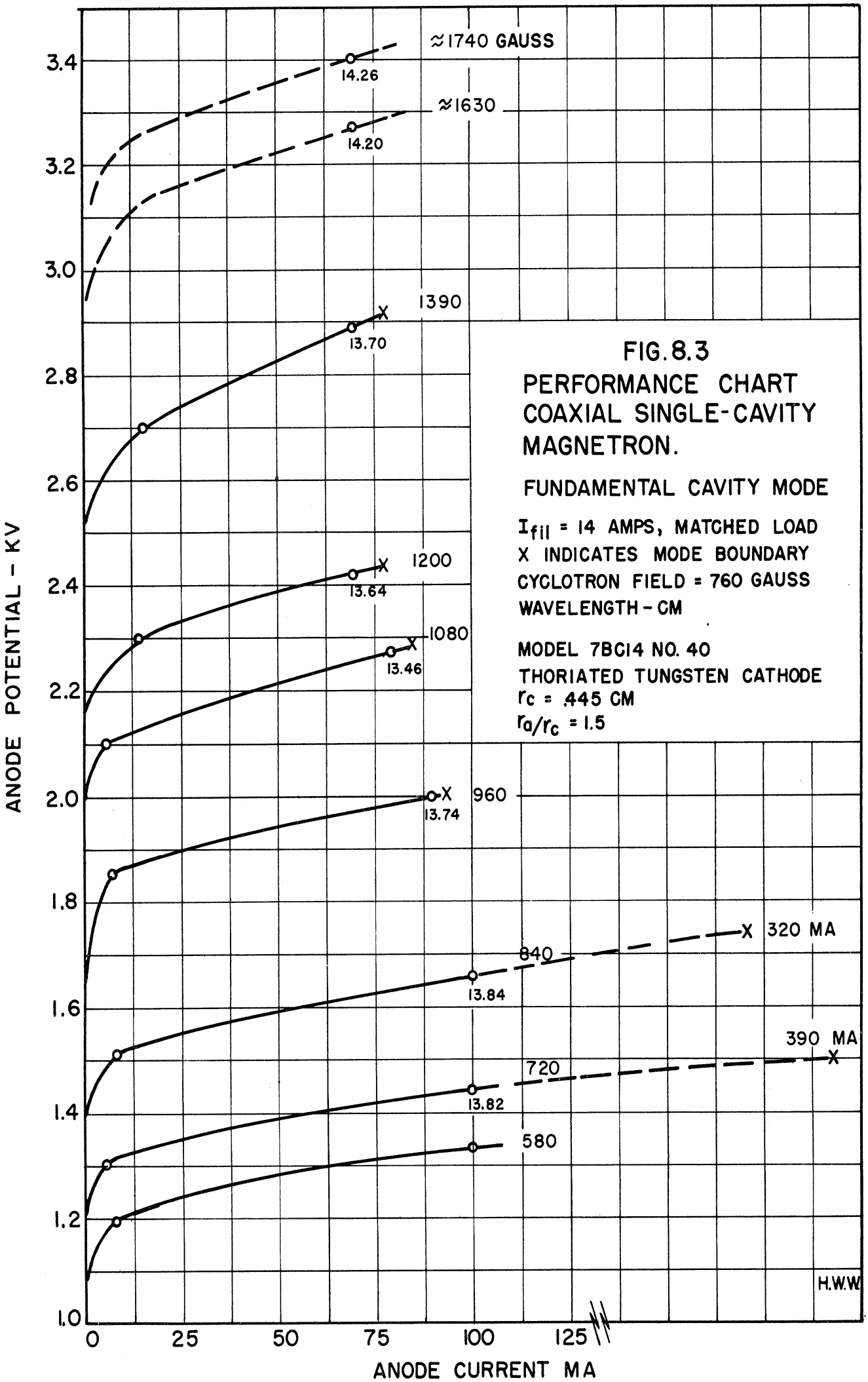

FIG. 8.3
PERFORMANCE CHART
COAXIAL SINGLE-CAVITY
MAGNETRON.

FUNDAMENTAL CAVITY MODE

I_{fil} = 14 AMPS, MATCHED LOAD
X INDICATES MODE BOUNDARY
CYCLOTRON FIELD = 760 GAUSS
WAVELENGTH - CM

MODEL 7BC14 NO. 40
THORIATED TUNGSTEN CATHODE
r_c = .445 CM
r_a/r_c = 1.5

be reviewed below. Most of the Model 7 tubes give similar performance characteristics except for mode-jump current so that this quantity is a good criterion of satisfactory operation.

No. 41 was built to test the effect of the large $\lambda/4$ bypass sleeve on the cathode line. This structure is shown in Dwg. No. B10,007C in Appendix A. The large bypass is intended to prevent completely any leakage of power by way of the cathode line and to provide a high impedance at the anode structure. The maximum mode-jump current obtained from pulsed measurements on this tube was 180 ma at 1290 gauss; this could be increased to 300 ma by unloading the tube with reflectors in the output line. This relatively high mode-jump current (180 ma) would indicate that very satisfactory performance should be expected from this tube when tested d-c with a thoriated tungsten cathode.

Tube No. 45 was built to test a modified vane-and-bar structure conceived for the purpose of equalizing the voltage between the cathode and the anode segments by balancing the capacitances between bars and cathode, and those between vanes and cathode. A drawing of this vane-and-bar structure is shown in radial-plane cross section in Fig. 8.4. It is seen that in the region between planes AA' and BB', the area of vanes exposed to the cathode is equal to the area of the bars exposed to the cathode. As a result of this capacitance balance it was thought that the cathode emitting surface would be at a potential midway between the vanes and bars. The effect of the region of the cathode line outside of the planes AA' and BB' is not, at present, definitely known; this effect will be reduced, however, by the use of a small-diameter cathode-support stem. This tube was operated under pulsed conditions only; the maximum mode-jump current observed was approximately 50 ma at 1390 gauss.

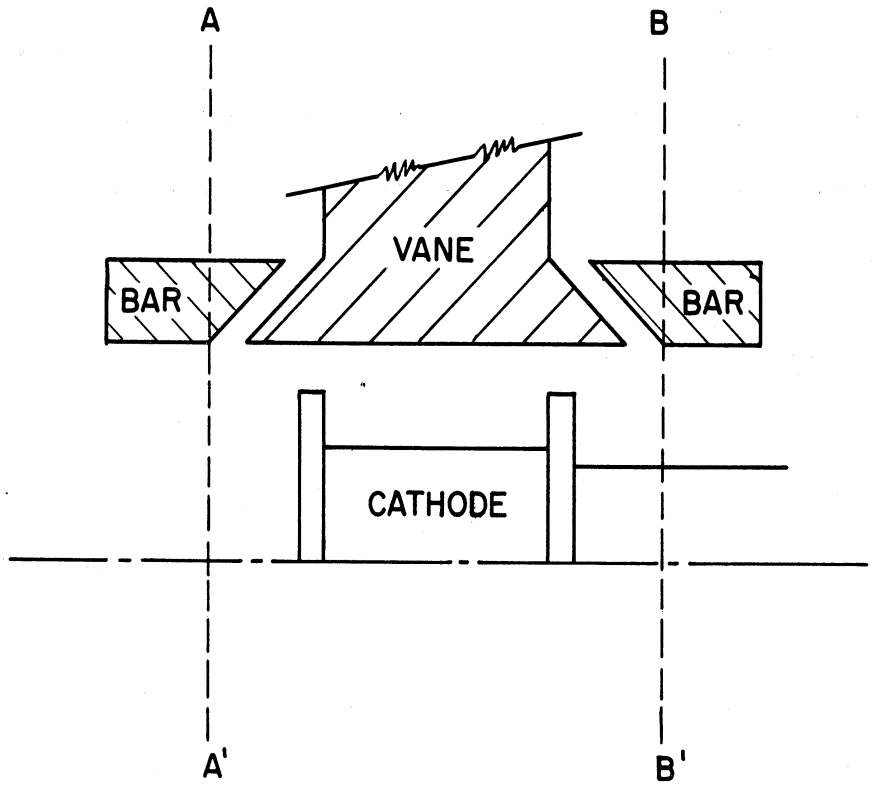

FIG. 8.4

VIEW SHOWING VANE PROTRUDING THROUGH SLOT. MODEL 7E

Model 7D No. 42 was constructed to determine the effect of heavier loading on tube performance. The output-coupling loop was designed with twice the area of the No. 33. This reduced the external Q from 354 on the No. 33 to 72 on the No. 42. It is seen from the performance chart of Fig. 8.5 that the maximum mode-jump current observed was 72 ma at 1690 gauss; a value less than that observed on No. 33. This tube is identical in structure (except for increased coupling) to the Model 7B No. 40. In this tube $r_a/r_c = 1.75$ and a backing ring is included to lower the vane resonant wavelength. Despite the relatively low mode-jump current this tube yielded output power as high as 150 watts for B = 1690 gauss with 58 per cent efficiency.

9. Model 6 F-M Magnetron (H. W. Welch, Jr.)

The Model 6 f-m magnetron has a coaxial resonant cavity, two anode sets, and two cathodes. There are sixteen anodes in the oscillator section and four in the modulator section. The oscillator section is exactly like the basic structure of the Model 7. Resonant wavelength in the desired mode is approximately 13 cm. For this mode, the coaxial cavity is one electrical wavelength long with a voltage maximum at each anode set. The tube is not, at present mechanically tunable; but because of the simplicity of the coaxial cavity, mechanical tuning could be easily accomplished. An assembly drawing is given in the Appendix. The design procedure for the Model 6 is exactly the same as for Model 7 after the anode geometries have been selected. Since the oscillator structure has been discussed in Sections 6 and 7, the remarks in this section will be restricted principally to the modulator section.

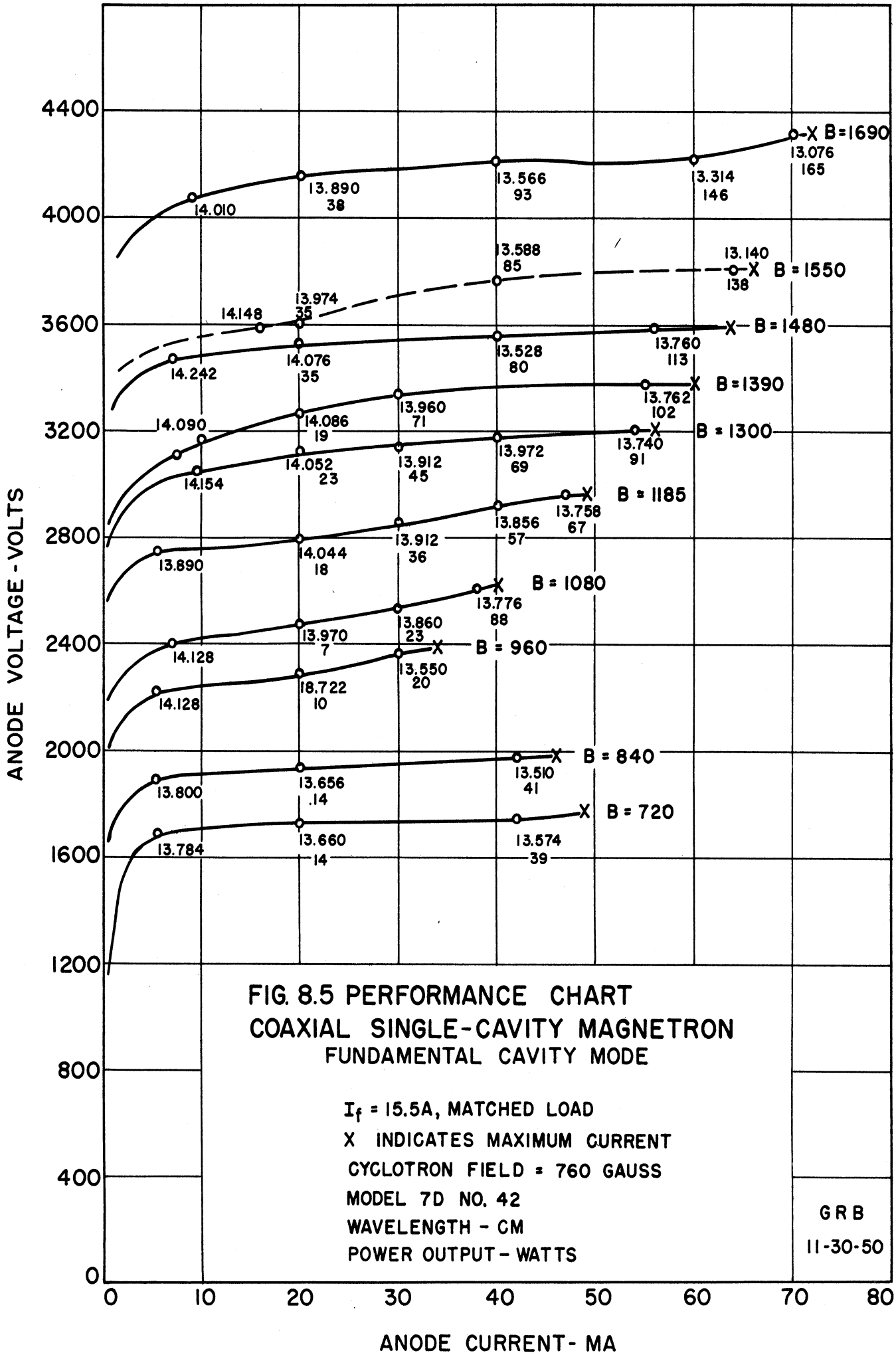

FIG. 8.5 PERFORMANCE CHART
COAXIAL SINGLE-CAVITY MAGNETRON
FUNDAMENTAL CAVITY MODE

I_f = 15.5A, MATCHED LOAD
X INDICATES MAXIMUM CURRENT
CYCLOTRON FIELD = 760 GAUSS
MODEL 7D NO. 42
WAVELENGTH - CM
POWER OUTPUT - WATTS

GRB
11-30-50

The amount of modulation to be expected for a given anode structure can be predicted approximately by the methods given in Technical Report No. 1. The necessary data are given in Table 9.1. Capacitances were calculated from flux plots by the method described in Appendix A of Report No. 6.

The formula for resonance in a half-wavelength cavity corresponding to the modulator half of the cavity is

$$\frac{\lambda}{2\pi c C_A} = \frac{1}{2} Z_o \tan\frac{2\pi \ell}{\lambda} , \qquad (9.1)$$

if the vane inductance is neglected. If C_A is changed by dC_A to produce a wavelength shift $d\lambda$, we may differentiate the above equation to obtain

$$\frac{d\lambda}{\lambda} = \frac{dC_A}{C_A} (1 + 2\,\theta \cos 2\theta)^{-1} , \qquad (9.2)$$

where

$$\frac{dC_A}{C_A} = \frac{\Delta C_c}{C_c} \frac{C_c}{C_A} \qquad (9.3)$$

and c = velocity of light in free space

$\theta = 2\pi\ell/\lambda$

ℓ = distance from vane to short circuit of coaxial cavity

C_c = capacitance to cathode surface

C_A = total modulator-anode capacitance

$\frac{\Delta C_c}{C_c}$ = percentage change in cathode capacitance caused by the space-charge swarm.

TABLE 9.1

MODEL 6 DESIGN DATA
(Dimensions in inches)

	N	r_a	r_c	C_A	C_c/C_A	E_o	B_o
Oscillator Section	16	.524	.300	4.88 $\mu\mu$f	----	355 volts	286 gauss
Modulator Section	4	.420(No.26) .450(No.31)	.300	1.36 $\mu\mu$f	5.51%	4200 volts 4800 volts	1680 gauss 1480 gauss

In an ordinary lumped-constant resonant circuit, Eq 9.2 has the form

$$\frac{d\lambda}{\lambda} = \frac{1}{2}\frac{dC_A}{C_A} \quad . \tag{9.4}$$

This may be written

$$\frac{d\lambda}{\lambda} = \frac{1}{2}\frac{dU}{U} \quad , \tag{9.5}$$

where U is the energy stored in the electric field. The modifying factor $F(\theta) = (1 + 2\theta \cos 2\theta)^{-1}$ in Eq 9.2 replaces the factor 1/2 of Eq 9.4 because all the electrical energy storage is not in the capacitance. This factor is plotted in Fig. 9.1. A substantial part of the energy is stored in the cavity in the coaxial-type magnetron.[1] In some cases this is not true, e.g., in the interdigital magnetron operating in the zero-order mode. In any distributed-constant circuit one must be careful in calculation of the effect of a capacitance change not to overestimate the resulting wavelength shift.

Eq 9.2 is only valid for a half-wavelength coaxial cavity loaded in the center by the modulator capacitance. If we include the other half of the cavity and the vane inductances, a simple relationship for the wavelength shift cannot be derived. It is, of course, possible to use the complete design formula and plot a curve of wavelength versus any one of the parameters. However, a reasonable approximation is made by assuming half of the energy storage to be in the oscillator half of the cavity. Then for the complete f-m magnetron

---

[1] See Eq 6.7.

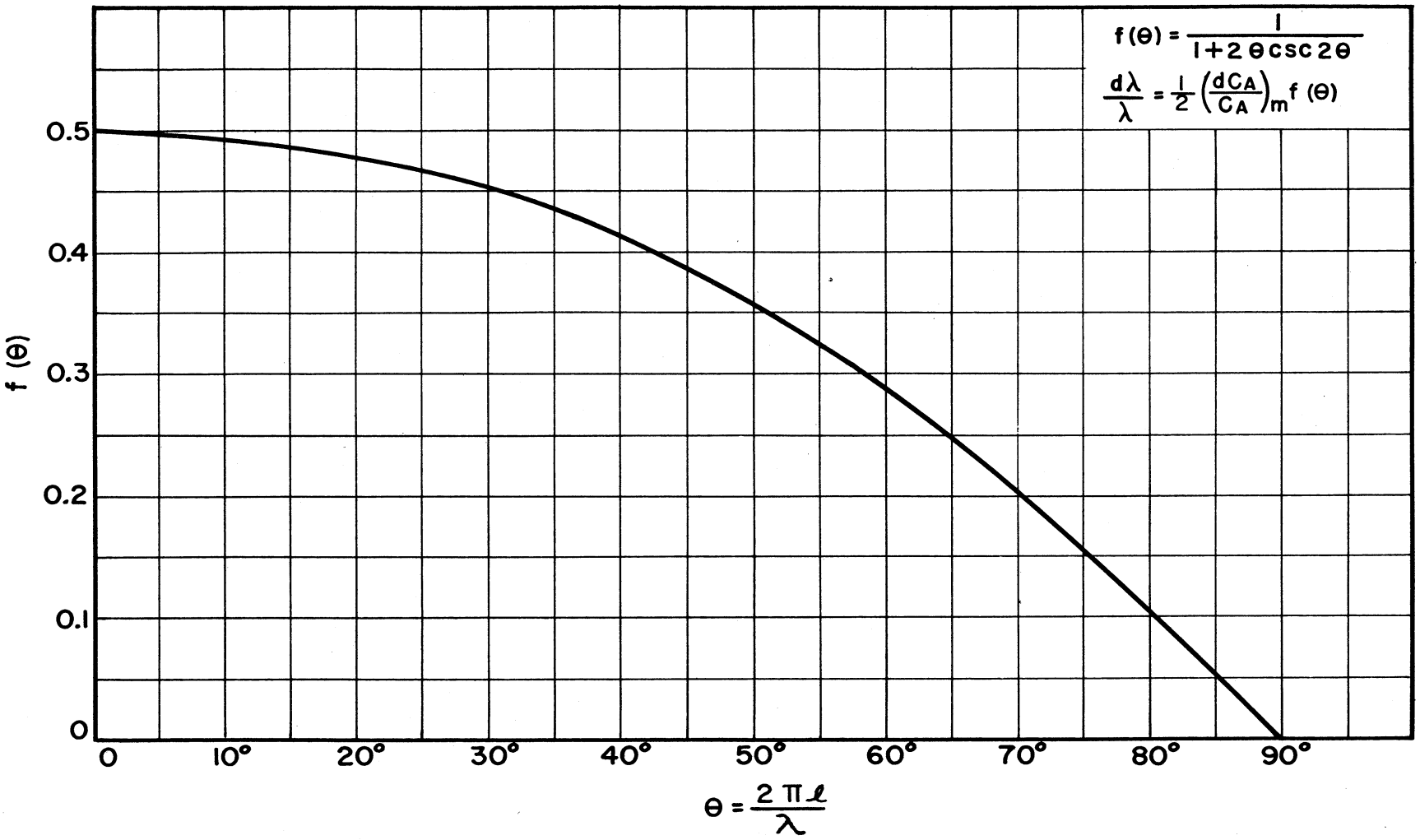

FIG. 9.1 FACTOR USED IN CALCULATING WAVE-LENGTH SHIFT IN MODEL 6

$$\frac{d\lambda}{\lambda} = \frac{1}{2}\left(\frac{dC_A}{C_A}\right)_m (1 + 2\theta \csc 2\theta)^{-1} , \qquad (9.6)$$

where $(dC_A/C_A)_m$ represents the change in the modulator capacitance and θ is the electrical-line length from vane to short circuit in the modulator half of the cavity.

This formula has been applied to a particular experiment where

$C_c/C_A = 5.51\%$

$\theta = 65°$

$\Delta C_c/C_c = 123\%$ for the maximum r_H/r_c used in the experiment,

where r_H/r_c is the ratio of the space-charge-swarm radius to cathode radius in the modulator interaction space. r_H/r_c is obtained from Eq 5.13 in Technical Report No. 1 (Eq 6 in Technical Report No. 4) and $\Delta C_c/C_c$ is given approximately by the following

$$\frac{\Delta C_c}{C_c} = \frac{\log r_a/r_c}{\log r_a/r_H} - 1 . \qquad (9.7)$$

(This is Eq 7.5 in Report No. 1 or 40 in Report No. 4.) The results of this calculation are compared with experimental results in Fig. 10.3. Actually, the reasonably good check on the results is probably, in part, accidental, since the stem of the modulator cathode is known to have an important effect on the resonant circuit and was not accounted for in calculation of C_c/C_A. Also, the measured magnetic field, 1400 gauss, is theoretically not quite large enough to make the space-charge swarm a totally reflecting medium.

The experimental work on the Model 6 magnetron was discontinued after about June 1 in order to give more attention to the voltage-tuning

problem and to attempt, through experiments on the Model 7 magnetrons, to obtain a better understanding of the problem of coupling to the cathode and the maximum-current-boundary limitation. These are the most pressing problems in the Model 6 design since, although the oscillator section of the tube performs satisfactorily without the modulator cathode (150 to 200 watts C-W at about 50 per cent efficiency), the insertion of the modulator cathode immediately limits operation by reducing the maximum-current boundary to very small values or even zero. The modulation tests could only be made under special loading conditions. The facts gathered from tests on the Model 6 do indicate that between 1 and 5 per cent frequency modulation can be obtained; a completely redesigned tube will be built as soon as possible. The following changes will probably be made:

a. The modulating voltage required in the present structure is excessive. This can be reduced by reducing the cutoff voltage in the modulator section. Using the data in Table 9.1, the cutoff voltage at 1400 gauss is 2950 volts. For a wavelength shift of greater than 1 per cent about 2500 volts are required. Cutoff voltage is given by

$$\frac{E}{E_o} = \left(\frac{B}{B_o}\right)^2 \tag{9.8}$$

or

$$E = \frac{e}{8m} B^2 r_a^2 \left(1 - \frac{r_c^2}{r_a^2}\right)^2 \tag{9.9}$$

Thus, if r_a/r_c is kept constant, E is proportional to r_c^2. The modulator should therefore be designed with as small as practical a cathode for minimum modulating voltage.

b. The coupling to the cathode is probably encouraged by the special design of the modulator anodes. By sacrificing a little of the predicted modulation possibility the anode design can be changed to make coupling to the cathode less. It should still be possible to get 1 or 2 per cent modulation. It also should be possible to reduce the leakage current (see Fig. 10.3).

c. In order to increase relatively the energy storage in the modulator capacitance it will be advantageous to decrease energy storage in other parts of the circuit.

The tube also needs to be made mechanically tunable. This will not be attempted until it has been demonstrated that power output is available with greater than 1 per cent modulation.

10. Performance of Model 6 F-M Magnetron (H. W. Welch, Jr., G. R. Brewer)

Eight tubes of the Model 6 design have been constructed. Of these, five were operated under oscillating conditions and two of the latter were modulated in frequency by the modulator space charge. In all these tubes considerable difficulty was experienced with power leakage out the modulator cathode line. This additional loading was usually sufficient to prevent oscillation unless the tube was unloaded from the output line. This effect is illustrated by the Model 6, No. 31, which oscillated very feebly only when no power was coupled out the output line. However, modulation data were obtained from this tube as shown in Fig. 10.1. It is seen that a wavelength shift of 0.07 cm or 0.5 per cent was obtained. The modulator cathode was removed from this tube, and Fig. 10.2 shows a performance chart of the tube as an oscillator only. It is seen that output power as high as 190 watts with 40 per cent efficiency was obtained.

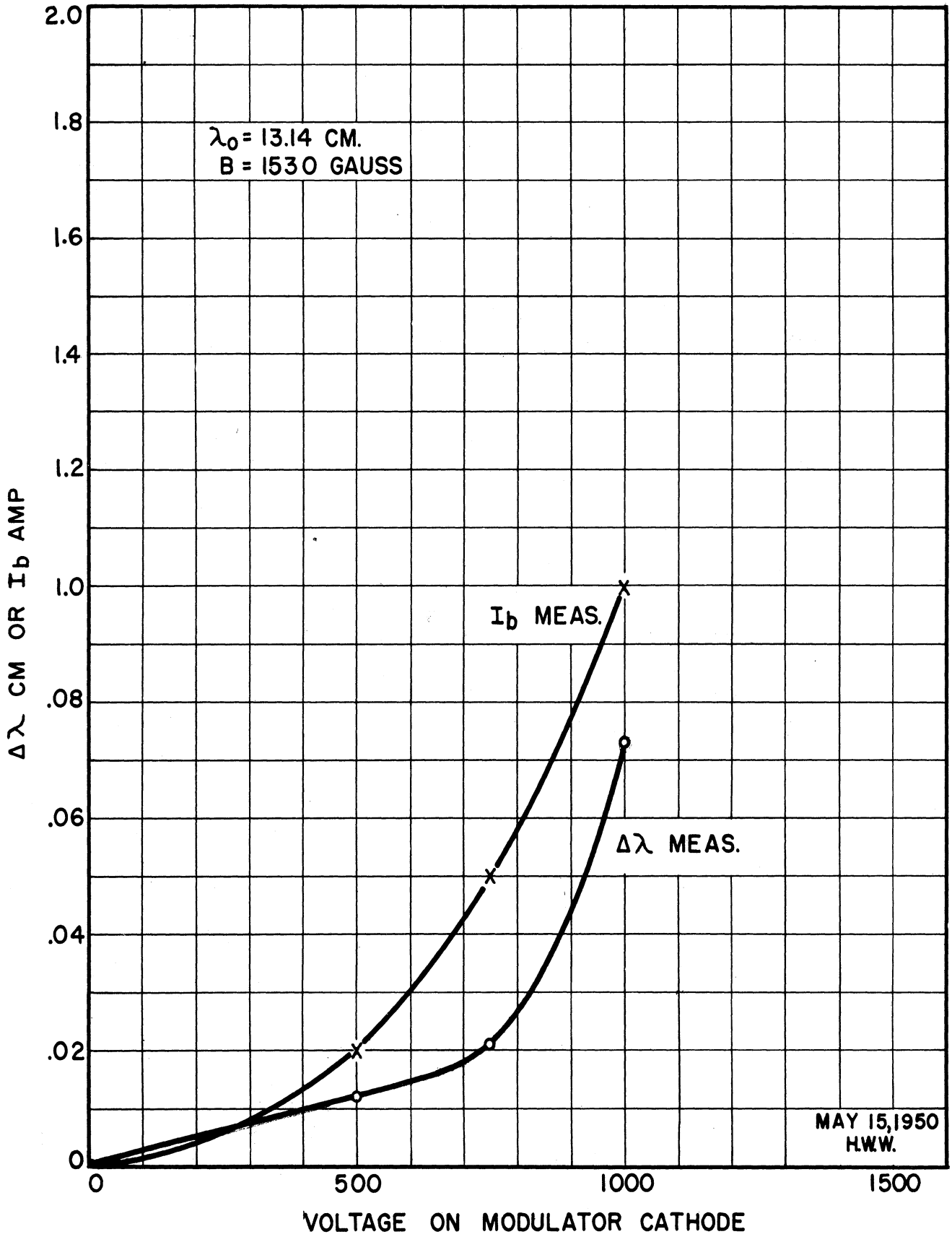

FIG. 10.1 MODULATION DATA ON MODEL 6 #31

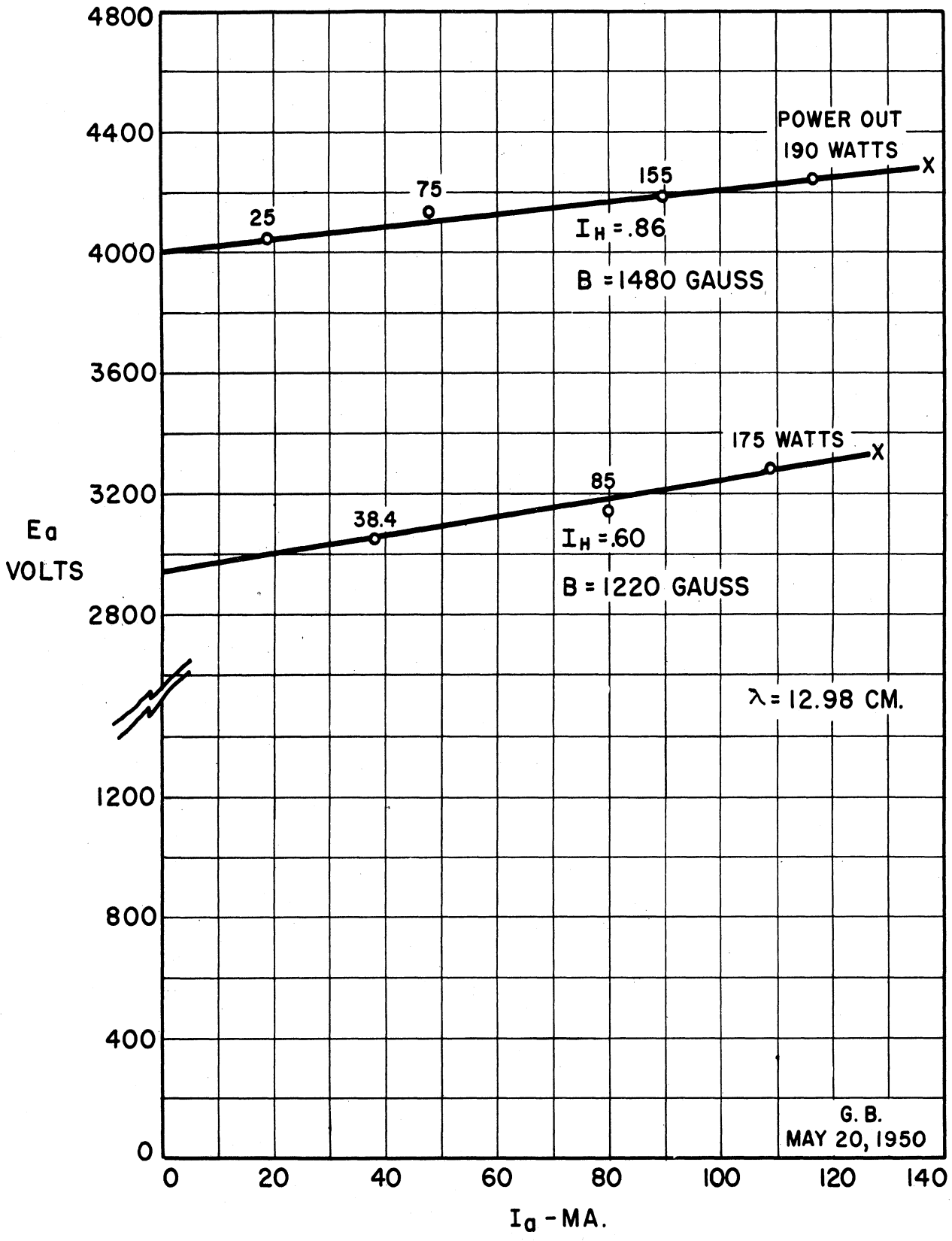

FIG. 10.2 PERFORMANCE DATA MODEL 6 NO. 31
WITHOUT MODULATOR CATHODE

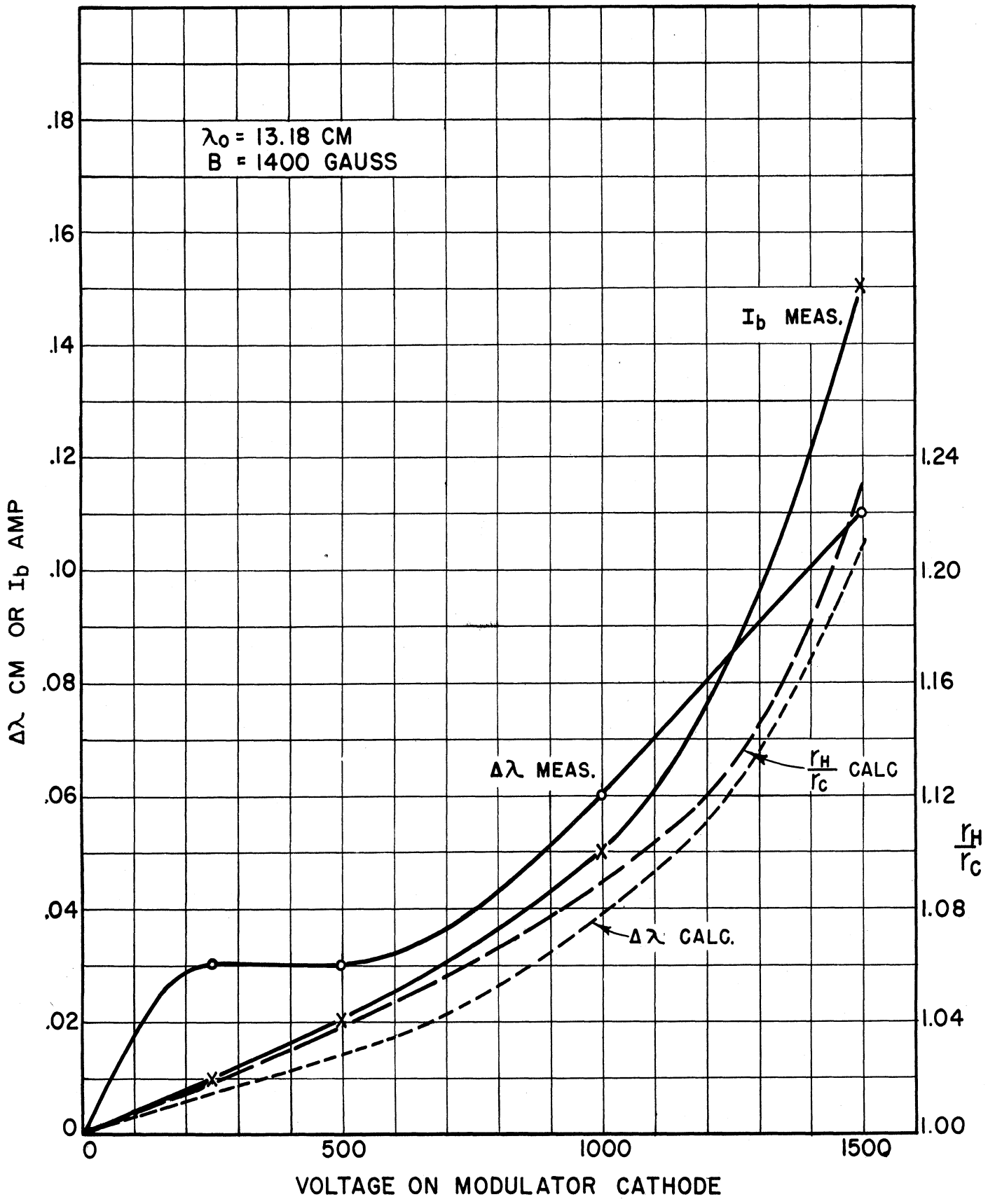

FIG. 10.3 MODULATION DATA ON MODEL 6 #26

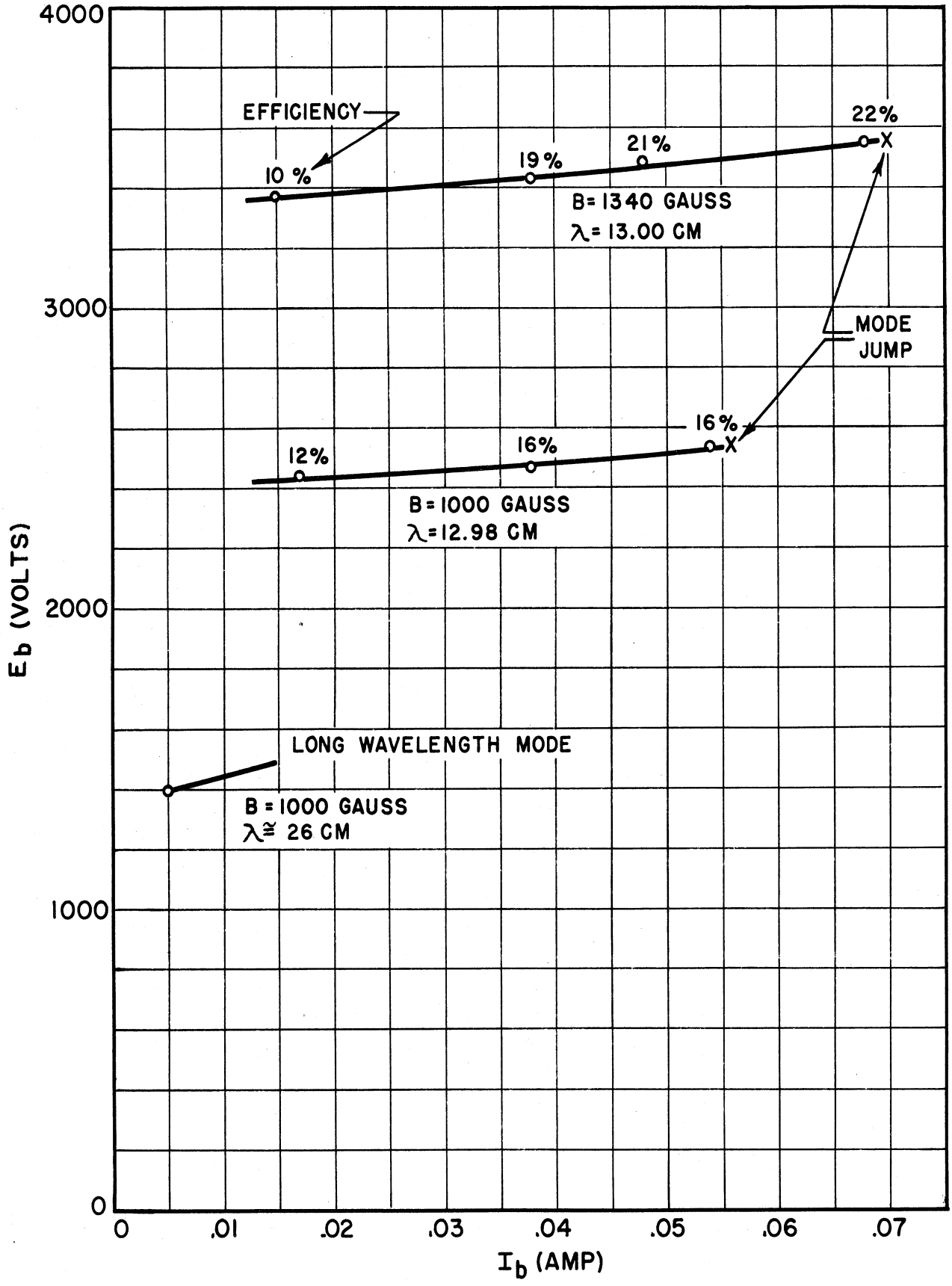

FIG. 10.4 PERFORMANCE CHARACTERISTICS MODEL 6 #26

MODULATOR CATHODE IS REMOVED

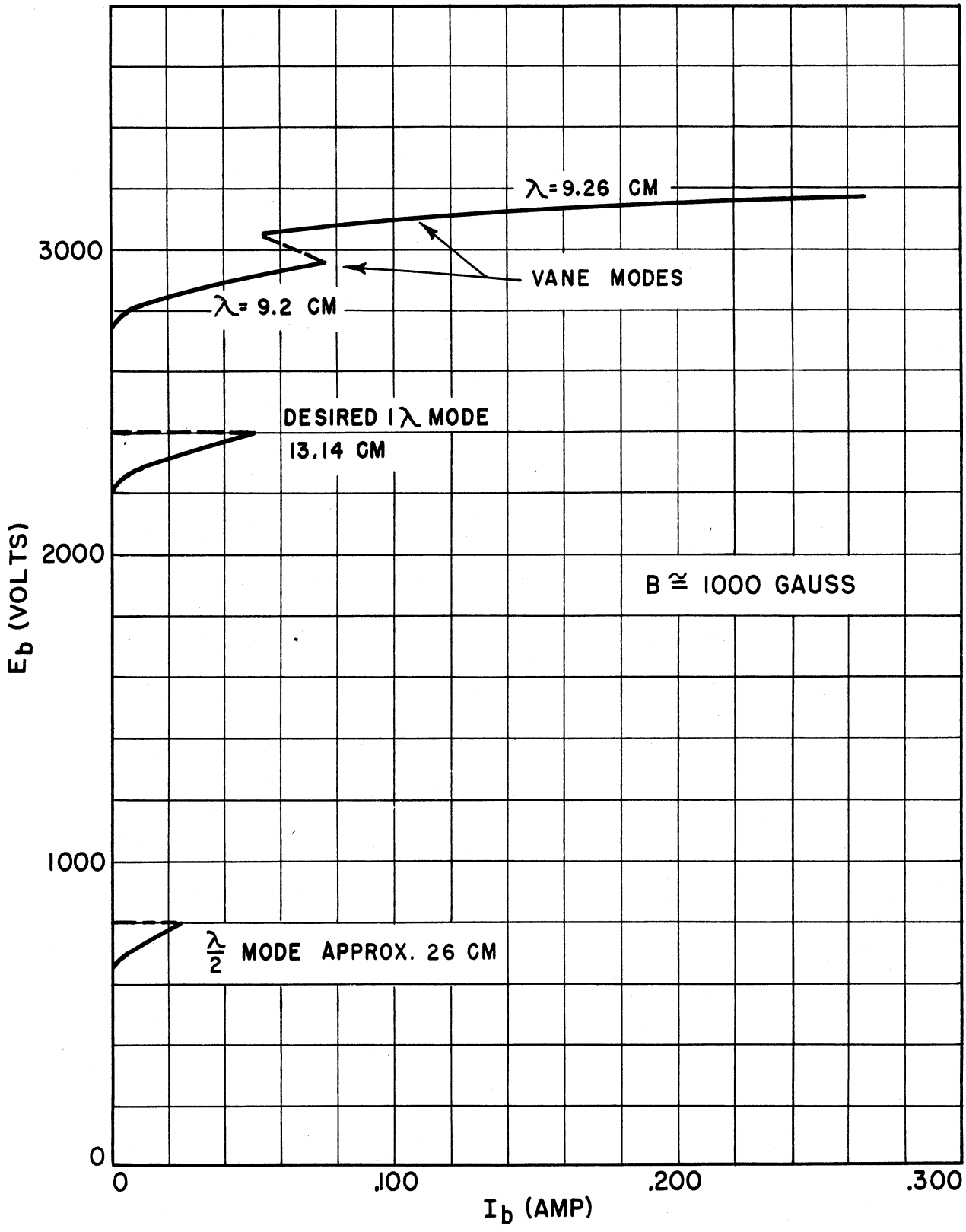

FIG. 10.5 VOLT-AMPERE CHARACTISTIC PULSED MODEL 6 #31

MODULATOR FILAMENT LEAD SEALS ARE SHIELDED. MAIN CATHODE SEAL IS NOT SHIELDED. THE 13.14 CM MODE DOES NOT APPEAR WITHOUT SHIELDS.

The Model 6, No. 26, yielded similar data. The modulation data for this tube are shown in Fig. 10.3, from which it is seen that the maximum wavelength shift is 0.11 cm or 0.85 per cent. Thesedata also show, for comparison, predicted values of r_H/r_c and $\Delta\lambda$. After removal of the modulator cathode this tube was operated C-W, and the performance chart of Fig. 10.4 was obtained.

After the problem of power leakage out the modulator cathode line was encountered, it was decided to carry on the development with the Model 7, which has the same oscillator section, and study the problems of cathode leakage and mode jump, etc., without the complication of the modulator section. This work is being carried out at present (see Section 8).

The nearest interfering mode is the 9.2-cm vane mode shown in a characteristic taken from pulse data in Fig. 10.5. In the first Model 6 this mode was at 10.96 cm, and the tube jumped directly from the 13-cm mode to the 10.96 mode. The backing ring, which is now included to shorten the vanes, shifts the vane mode to 9.2 cm, and the tube jumps out of oscillation before starting in the shorter-wavelength mode. It is believed, therefore, that mode competition is not responsible for the low maximum-current boundary in this tube. The long-wavelength mode occurringat low voltage is not troublesome.

11. Model 8 Double-Anode-Set Interdigital Magnetron (J. R. Black, H. W. Welch, Jr.)

The Model 8 double-anode magnetron was conceived as a structure adaptable to f-m use. Due to difficulties encountered in the Model 5 and Model 6 f-m magnetrons, a stronger emphasis was placed on the study of the Model 8 structure in the latter part of 1950. A photograph and assembly

drawing of the Model 8 are shown in Fig. 11.1 and in Dwg. No. B10,008 in Appendix A. It is essentially a capacity-loaded full-wavelength rectangular cavity having two sets of interdigital anodes, each placed at a voltage maximum. The structure would form an f-m magnetron if one set of anodes were designed as an oscillating magnetron and the other to form a variable reactance. It is apparent that the power output of such a structure, having both sets of anodes designed as oscillating magnetrons, would be considerably greater than that derived from a single-cathode structure. It is believed that extremely high-power magnetrons might be developed by lengthening the cavity and employing several sets of anodes and cathodes.

A sketch of a brass Model 8 cavity for cold testing is shown in Fig. 11.2. The ratio of length to width of the cavity was made exactly 2 to 1 in an attempt to eliminate complex resonances observed in an earlier cavity. (See Section 13C of Final Report, Technical Report No. 3.) The brass model was built with the same anode design as used in the Model 4 magnetron. The field was determined by inserting a small probe through the seven holes evenly spaced along one side of the cavity. Fig. 11.3 shows the field patterns observed by means of the probe for the zero, first, second, and third-order modes. The two shaded areas indicate the positions of the two sets of anodes. The desired mode for this model is the first-order mode at 16.08 cm; however, the zero and second-order modes could be suppressed by short circuiting them in the center of the cavity where the desired mode has a node.

A working model of this structure was constructed from the data obtained from this cold model. A new interaction-space design was used in

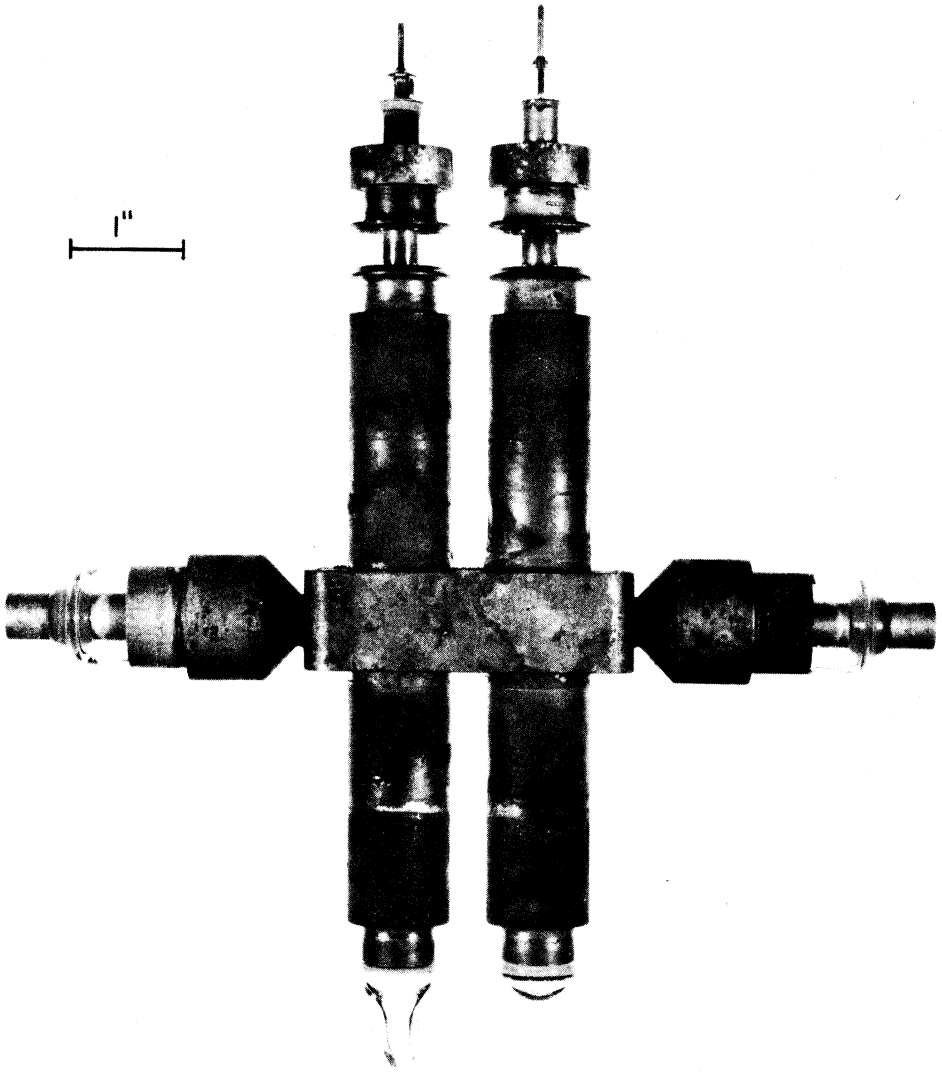

FIG. II.1 MODEL 8 NO. 36 DOUBLE ANODE MAGNETRON

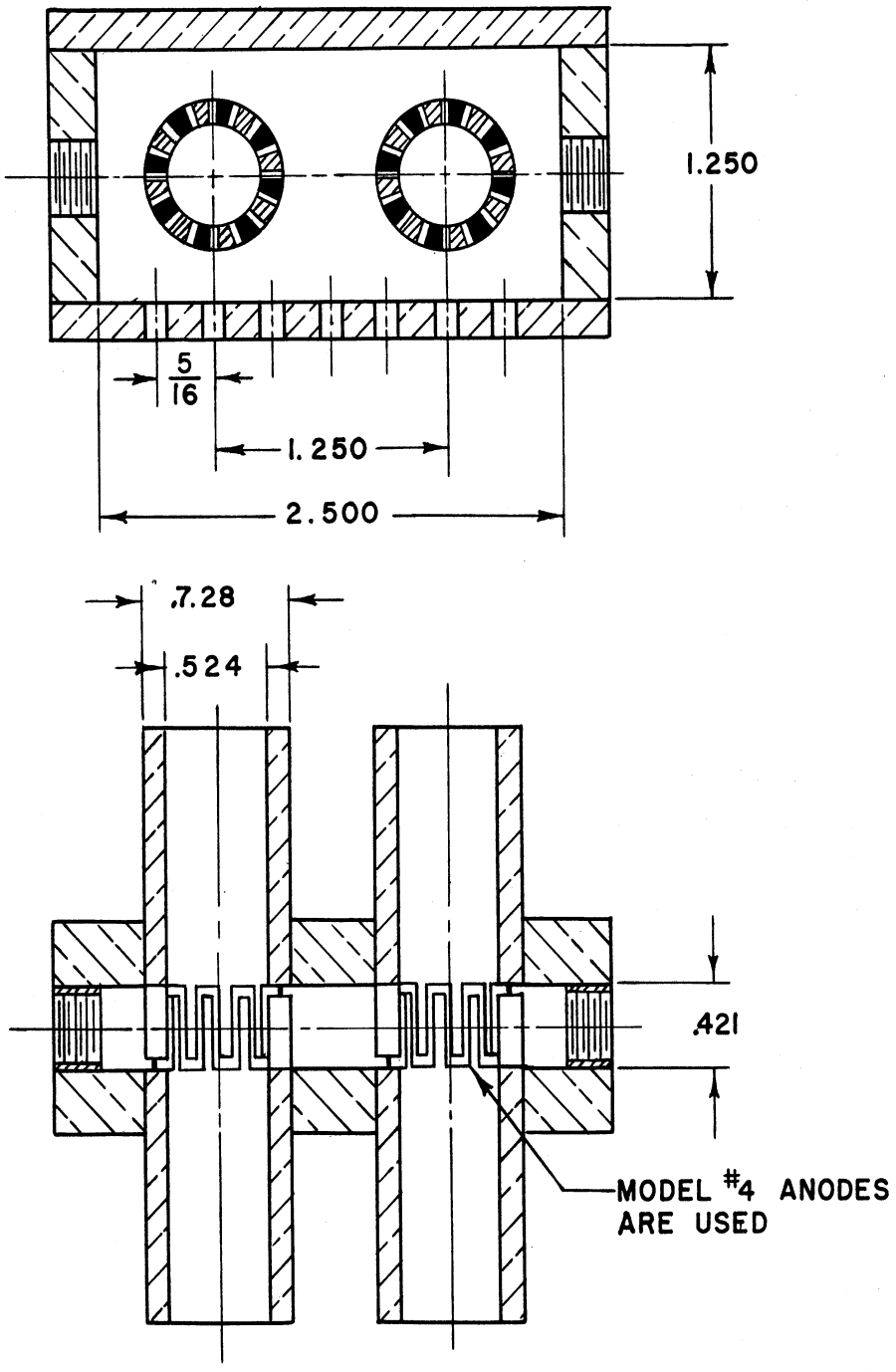

FIG. 11.2 SKETCH OF MODEL #8 MAGNETRON USED FOR COLD TEST

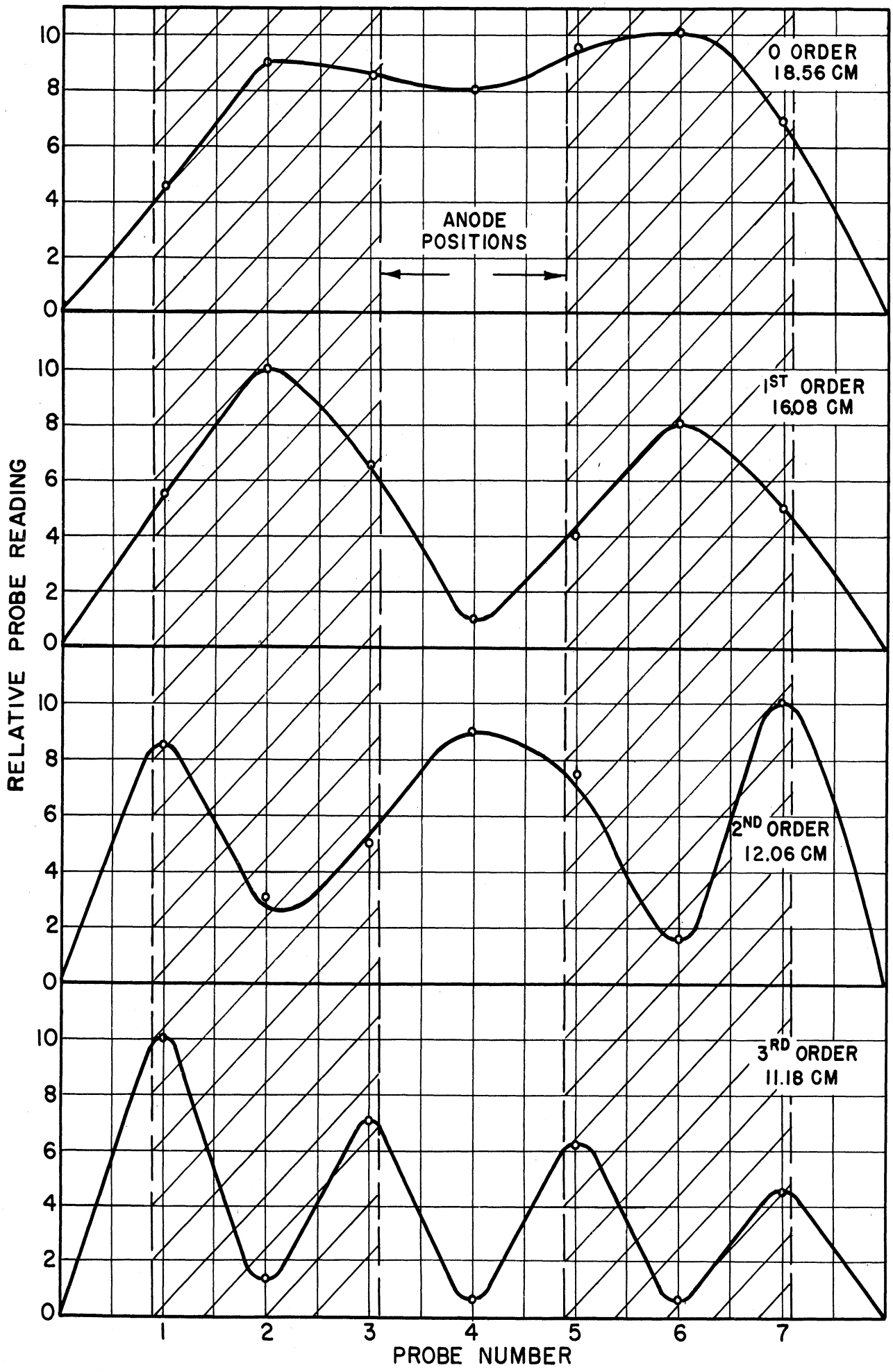

FIG 11.3 RESONANCES IN RECTANGULAR CAVITY MAGNETRON

the hot model which would be more efficient than that used in the cold model and in Models 4,5, and 6. An attempt was made to scale the frequency to 13 cm on the hot model.

The following are design parameters used for the Model 8 tube. For symbols used, see Fig. 11.4.

r_a	—	.45 cm	cavity	—	3 x 6 cm
r_c	—	.30 cm	h	—	1.02 cm
r_a/r_c	—	1.5	ℓ	—	.90 cm
L	—	.724 cm	d	—	.089 cm
R_a	—	.762 cm	N	—	16
			C_A	—	4 $\mu\mu$f

In this tube both sets of anodes were designed as oscillatory structures in order to check the possibility of push-pull (or parallel) type of operation as well as f-m features of the structure.

Due to the fact that probes could not be inserted within the hot model, it was most difficult to determine the exact frequency of operation before the cathodes were sealed. The chokes were therefore designed to operate at the expected 13-cm wavelength. Two output loops were used to facilitate cold tests.

Because of the close spacing of the cathode glass seals to one another in Model 8, the tube was designed so the glass seals could be made by means of an induction heater. Stainless-steel spacers were utilized to align the cathodes accurately within the interaction space.

Performance results of this tube are given in the next section.

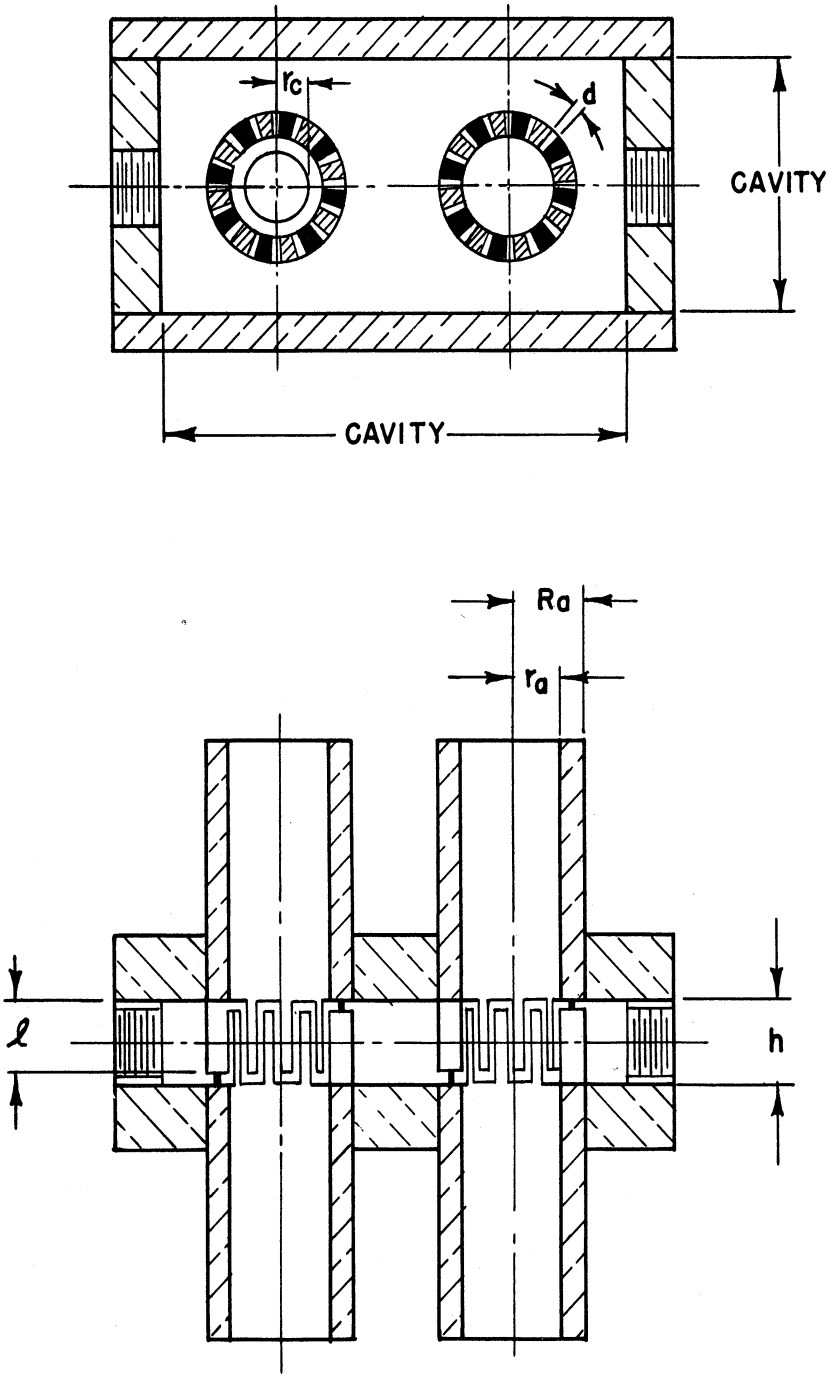

FIG. II.4
SKETCH OF MODEL #8 MAGNETRON

12. Performance of Model 8 Magnetron (J. R. Black, H. W. Welch, Jr.)

Model 8, Tube No. 36 was constructed using the design parameters discussed in Section 11 of this report. The operation of this model indicated clearly that the two sets of anodes lock in on the same frequency, and the power input to the structure is approximately double that of a single tube. Figs. 12.1, 12.2, and 12.3 show voltage-current curves of the tube for these different magnetic fields under pulsed conditions. Curves are plotted for each anode operating individually as well as both of them operating in parallel. These curves were taken from an oscilloscope with a voltage scale approximately 330 volts per division. Fig. 12.4 is a d-c voltage-current plot of the tube operating in a magnetic field corresponding to that in Fig. 12.2. All the above curves were taken with a load placed on only one of the two output connections.

As the above curves indicate, the tube did not operate in the expected 13-cm mode; preliminary cold tests of this model indicate that the desired first-order mode is at 16.9 cm and therefore would not operate with cathode chokes designed for 13 cm.

A crack developed under test in one of the cathode seals, limiting further tests; however, extensive study of this tube is being planned for the immediate future including f-m as well as the parallel-operation feature.

The operating characteristics of this type of structure indicate that it holds great promise for the development of high-power magnetrons. A geometry consisting of a wave guide bent to form a ring having several sets of anodes and cathodes would probably be a desirable form for a high-powered tube.

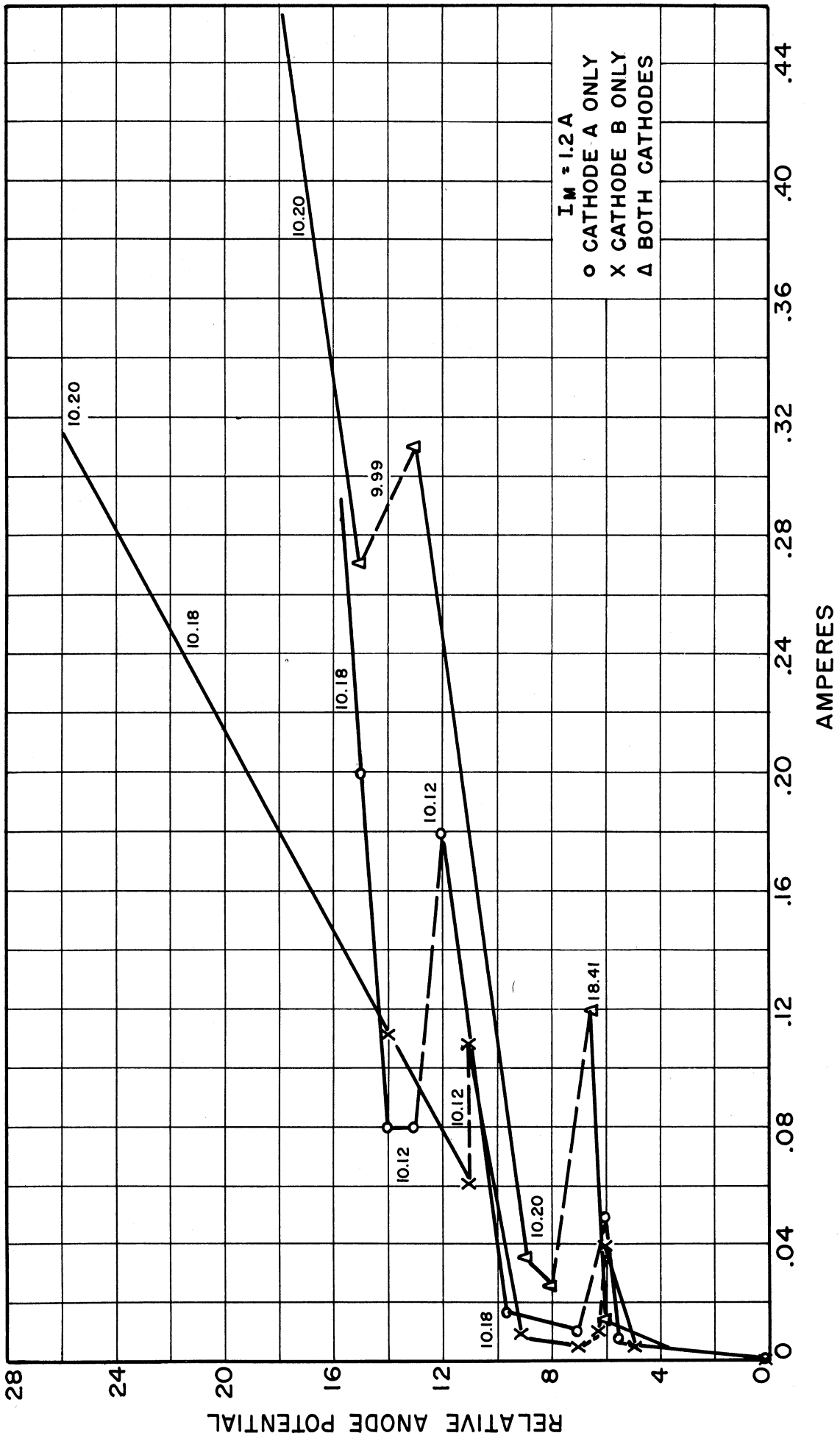

FIG. 12.1
PERFORMANCE CHARACTERISTICS MODEL 8 #36 (PULSED)
FROM OSCILLOSCOPE SCREEN, VERTICAL SCALE APPROX. 330 V/UNIT

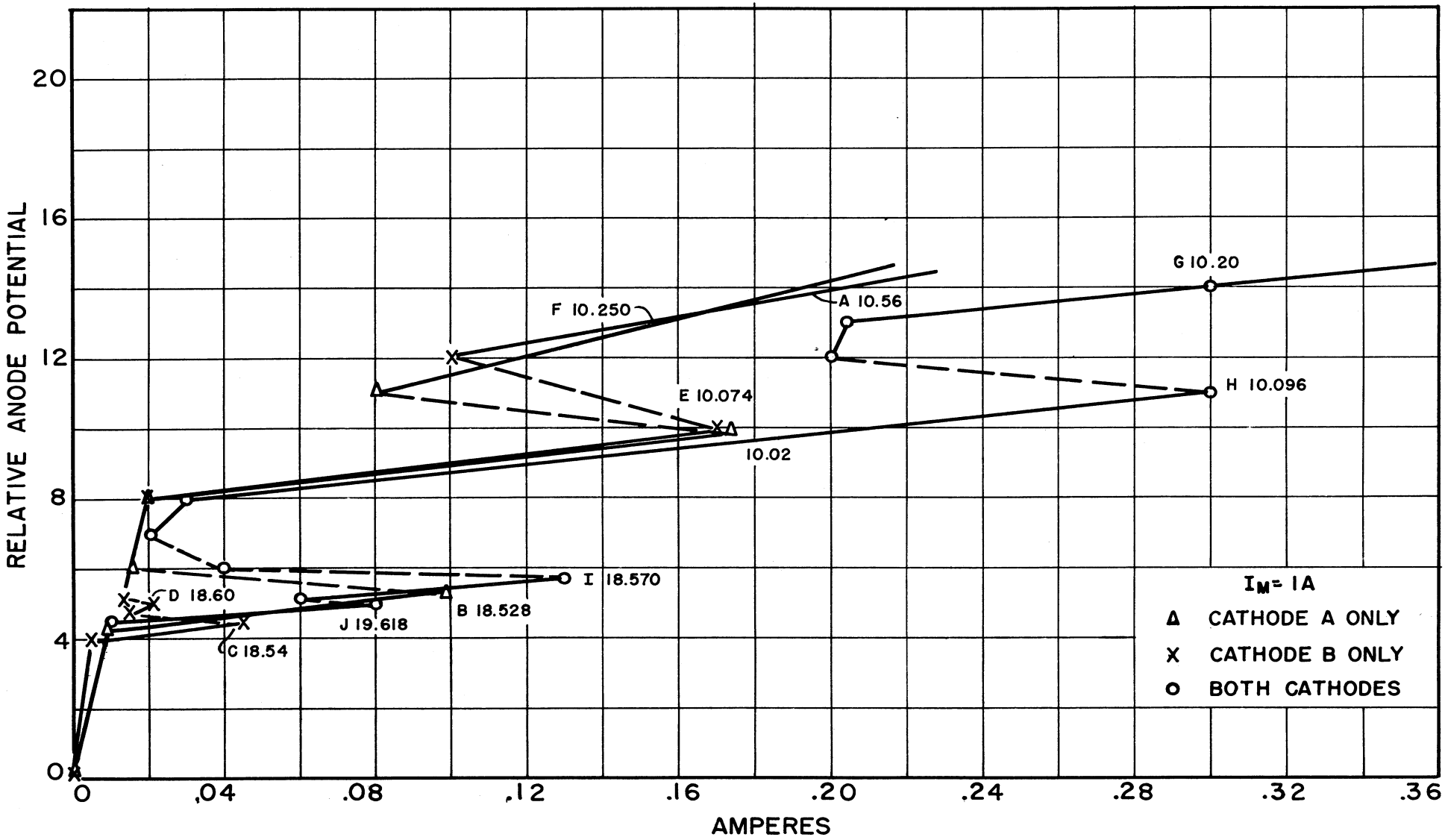

FIG. 12.2

PERFORMANCE CHARACTERISTICS MODEL 8 #36 (PULSED)

FROM OSCILLOSCOPE SCREEN. VERTICAL SCALE APPROX. 330 V/UNIT

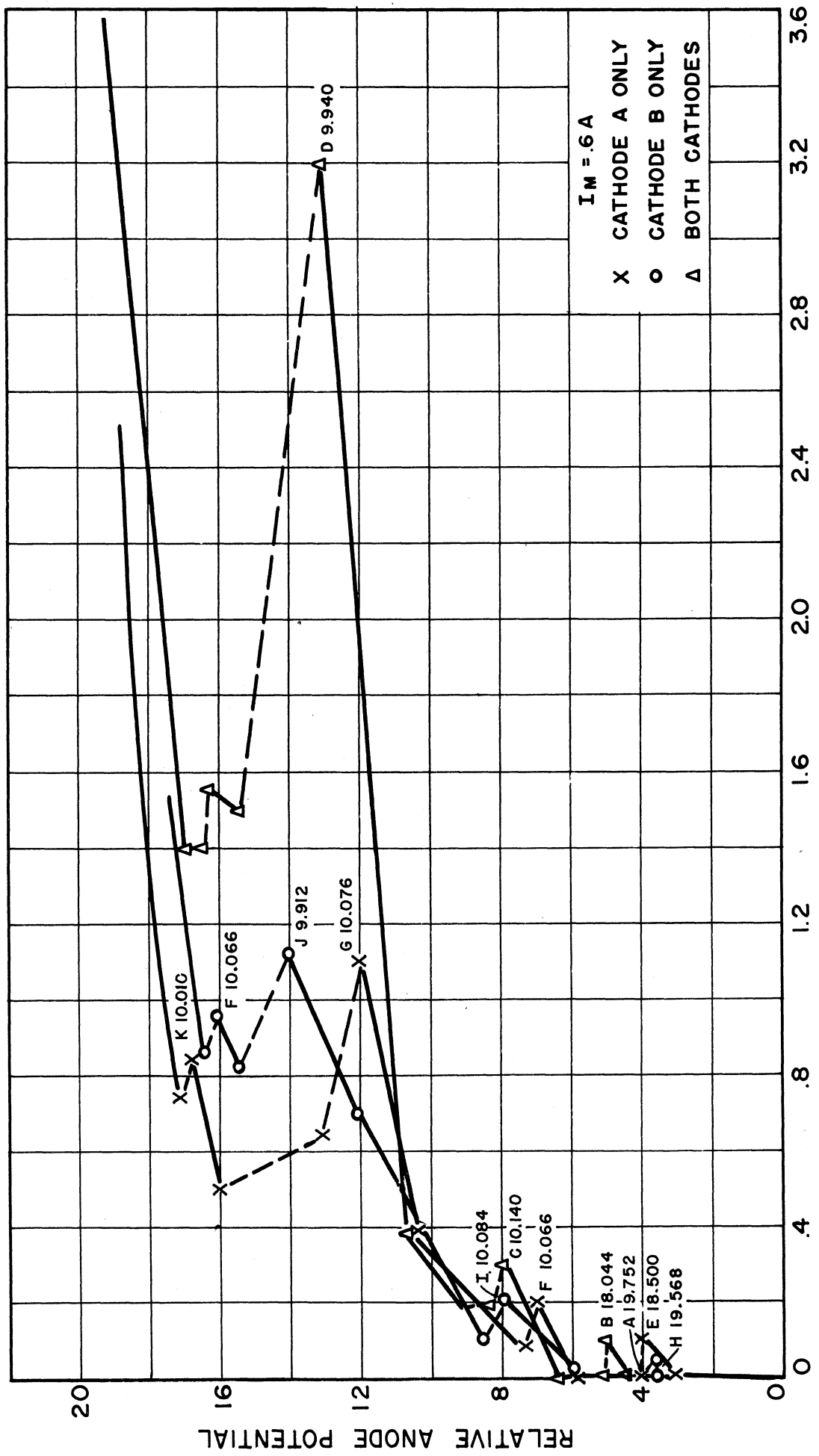

FIG. 12.3
PERFORMANCE CHARACTERISTICS MODEL 8 #36 (PULSED)
FROM OSCILLOSCOPE SCREEN. VERTICAL SCALE APPROX. 330 V/UNIT

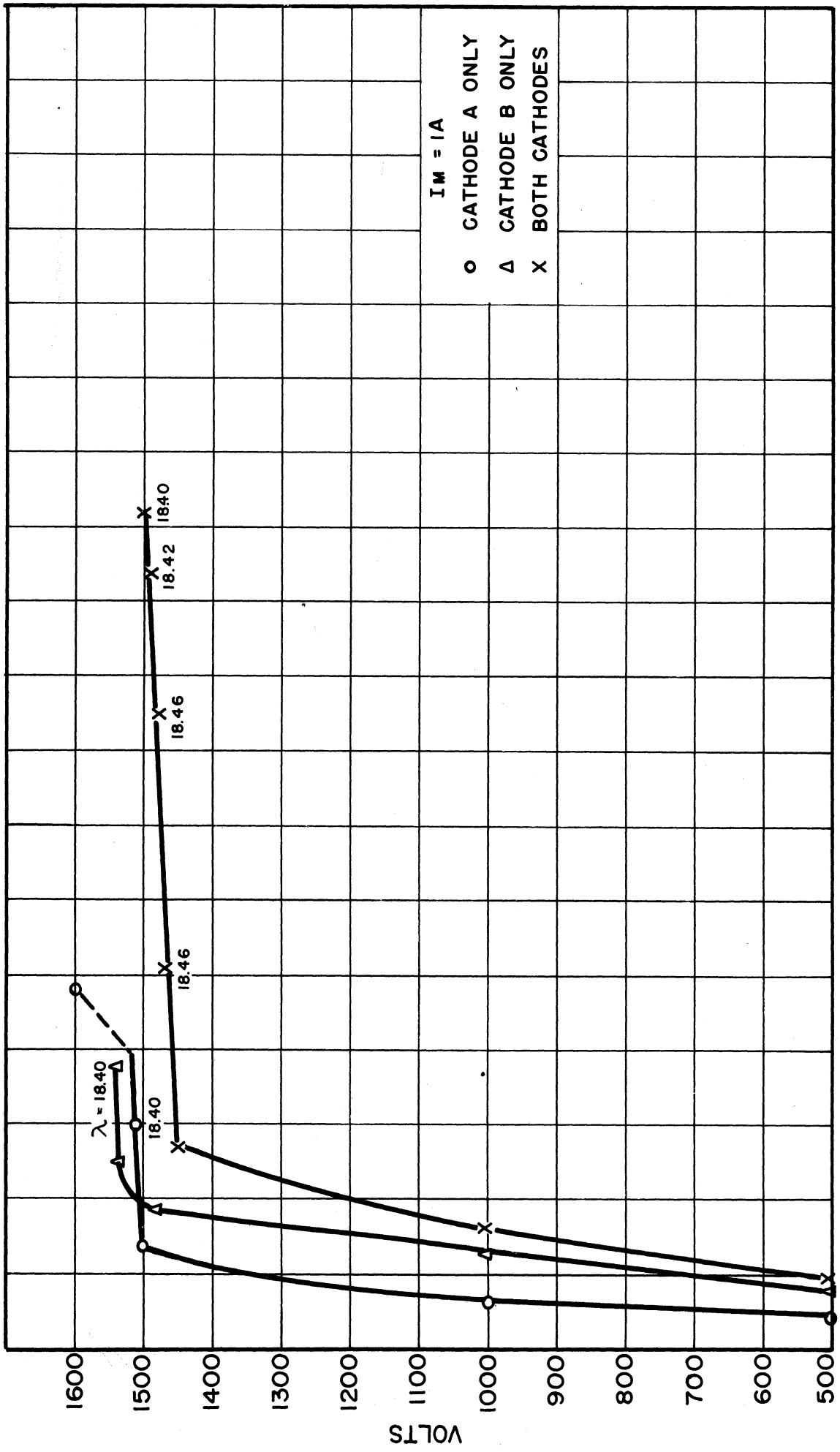

FIG. 12.4
PERFORMANCE CHARACTERISTICS MODEL 8 #36,

A low-Q tube based on this structure will be studied in the near future. It is proposed to employ one-half the Model 8 structure coupled directly into a wave guide through a window. This structure would be used in studies of the voltage-tuning phenomena.

13. Model 9 Low-Power Insertion Magnetron (J. S. Needle)

In order to achieve more flexibility in the experimental program for study of low-Q operation and to develop at the same time a tube usable in this type of operation at microwave frequencies, a low-power insertion magnetron was constructed in this laboratory. The assemblies for three models of this tube are given in Dwg. Nos. B10,009, B10,009A, and B10,009B in Appendix A. The resonant system for this tube is the coaxial type discussed in Section 6 of this report. Only the capacitive portion of the resonant circuit is incorporated within the vacuum envelope of the tube, allowing changes in external cavities to be readily made.

The Model 9 structure consists of six radial vanes attached to the outer cylinder and protruding through six axial slots in the inner cylinder. Thus a 12-anode set is formed with dimensions based on an interaction space designed for 10-cm operation. The cathode is a standard oxide-coated nickel-mesh on nickel-base emitter.

Design factors for the Model 9 structure are given in the following table.

λ	—	10 cm	E_o	—	280 volts
$n\lambda$	—	60	E	—	1400 volts
$n = \frac{N}{2}$	—	6	B_o	—	554 gauss
r_a	—	.317 cm	B	—	1662 gauss

r_c — .190 cm $\qquad\qquad$ $\frac{B}{B_o}$ — 3

$\frac{r_a}{r_c}$ — 1.66

Three very desirable features inherent in the Model 9 magnetron are valuable for the study of magnetron behavior: (a) the size and shape of the external oscillator cavity can be easily changed; (b) the loading can be easily changed; (c) the two halves of the anode may be operated at different d-c potentials. This flexibility in structure suggests the following possibilities in its application to work now in progress at the University of Michigan:

a. to be used as basic geometry in the development of a widely-tunable magnetron suitable for local oscillator or signal-generator use,

b. a tool for a study of effect of loading on maximum-current boundary and pushing,

c. to serve for the investigation of the optimum shunt impedance for higher-power coaxial-line oscillator structures,

d. to provide information as to the possibility of frequency modulating the oscillator by employing a variable voltage on one set of anodes with respect to the other (see G. E. Report No. RL 341, April 1950),

e. to provide design experience for the construction of higher-power ceramic-seal tubes of similar geometry.

Dwg. No. B10,009 in Appendix A shows the first model of this tube (Model 9). This model reached the vacuum-pump stage in its assembly when a leak in the glass-to-metal seal at one of the Kovar cups was discovered. Several attempts to repair this seal failed, and the leak was attributed to the difference in axial expansion between the inner and outer anode structures.

In order to overcome the glass-sealing problem, the design of Model 9 was modified and designated Model 9A (see Dwg. No. B10,009A in Appendix A). The outer anode ring of Model 9A consists of a Kovar ring to which the anode vanes are brazed. The inner anode of Model 9A differs from Model 9 in that a sliding fit was incorporated between one end of the copper portion of the anode and its connecting Kovar cylinder. This sliding fit overcomes the effects of the difference in axial expansion between the inner and outer conductors of the coaxial line, thus removing strain from the glass seals.

The choke and bypass system built onto the cathode stem to prevent leakage of power out the cathode line was designed for 10 cm. Power is to be coupled out of this tube by means of a probe or an inductive loop placed in the external cavity.

Another model, designated Model 9B (see Dwg. No. B10,009B in Appendix A) was designed to couple power out of the tube along the cathode line. This was done to avoid the use of a relatively narrow-band choke system which would limit the operating frequency range of the tube. This type of tube is desirable for wide-range frequency-pushing studies as well as for a wide-range mechanically tunable tube. Model 9B differs from Model 9A in that the cathode stem is longer in the 9B and the choke has been omitted. Originally, a thin ring of beryllium copper was brazed on the outside at the center of the tube for holding it in the external cavity; however, this is now to be omitted on all future tubes and is replaced by beryllium-copper fingers which slip over the outside of the shell.

Photographs of the partially assembled and the assembled tube are shown in Figs. 13.1 and 13.2.

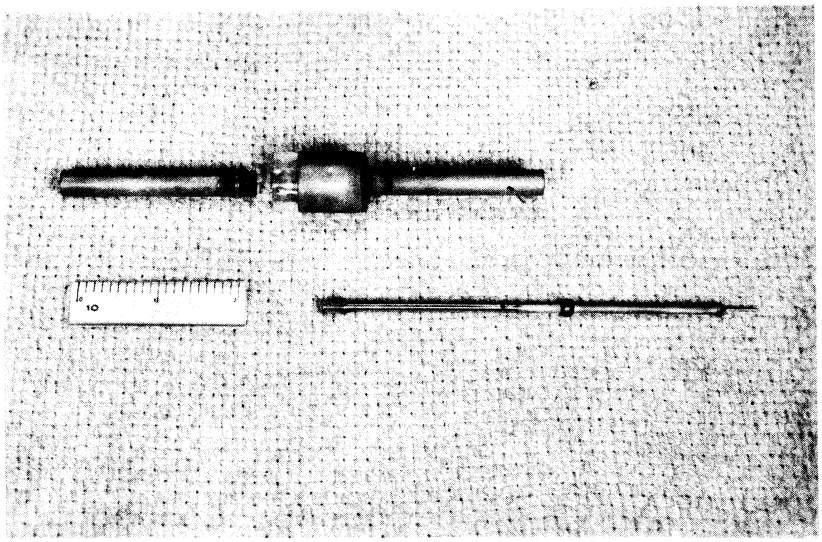

FIG. 13.1
PARTIALLY ASSEMBLED MODEL 9B

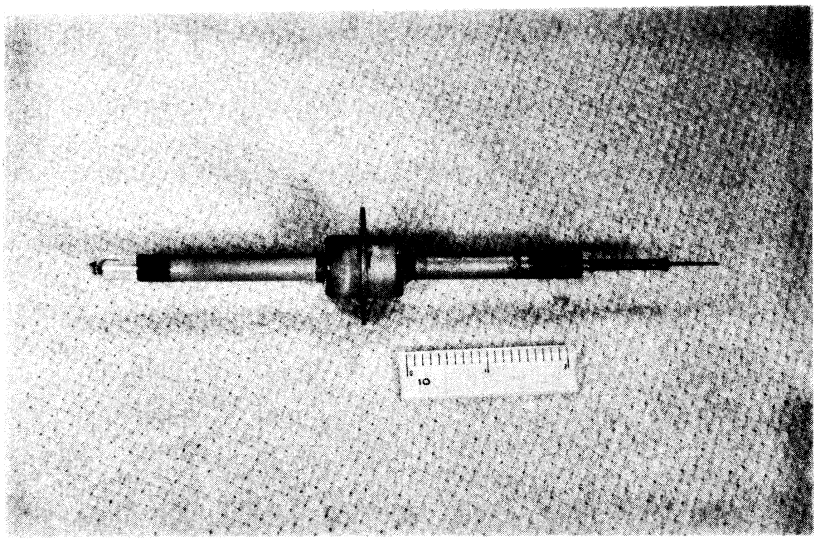

FIG. 13.2
ASSEMBLED MODEL 9A

14. Model 9 Performance (J. S. Needle)

The Model 9A and 9B tubes were tipped off the pumps immediately before the writing of this report, allowing little time to accumulate experimental data. The following are the initial results obtained from these models:

The Model 9A No. 39 insertion magnetron has been pulse-operated in a coaxial resonator, and oscillations were observed in the 3/2-wavelength cavity mode at 10.7 cm and also in the 1/2-wavelength mode at approximately 30 cm. Pulsed-performance oscillograms for operation in the 10.7-cm mode are shown in Fig. 14.1. These oscillograms show the effect of cathode heater input on leakage current. The leakage current is presumably due to end-hat emission. Cathode power input with 2.0 amperes of heater current is 7.2 watts. The anode voltage is approximately 900 volts for 10-cm operation with 1300 gauss. No C-W data on this model are available at the present time.

Model 9B No. 43 differs from the Model 9A insofar as it does not incorporate a choke and bypass inside the evacuated portion of the tube. This tube operated in the 1/2-wavelength cavity mode under pulsed conditions, but no oscillations were observed in the 3/2-wavelength mode. C-W operation with an external bypass in the cathode line gave an output of 900 milliwatts at 15.5 per cent efficiency. This operation was at 17.75 cm in the 1/2-wavelength cavity mode.

Experiments with heavy loading will be started in the immediate future.

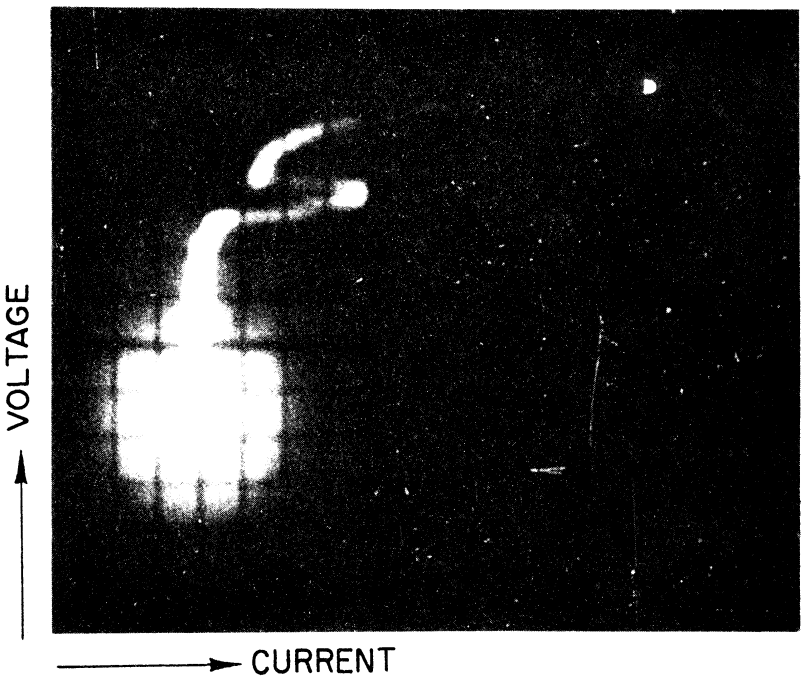

(a)

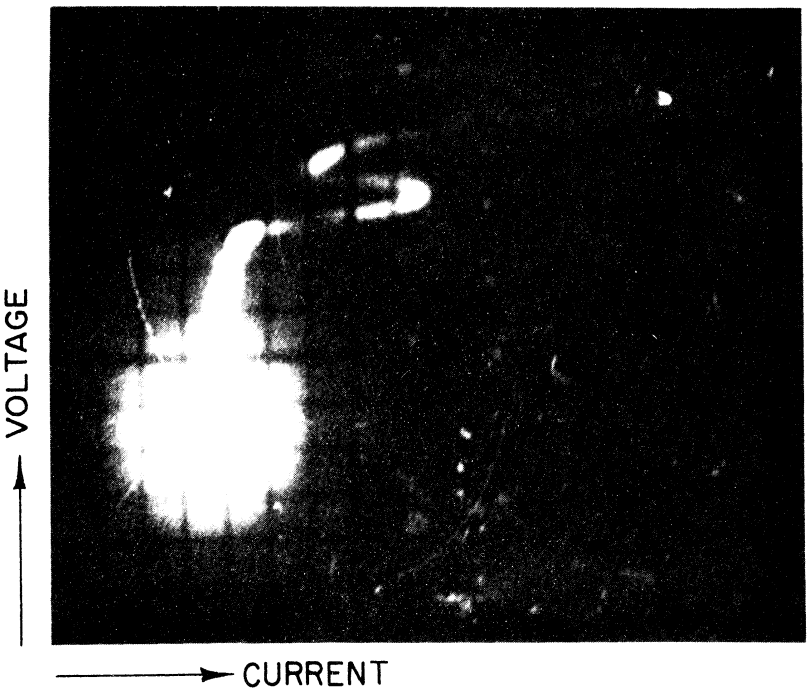

(b)

FIG. 14.1 PULSED PERFORMANCE OSCILLOGRAMS OF MODEL 9A MAGNETRON

CURRENT CALIBRATION = 25 MA. PER DIV.
VOLTAGE CALIBRATION ≅ 330 V. PER DIV.

15. The Trajectron, A Tube for Study of Magnetron Space Charge (W. Peterson)

The purpose of this experiment is to attain a more complete understanding of the magnetron by studying the space charge in a smooth-bore d-c magnetron.

The theoretical analysis of the space charge in a magnetron began about 30 years ago. In 1924 A. W. Hull suggested the solution of the magnetron equations (which often bear his name) in which the radial velocity is everywhere zero.[1] This is still widely used as a model for the actual space charge because of its simplicity.

In 1941 the general solution for the plane magnetron neglecting initial velocities appeared in reports by Slater.[2]

Allis then worked out an approximate solution for the cylindrical case which showed clearly the nature of the solutions for this case.[3]

Dr. Brillouin, while he was with the Applied Mathematics Panel at Columbia University, treated the magnetron in a manner similar to Lewellyn's treatment of conventional tubes and found a method for finding the magnetron voltage for a given current.[4] The equations could be solved for simple currents in a plane magnetron, but in the cylindrical case the equations had to be solved by approximate methods. Dr. Brillouin's reports include some solutions obtained by using a differential analyser.

---

1 Hull, A. W., "Paths of Electrons in the Magnetron", Physical Review, 23, 112 (abstract), January 1924.

2 Slater, J. C., "Theory of the Magnetron Oscillator", M.I.T. Radiation Laboratory Report 118, (V-5S), August, 1941. Also: Slater, J. C., Micro-Wave Electronics, New York, D. VanNostrand Company, 1950.

3 Allis, W. P., "Theory of the Magnetron Oscillator, Electronic Orbits in the Cylindrical Magnetron with Static Fields", Radiation Laboratory Report 122, (V-9S) Section 5 (122), 1941.

4 Brillouin, L., "Electronic Theory of the Plane Magnetron", O.S.R.D. Report No. 4510, A.M.P., Columbia University, 1944. Also: Brillouin, L., "Electronic Theory of the Cylindrical Magnetron", O.S.R.D. Report No. 47.

R. G. Twiss investigated the effects of including initial velocities in the equations for the plane magnetron.[1] He finds that one cannot consider only normal initial velocities and get a true picture of the space-charge distribution. However, when the tangential velocities are considered, the solution is similar to the double-stream solution found by Slater. Such things as current, time for electron to travel one loop, and distance traveled in one loop are to a first approximation independent of temperature. Consideration of initial velocities did not fully account for the noise in magnetrons and the extremely high electron temperatures observed. There are definitely questions which must yet be answered.

The recent experimental work on magnetrons includes some experiments by Regnar Svensson, Stockholm, Sweden, who had moderate success sending a beam of electrons through a magnetron. Reverdin and Marton, at the Bureau of Standards, have also done some experiments on a d-c magnetron. The results were presented at the Mexico meeting of the American Physical Society in June, 1950, and are supposed to appear soon in the Journal of Applied Physics. A project is underway at Columbia University to measure space-charge distribution in a magnetron by a unique method. A beam of helium atoms is to be injected into the space charge, and the number of atoms excited to certain metastable states will be measured. It is felt that there is certainly room for more experimental work along this line, both to verify the theory which has been worked out and to point the direction for new theoretical investigations.

What we propose to measure is an electron's position as a function of the time after it leaves the cathode. It is obvious, then, that from

---

[1] Twiss, R. G., "On the Steady State and Noise Properties of Linear and Cylindrical Magnetrons", Doctoral Thesis, M.I.T., 1949.

these data we can calculate the electron velocities at any radius and the trajectories of the electrons. The potential distribution can be calculated from the conservation of energy relationship, using the electron velocities from the experiment. The best way of finding the space-charge distribution would probably be to use the fact that radial current must be constant. Thus, the space-charge density is inversely proportional to the product of radial velocity and radius. This will not yield the total amount of space charge, but this might be found from the potential distribution with fair accuracy.

The tube which will be used for this work is a d-c smooth-bore magnetron with an electron gun in the same envelope arranged so that a beam of electrons can be sent into the magnetron space charge in an axial direction just grazing the cathode. The exit point of the beam will show on a fluorescent screen. This tube has been named the trajectron.

Theoretically, the Z-direction forces are independent of the r and θ displacements and velocities, and the r and θ forces are independent of the Z position or velocity. Thus, as far as r and θ are concerned, the beam electrons must move in just the same manner as emitted electrons. To find the displacement of an emitted electron in t seconds, we adjust the beam velocity so that the beam electrons spend t seconds in the magnetron space charge. We read the r and θ displacements from the fluorescent screen.

The first model of the trajectron, which was completed in September, 1950, is shown in Figs. 15.1 and 15.2. The assembly drawing of the trajectron is given in Appendix A, Dwg. No. B11,004. The large cathode on this tube failed while the tube was being evacuated. It was modified and the second model, completed in November, was lost in a freak accident in

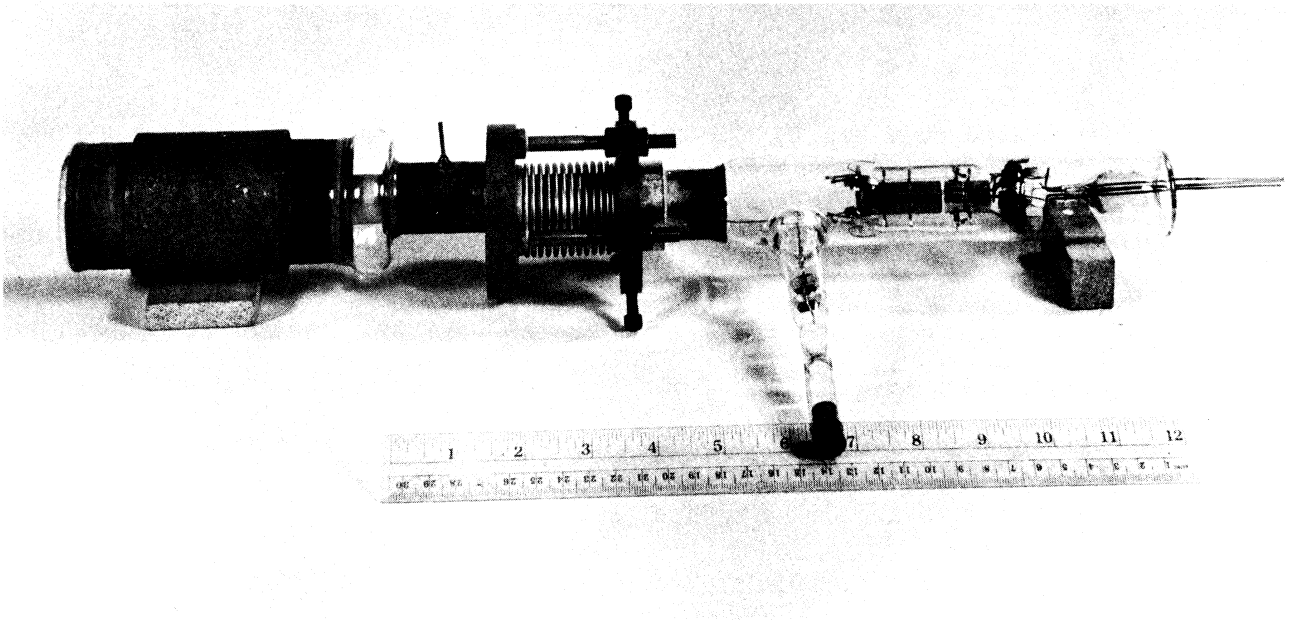

FIG. 15.1
TRAJECTRON

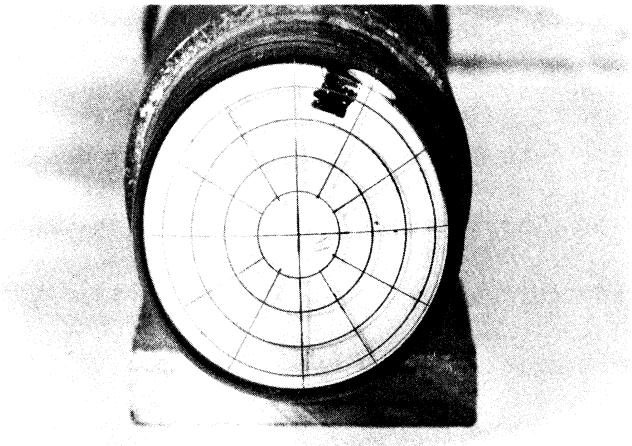

FIG. 15.2
TRAJECTRON VIEW SCREEN

which the ionization gage broke while the trajectron cathode heaters were on. It was rebuilt again and successfully evacuated. In initial tests (as this report is being written) it was found that the Kovar, used for glass seals, distorts the magnetic field so much that it is extremely awkward to align the beam. Also, heating the large cathode to operating temperature causes some gas to appear in the tube; but this condition has not yet become bad enough to make the tube useless. Work is being continued on this experiment.

16. Model 5 F-M Magnetron (H. W. Welch, Jr., J. R. Black)

The Model 5 f-m magnetron is a nontunable interdigital tube utilizing coupling to the cathode line in the zero-order mode to introduce effects of the modulating space charge supplied by a second cathode. Dwg. No. B10,005 shows an assembly drawing of the Model 5 magnetron. The interdigital oscillator, anode structure, chokes, and output assembly are the same as employed in the Model 4 interdigital magnetron (see Interim Report). The modulator anode is simply a smooth-bore anode placed 1/2 wavelength from the oscillator-cathode surface. The upper cathode structures are designed to form an r-f short between the two cathodes and are spaced by means of a lava insulator.

Extensive data on brass models of the Model 5 are given in Technical Report No. 3. These data correlated with results given on the Model 4B (see Interim Report) give a fairly complete basis for the present design.

The first model of this type was completed in January, 1950. It would not oscillate in the zero-order mode, and sparking between the oscillator and modulator cathode was observed when pulsed voltages were applied to the oscillator cathode. X-ray showed the modulator cathode to be

distorted and making near-contact with the oscillator cathode in the bypass sleeve between them. Upon taking the tube apart it was discovered that a lava spacing insulator (not shown in the drawing) had been displaced and wedged between the cathodes in such a way as to cause distortion on expansion of the cathodes when they were heated.

The tube was reassembled without the lava spacer, and the results of hot tests may be summarized as follows:

a. Oscillations were observed in the desired mode at 15.34 cm only by unloading the tube to the point where power output was not measurable.

b. Rather strong coupling to both cathodes was observed at 15.34 cm. This is to be expected, since the cathode chokes were designed for 14 cm. A check of data on the Model 4 magnetron, which has the same oscillator section, indicates that the anode spacing should be .080 inch instead of .050 inch as it is in the Model 5 for 14-cm operation. (See Interim Report for details of Model 4.) In order to shift the resonant wavelength of this particular tube the cathodes were removed and the chokes (Part No. 10 in Dwg. No. B10,005) shortened by the insertion of a copper sleeve, .75 cm in length, between the cathode stem and bypass sleeve at the base of the choke. Effectively the cathode line, which is part of the resonant circuit, is shortened 1.5 cm. This should change the resonant wavelength about the same amount; however, the tube was lost on reassembly.

c. No modulation data were obtained because of the erratic behavior of the oscillator.

Further work on this model was dropped in March, 1950, due to its complex structure and due to the promising results obtained from Models 6 and 8.

17. Summary of Construction Techniques (J. R. Black)

Most of the tube-construction techniques employed in the Michigan Vacuum Tube Laboratory are in general widely used in the art. Most of the techniques have been discussed in Section 14 of "Theoretical Study, Design and Construction of C-W Magnetrons for Frequency Modulation", Final Report No. 3. It should be stressed that nearly all parts have been constructed at the University of Michigan Vacuum Tube Laboratory, starting from raw stock.

All the tubes constructed to date are tipped off the vacuum system before they are operated. Getters have been employed only in the trajectron tube which has a relatively large volume; however, these are used only as a precaution and have not as yet been flashed. The tubes undergo severe bake-out while on the pumps and are tipped off at vacuums less than 5×10^{-7} mm Hg.

Most of the brazing on the tube body is done with gold-copper (37 per cent gold) solder, which allows several successive brazes to be made on the same tube without danger of previous brazes letting go. All Kovar parts are brazed with this solder. Output seals are brazed to the tube bodies after glassing, using the lower-melting point BT silver solder (eutectic).

Pure copper and pure platinum are sometimes used as solders on the cathode where high temperatures are involved.

All brazing is done in one of the four hydrogen furnaces listed in Section 18. Kovar is brazed only in the small hydrogen bottle, where it can be easily observed and the temperature reduced immediately after the gold-copper solder flows. Oxidized stainless-steel jigs are used for holding parts in position while being brazed.

Tungsten and molybdenum parts are arc-welded in a hydrogen atmosphere to prevent oxidation. A carbon electrode is used with d-c power for these welds.

The glass-to-metal seals are Kovar to Corning 7052 glass. These are made by our laboratory personnel on Litton glass lathes or by means of a 20-kw induction heater. Accurate alignment is maintained to within .002 or .003 in. by machinists' indicators on the glass lathe and by jigs on the induction heater. Nitrogen which has passed over methyl alcohol is used for blowing on the glass lathe to prevent oxidation of the tube during glassing.

Iron employed in the magnetic circuit within the magnetron is hot-rolled SAE1020. Hot-rolled steel has less tendency to have axial cracks than cold-rolled steel, thus assuring vacuum tightness. The iron is copper-plated in a copper cyanide-Rochelle salt bath to provide low electrical losses and to insure good brazing.

The oxide cathodes were of the triple-carbonate type applied to grade "A" nickel mesh sintered to a grade "A" nickel sleeve. The tungsten heaters are sprayed with an Al_2O_3 insulator mixture supplied by R.C.A. and fired in a hydrogen furnace at 1650°C.

IV. LABORATORY FACILITIES

Most of the equipment and facilities of the Electron Tube Laboratory are shown in the drawings and photographs on the following pages. The laboratory is housed in three rooms on the third floor of the new Engineering Building and has a total floor space of 2400 sq. ft. One room is devoted primarily to test equipment, one to assembly and processing equipment, and one to the machine shop. Desk and work-bench space is divided between the three rooms. Two offices, an electroplating room, and a room for cathode work are built into the assembly room.

Each room has plug-in molding strips on the walls supplying 115-volt 60-cycle power. Outlet boxes conveniently arranged about the rooms supply a variety of outlets for 115 or 230-volt d-c, 230-volt 3-ϕ 60-cycle power and 115-volt 3-ϕ 60-cycle power. All combinations of these voltages can be connected to any outlet box by means of a master distribution panel located in each room. Water, air, and gas are also furnished to the rooms.

Approximately two-thirds of the equipment in the laboratory has been provided by the University of Michigan, while the remainder has been provided by the Signal Corps. It should be pointed out that this laboratory has the enviable position of being able to draw on the laboratory equipment and the facilities of the entire University.

18. Test Laboratory (J. R. Black)

A floor plan of the test laboratory is shown in Fig. 18.1. Work space for four or five sets of apparatus is available plus space for

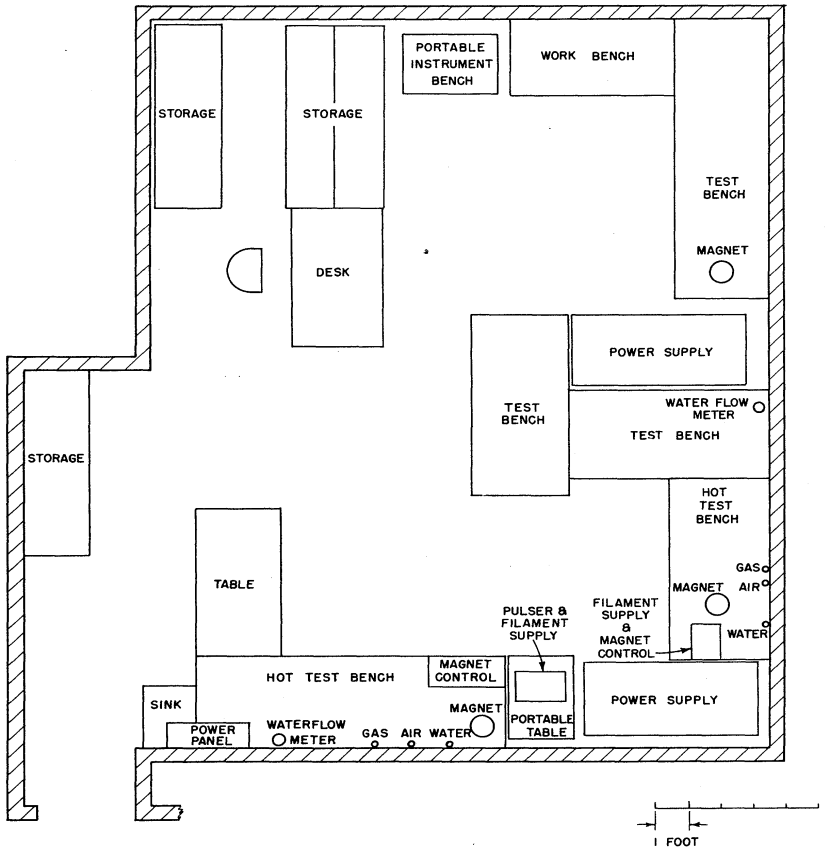

FIG. 18.1 TEST LABORATORY.

ALL DIMENSIONS UNLESS OTHERWISE SPECIFIED MUST BE HELD TO A TOLERANCE - FRACTIONAL ± 1/64" DECIMAL ± .005" ANGULAR ± ½°

ENGINEERING RESEARCH INSTITUTE UNIVERSITY OF MICHIGAN ANN ARBOR MICHIGAN		DESIGNED BY	APPROVED BY
		DRAWN BY MM	SCALE 3/8" = 1'-0"
		CHECKED BY	DATE 12-18-50
PROJECT M-762		TITLE FLOOR PLAN TEST LABORATORY	
CLASSIFICATION		DWG. NO. C-	
ISSUE	DATE		

computation and for storage of equipment. A large portion of the microwave equipment was built by this laboratory, partly because of lack of availability shortly after the war, and partly because certain special-purpose equipment was necessary.

The hot-test bench near the door (Fig. 18.2) is used for hot-testing magnetrons built in this laboratory. A magnetron under test can be seen in an electromagnet, the controls of which are mounted on the panel under the bench. This bench is equipped with a 1-5/8-inch coaxial line with its associated taper, slotted section, and water load mounted on an adjustable carrier. On the wallcan be seen a Schutte-Koettering water-flow meter and a Foxboro differential thermometer for determining power delivered to the water load. A filament power supply with a bridge to compensate for back-bombardment power is shown to the left of the magnet. On the table to the right of the picture is shown one of the two Model 1SS-4SE, Type 107 spectrum analyzers designed by M.I.T. and built by Sylvania. Also, on this table there is a 707B signal generator with its power supply. All the equipment shown in Fig. 18.2 was built at this laboratory except the water-flow meter, the differential thermometer, and the spectrum analyzer.

Fig. 18.3 shows the hot-test bench setup in the corner of the room. The box to the right contains a filament supply and the control circuit for the electromagnet pictured to the left of the box. A 1-5/8 inch coaxial line with its taper, slotted, and water-load sections is shown on an adjustable carrier, while on the wall can be seen a differential thermometer and water-flow meter.

The present setup on the wall test bench near the work bench is pictured in Fig. 18.4. The large power supply to the right has a variable

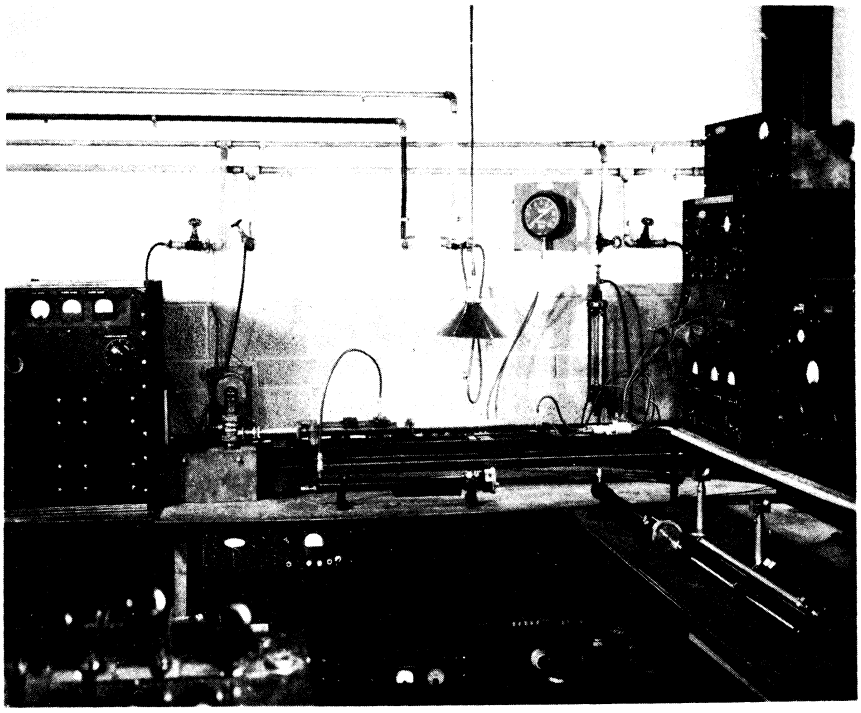

Fig. 18.2 Hot-Test Bench

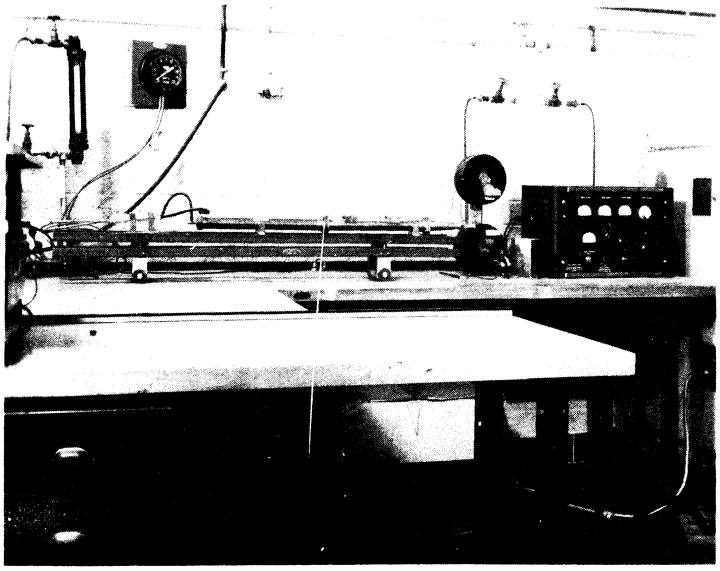

Fig. 18.3 Corner Hot-Test Bench

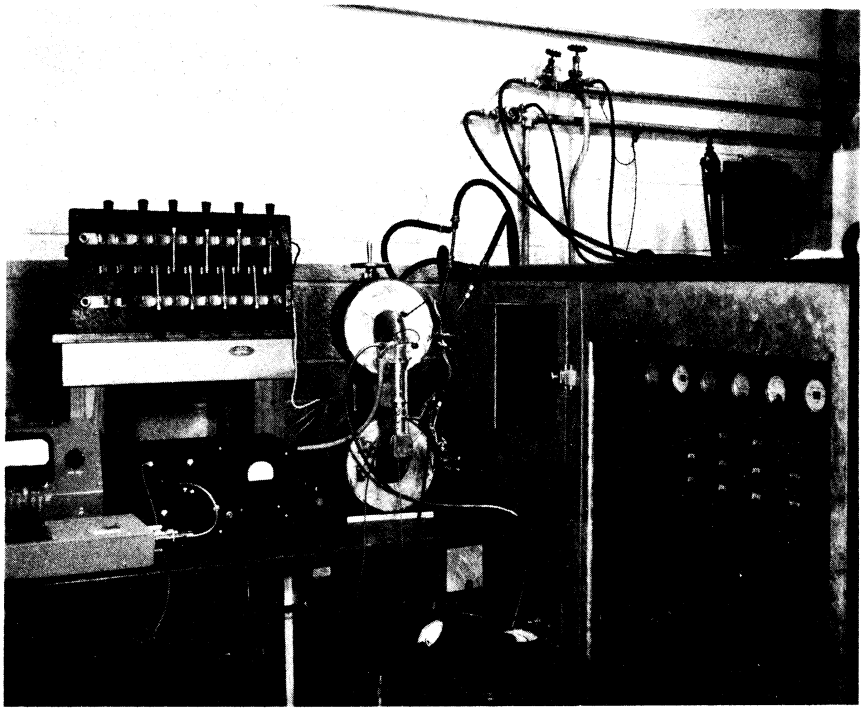

Fig. 18.4 Test Bench

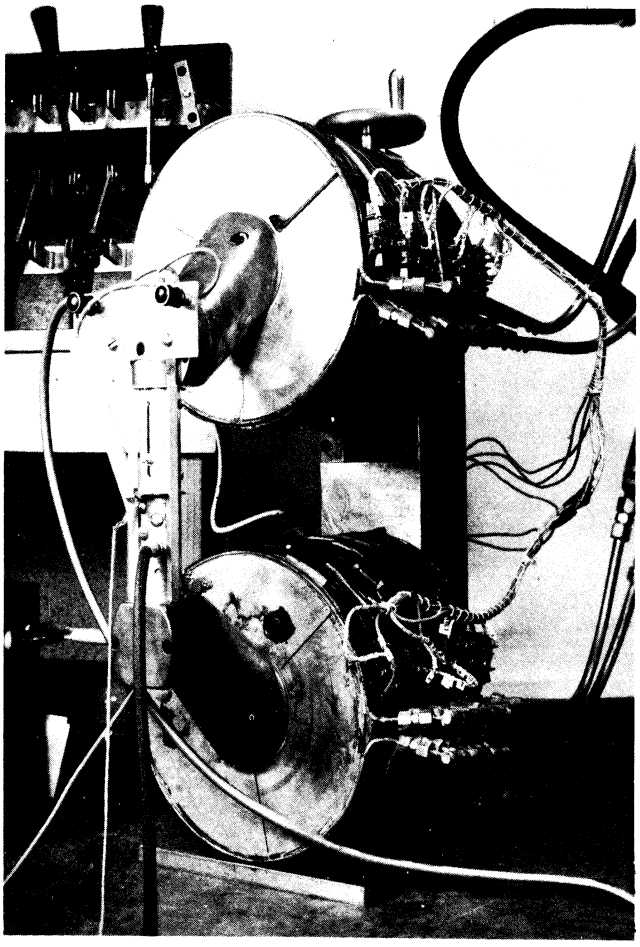

Fig. 18.5 Large Electromagnet

output up to 15,000 volts at 7.5 kva. This is one of the three war-surplus power supplies in this laboratory which have been cut down to one-half their original volume and rewired for convenient use in the laboratory.

The magnet in the center of Fig. 18.4 is pictured holding a Model 9 tube within its external cavity. A closeup view of this magnet, which was constructed in this laboratory, is shown in Fig. 18.5. The water-cooled coils consist of twelve separate coils which can be used in any desired combination. Each coil produces one thousand ampere-turns, giving a total maximum mmf of 12,000 ampere-turns which in this magnet will produce 10,000 gauss across a one-inch air gap using 1-1/2-inch solid pole pieces. The gap width between the pole pieces can be varied from zero to 8 inches by means of the wheel shown at the top of the magnet yoke. A Fluxmeter (Model F, Sensitive Research Company) is used to measure magnetic flux and proves to be a versatile and useful instrument.

Three other electromagnets have been constructed for operation at 220 volts d-c, two having a maximum field of 2500 gauss and one of 4400 gauss across a 3/4-inch gap. The smaller type is that shown in Fig. 18.2, while the larger is pictured in Fig. 18.3.

To the left of Fig. 18.4 is shown a resistance control box for the electromagnet, a filament power supply, and a power bridge consisting of a Hewlett Packard Bolometer Mount, Model 430A and a Tunable Bolometer Mount, Model 475B.

A 2 x 4-inch wave guide has been built by our shops with its associated water loads, dummy loads, slotted sections, coax-to-wave-guide matching sections, probes, etc. This wave guide was built at the laboratory to fit the special frequency range involved, since a suitable guide was not available on the market at the time.

A rotary probe set for measuring field distributions in magnetron models was designed and built at the University and has proven to be a most useful instrument.

Two signal generators, of the type shown in Fig. 18.6, using type 707B tubes in a coaxial-line resonator have been built in this laboratory. They cover a wavelength range from 8 to 21 cm and have a power output of approximately 75 milliwatts. One great difficulty with the above oscillators is that they operate in various modes making it impossible to tune them continuously. As a result of this, four other signal generators employing a wave-guide cavity and the 707B tube are being built. One is shown in Fig. 18.7. They tune from 8.25 to 17 cm with a power output of approximately 100 milliwatts. The great advantage of this type of signal generator is that no holes were observed in the frequency spectrum.

Three type 208 Dumont oscilloscopes, a Browning Laboratory Type P-4E Synchroscope, a Tetronix 512 Oscilloscope, a Ferris Instrument Company Model 22A Signal Generator (85 kc to 25 mc), a General Radio vacuum-tube voltmeter type 726A, an M.I.T.-designed Thermistor Bridge type TBN-3EV, a 1-mc modulator delivering 1 kw into a 500-ohm load built at this laboratory, crystal and bolometer mounts, and various pieces of microwave plumbing complete the equipment. Other equipment is, of course, available for use from the Electrical Engineering Department stock room.

19. Assembly Equipment (J. R. Black)

The assembly-room floor plan is shown in Fig. 19.1. This room contains a cleaning and plating room, a cathode room, processing equipment, storage space, work-bench space, drafting space, and two separate offices for desk space.

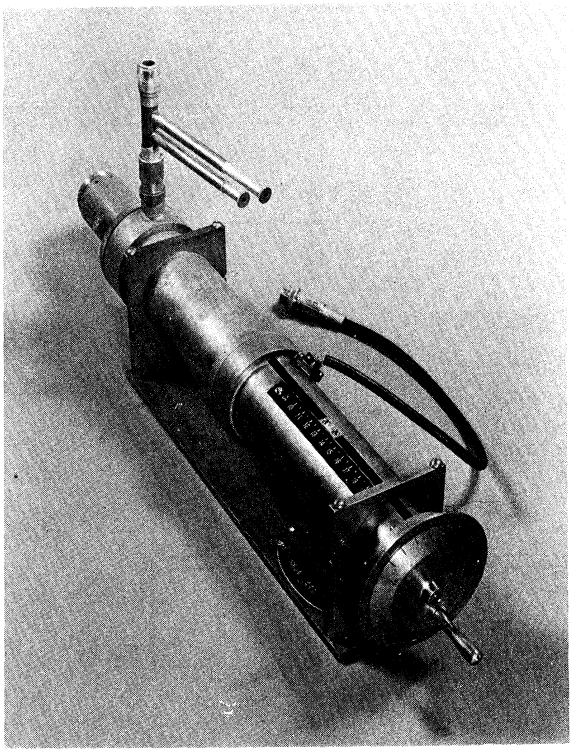

Fig. 18.6 Coaxial-Cavity Signal Generator

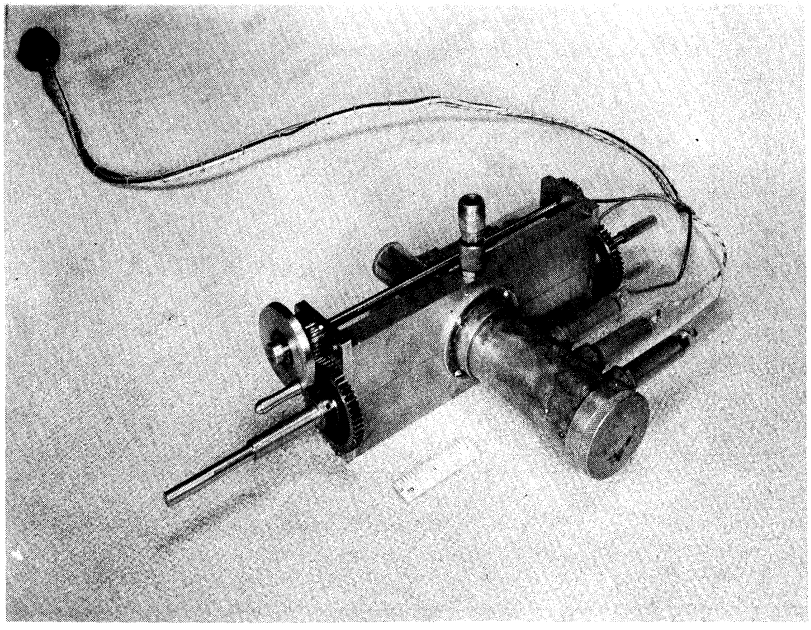

Fig. 18.7 Rectangular-Cavity Signal Generator

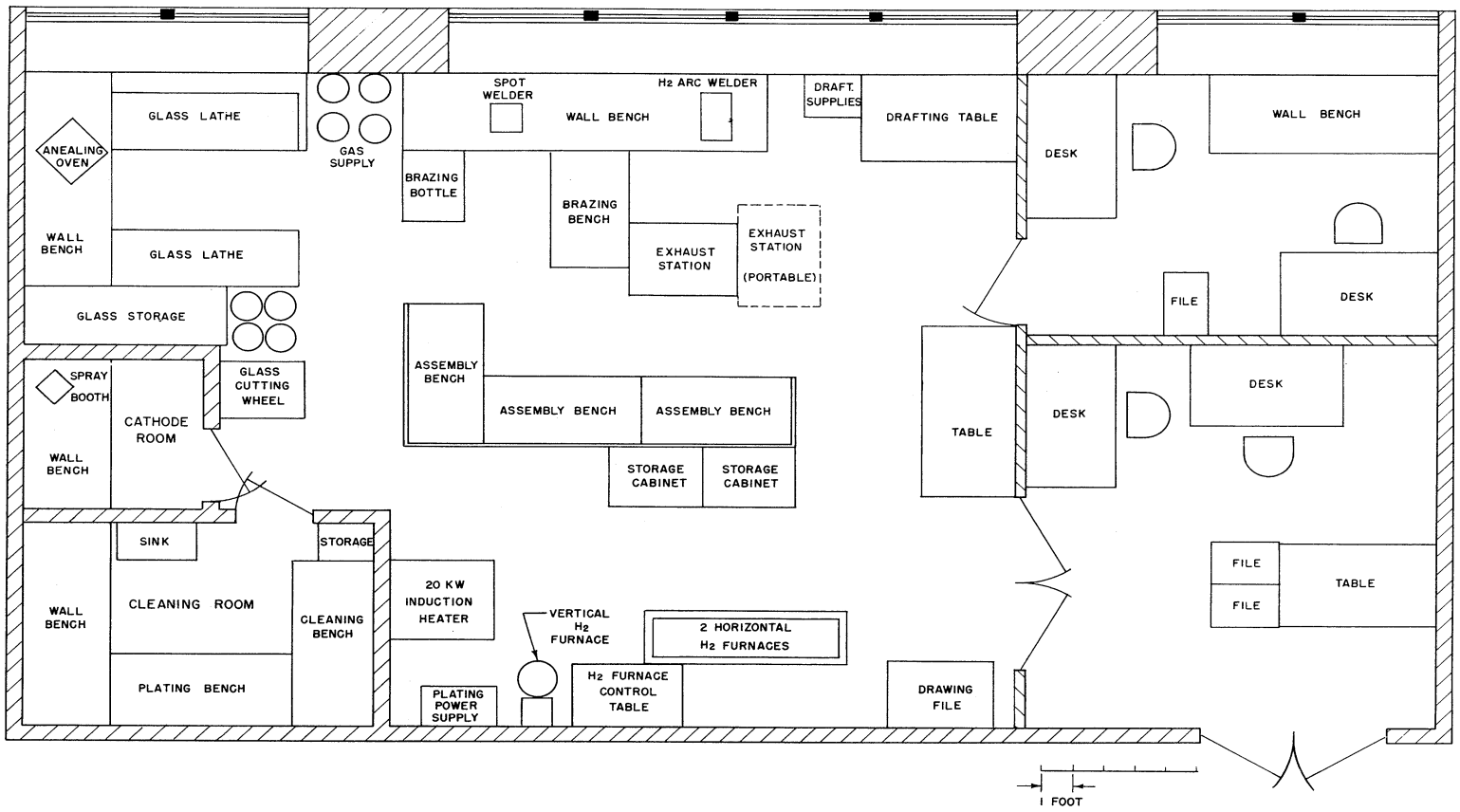

FIG. 19.1 ASSEMBLY LABORATORY

ALL DIMENSIONS UNLESS OTHERWISE SPECIFIED MUST BE HELD TO A TOLERANCE - FRACTIONAL ± 1/64" DECIMAL ± .005" ANGULAR ± ½°

ENGINEERING RESEARCH INSTITUTE UNIVERSITY OF MICHIGAN ANN ARBOR MICHIGAN		DESIGNED BY	APPROVED BY
		DRAWN BY 777	SCALE 3/8" = 1'-0"
		CHECKED BY	DATE 12-14-50
PROJECT M-762		TITLE FLOOR PLAN ASSEMBLY LABORATORY	
CLASSIFICATION		DWG. NO. C-	
ISSUE	DATE		

A view of three hydrogen-atmosphere furnaces is shown in Fig. 19.2. The smaller of the two horizontal hydrogen furnaces placed one on top of the other in the foreground has a 1.5-inch manifold and is capable of 1650°C operation. The larger of these two furnaces has a 5.25-inch manifold capable of attaining 1100°C and is automatically temperature-regulated. The control board for these two horizontal furnaces is on the stand supporting them. Water-jacket cooling sections allow continuous brazing operations to be made in each of these furnaces.

The large vertical cylinder shown in the rear of Fig. 19.2 is a new vertical hydrogen furnace having a 7-inch manifold and capable of attaining 1100°C operation. A quartz window is built into this furnace to enable visual observation of the brazing operation. The work is supported on a stand from the floor, and the furnace is lowered on rails over the work. The furnace element is located at the top of the cylinder, while a water-cooling chamber is located at the bottom. After a braze is completed, the furnace is raised part way to bring the cooling section around the work. This arrangement permits many brazes to be made in a working day, since the heating element is maintained at operating temperature throughout the brazing cycle. The work remains stationary on its stand throughout the brazing operation, thus minimizing misalignment due to shifting of jigs and parts. A thermocouple leading up the stand and mounted on the work measures the temperature; however, by viewing the work through the quartz window, the work can be cooled immediately after the solder flows. This procedure is convenient for silver-solder brazing as well as for brazing Kovar with gold-copper solder.

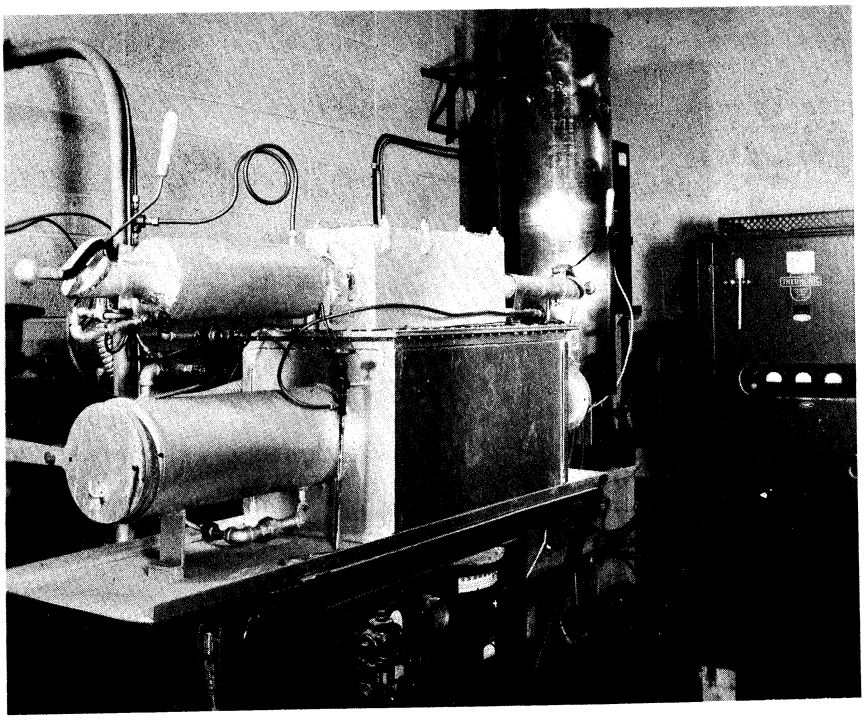

Fig. 19.2 Hydrogen Furnaces

Fig. 19.2 also shows a portion of the 20-kw Ther-monic Induction Generator, Model 1070. Transmission lines carry the power to the hydrogen brazing bottle and to the brazing bench, where it is utilized for brazing tube parts in a hydrogen atmosphere or for making glass-to-Kovar seals.

A portion of the cleaning and electroplating room is shown in Fig. 19.3. Two cleaning baths, two electroplating tanks, and a wash tank are visible in this picture. The rectifier for plating supplies 100 amperes at 6 volts. An exhaust fan is used for ventilating the cleaning and electroplating room and the cathode room. These rooms are normally shut off from the rest of the laboratory, air being supplied through dust filters.

A view showing a portion of the interior of the cathode room is shown in Fig. 19.4. A spray booth and a chuck for rotating parts to be sprayed are shown on the bench, while a three-jar ball mill is shown under the bench.

The glass-working section of the laboratory is shown in Fig. 19.5. The large glass lathe is a Litton Model HSA lathe, while the small glass lathe is a Litton Model F lathe. A glass-annealing oven is shown on the bench to the left of the Model F lathe. Machinists' indicators and jigs are employed to align parts accurately to within 0.002 inch.

Temperatures in excess of 1800°C can be reached on small parts in the hydrogen brazing bottle shown in Fig. 19.6. Parts are heated by radiation from a molybdenum filament or by means of the 20-kw induction heater. The molybdenum filament receives its power from the large variable transformer shown under the bench. A mercury manometer for indicating hydrogen flow is pictured at the back of the table. The pyrex jar is

Fig. 19.3 Cleaning and Electroplating Room

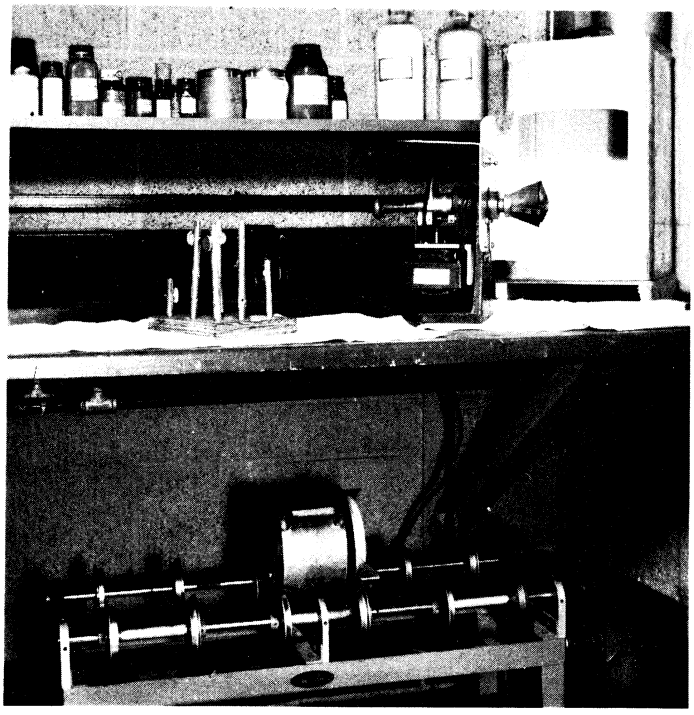

Fig. 19.4 Cathode Room

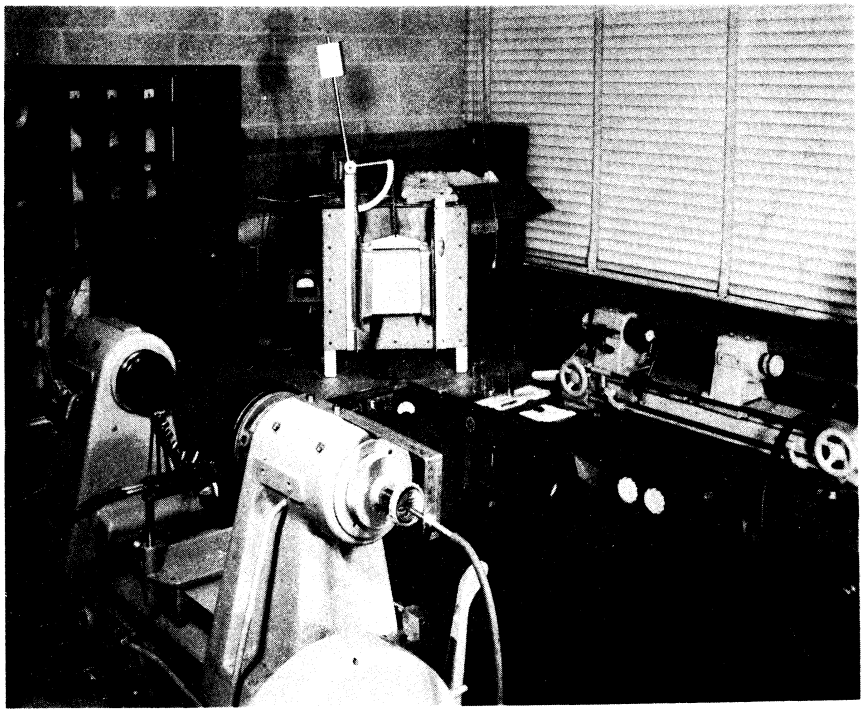

Fig. 19.5 Glass Lathes

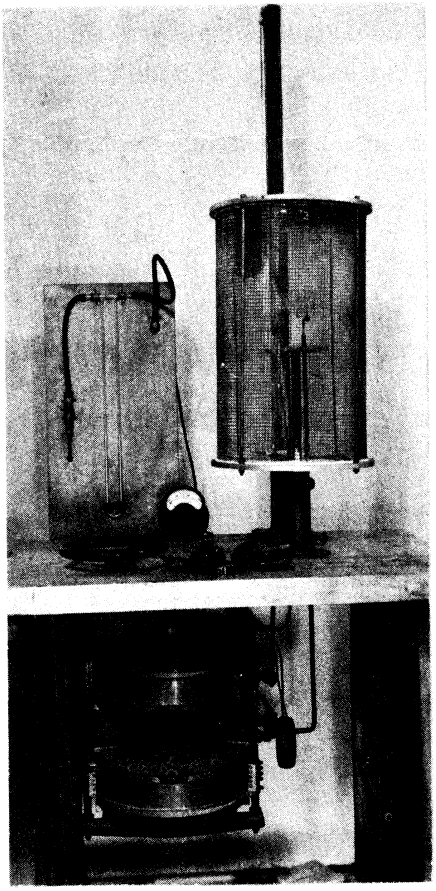

Fig. 19.6

Hydrogen Brazing Bottle

raised or lowered on a ball-bearing track and has a "weightless"-type window-sash counterbalance.

The hydrogen-atmosphere-carbon arc welder is shown in Fig. 19.7. An arm holding the carbon electrode protrudes through a hole in the heavy glass window. A small fluorescent light in the hood provides illumination for the work. An air cylinder controlled by a foot valve raises and lowers the hood over parts to be welded. To the left are shown the hydrogen valves and flowmeter as well as a timer which controls the length of time the arc is on. Under the table (not shown in the picture) is a rectifier for supplying power to the welder. High-melting-temperature materials are joined together in this welder.

The stationary evacuation station is pictured in Fig. 19.8, showing a tube sealed to the manifold. The upper right panel contains an automatically regulated ionization-gage circuit and a thermocouple-vacuum-gage circuit. The upper left panel contains controls for the station, i.e., switches for the pumps, oven, filament supply, and vacuum interlock as well as the thermocouple meters and filament meters. The lower left panel contains controls for the oven, filament, and pumps. The large aluminum box seen just below the upper panels is an oven to be lowered over the tube for baking at 425°C. A small portable oven can also be used to bake the metal portions of the tube at 625°C. An oil-vapor diffusion pump, having an activated-charcoal baffle, produces vacuums of the order of 5×10^{-7} mm Hg.

Fig. 19.9 shows a portable vacuum station which uses a Litton Oil Diffusion Pump and Charcoal Baffle, Series 250. The system is arranged for bell-jar operation or for tube evacuation. The glass manifold to which the tubes are sealed can be seen protruding above a transite heat shield which

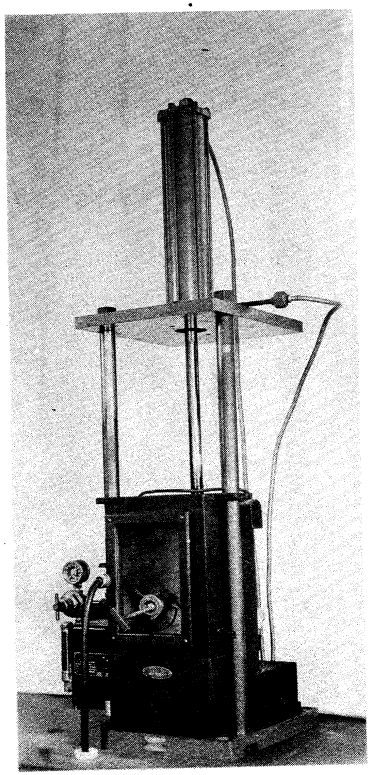

Fig. 19.7

H_2 Atmosphere Arc Welder

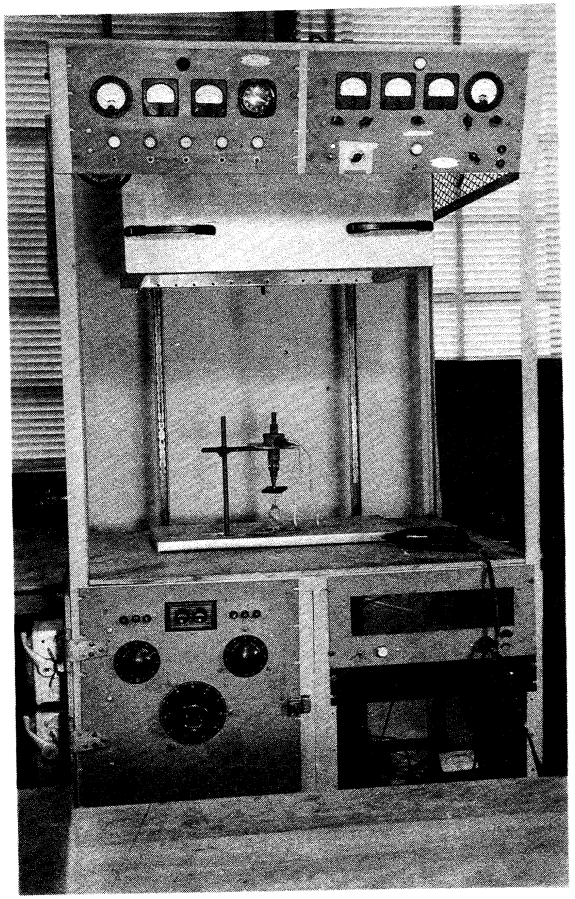

Fig. 19.8

Stationary Vacuum Station

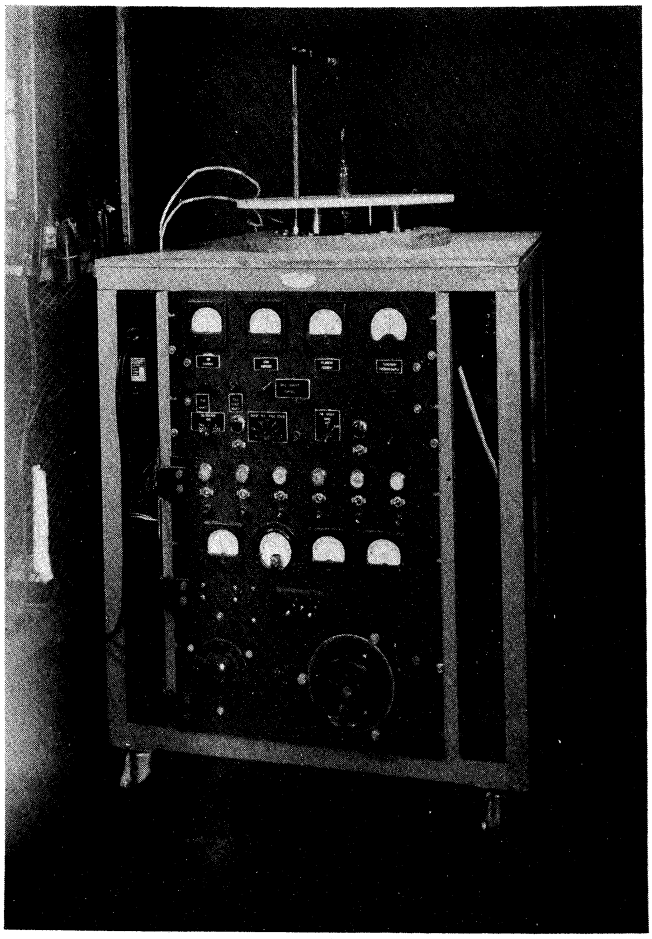

Fig. 19.9 Portable Vacuum Station

Fig. 19.10 Tube-Assembly Space

protects the bell-jar plate. A portable oven fits over the tube and rests on the transite heat shield for baking out the tubes. The top panel contains an ionization gage and thermocouple gage as well as a poor-vacuum interlock. The lower panel contains power circuits for the pump, tube filament power supply, oven control and thermocouple temperature-measuring circuits. Plug-in hoses for cooling water and a plug-in power source make this station extremely versatile. Vacuums of the order of 2×10^{-7} mm Hg can be obtained with this system.

A general view of the assembly-bench space, stationary vacuum station, brazing bottle, and the glass-working space is given in Fig. 19.10. The exhaust fan for the cleaning and electroplating room and the cathode room can be seen on the wall above glass storage cabinets.

A glass-cutting wheel, a 1-kva spot welder with timer, a "hot" box for storing tube parts, and an R.C.A. grid-winding machine are not shown in this report.

20. Machine Shop (J. R. Black)

The floor plan of the machine shop is shown in Fig. 20.1. Fig. 20.2 shows a view taken from the doorway down to the raw-stock rack. To the left can be seen three drill presses. They are a Motor-Avery high-speed drill press, Type C, a Walker-Turner 1/2-inch drill press and a heavy-duty Allen drill press. At the rear of the picture next to the raw-stock rack is a 10-hp Hobart d-c-generator arc welder. To the right of the picture are a No. 2 Brown and Sharp universal mill and a Bridgeport vertical milling machine with a universal head and a slotting attachment.

Fig. 20.3 shows another view of the machine shop down the second aisle. To the left is shown a Sheldon 10-inch lathe, an Ammco 7-inch shaper

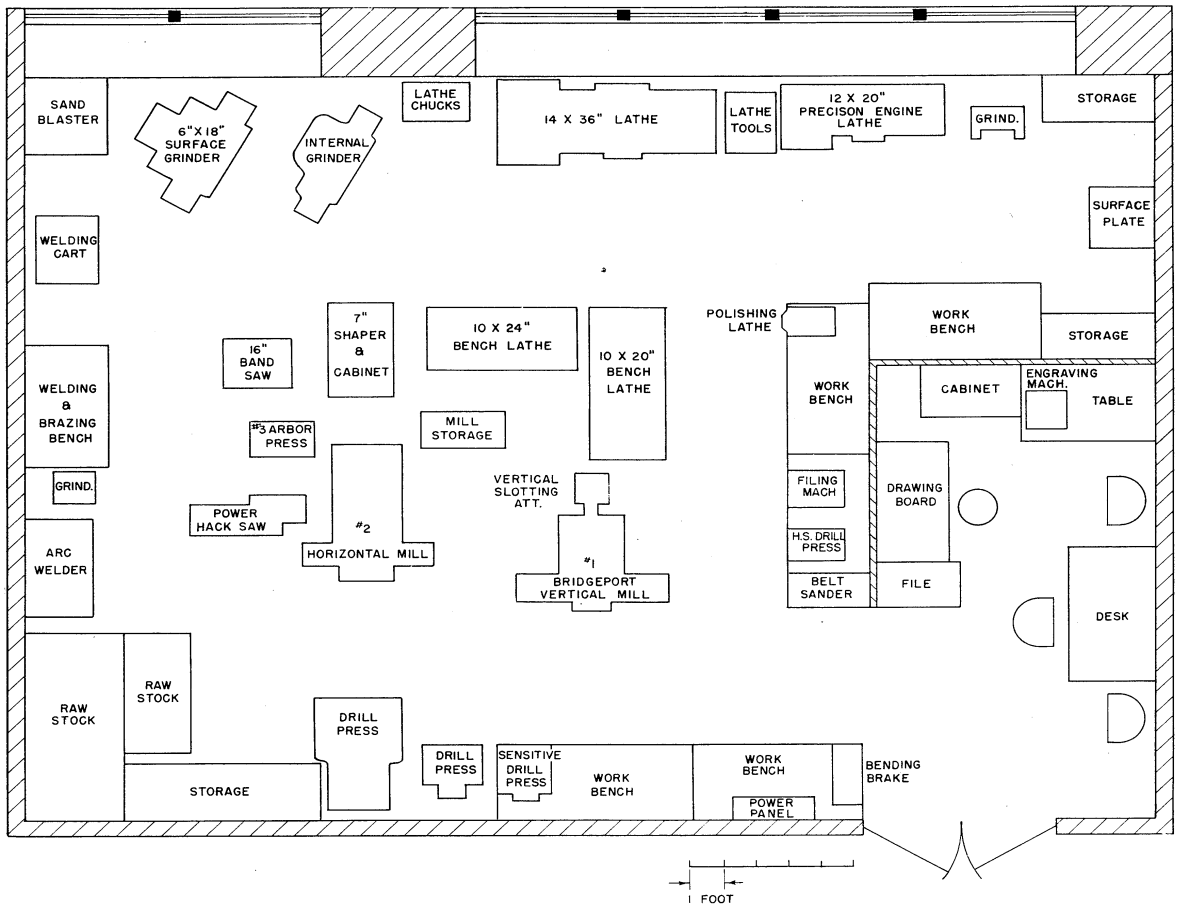

FIG. 20.1 MACHINE SHOP

ALL DIMENSIONS UNLESS OTHERWISE SPECIFIED MUST BE HELD TO A TOLERANCE - FRACTIONAL ± 1/64" DECIMAL ± .005" ANGULAR ± 1/2°

		ENGINEERING RESEARCH INSTITUTE UNIVERSITY OF MICHIGAN ANN ARBOR MICHIGAN	DESIGNED BY DRAWN BY 777 CHECKED BY
		PROJECT M-762	TITLE FLOOR PLAN MACHINE SHOP
ISSUE	DATE	CLASSIFICATION	DWG. NO. C-

APPROVED BY
SCALE 3/8" = 1'-0"
DATE 12-16-50

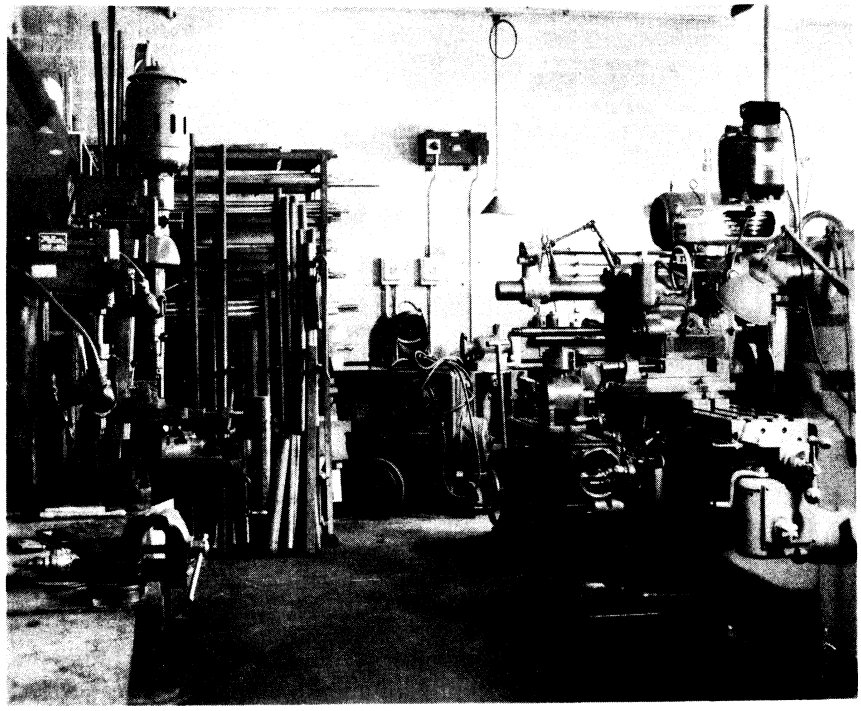

Fig. 20.2 Machine Shop

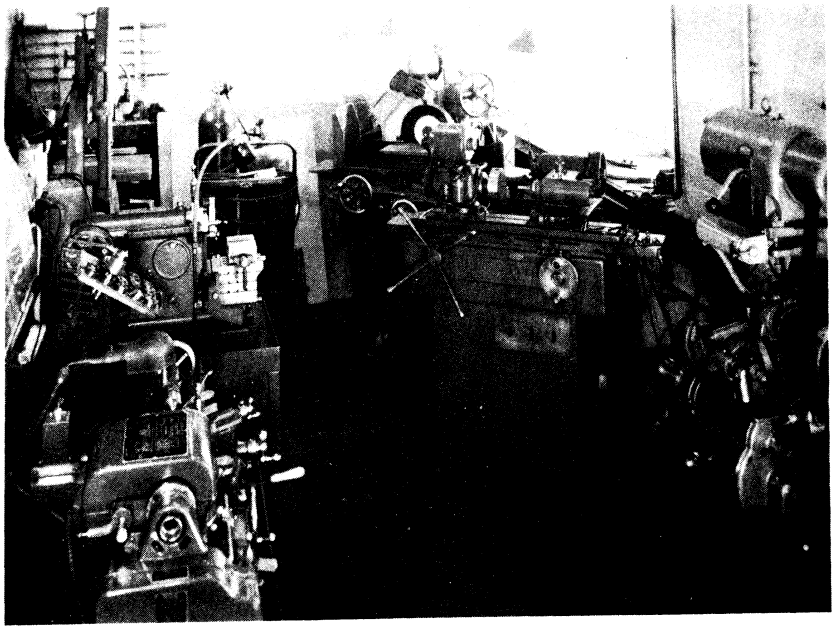

Fig. 20.3 Machine Shop

and a Walker-Turner metal-cutting band saw. Directly at the rear in Fig. 20.3 can be seen the oxy-acetylene welding equipment and to the right a Mott sand blaster. A portion of a Norton hydraulic surface grinder can be seen behind a Majestic internal grinder on the right-hand side of the picture. To the extreme right can be seen a portion of a 14-inch Handy tool-room lathe.

A close-up view of the 10-inch Monarch tool maker's lathe is given in Fig. 20.4.

Not shown in the photographs are a 9-inch Ames speed lathe, a Shaver polishing lathe, a jeweler's lathe, a watchmaker's high-speed drill press, a pedestal grinder, a bench grinder, a 24 x 24-inch surface plate, a Toledo power hack saw, a hand bending brake, a filing machine, an arbor press, and an engraving machine. Precision measuring equipment, such as Johanasson blocks, height gages, Sheffield visual indicator, angle plates, cubes, bench centers, micrometers, etc., complete the tool-room equipment.

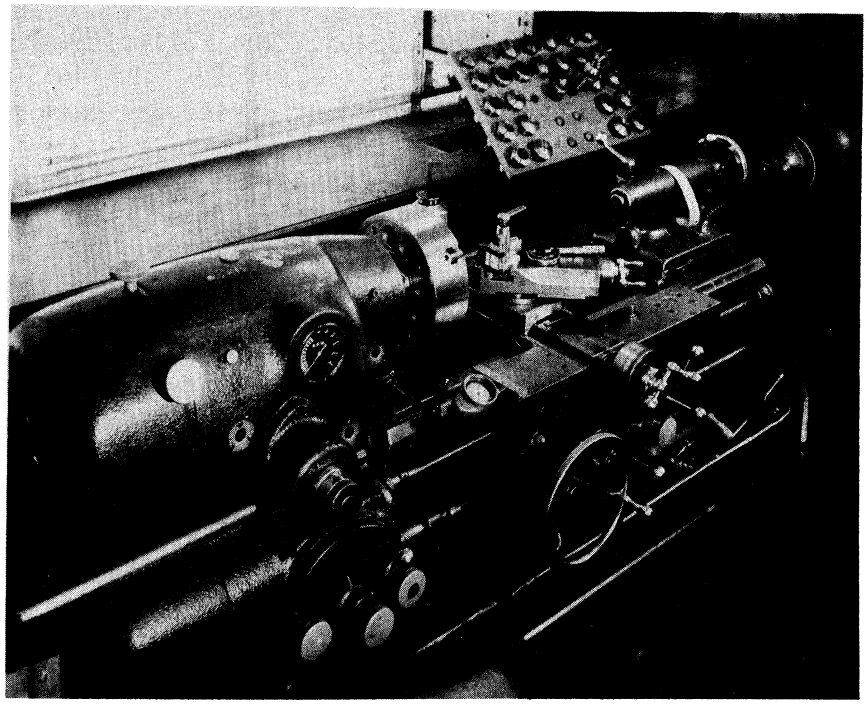

Fig. 20.4 10-inch Monarch Lathe

V. CONCLUSIONS

21. Summary of Results (H. W. Welch, Jr.)

The nature of the research which has been carried on under this contract is such that it is not possible to bring every phase of the work to a satisfactory conclusion by a given date. However, progress is always being made, and one may give evidences of such progress as a summary of the results of working for a specified period. The following are considered the most important results of this project during the past year.

a. Definite progress has been made toward an increased theoretical knowledge of maximum-current boundary, frequency pushing, and voltage tuning under heavily loaded conditions.

b. A new resonator structure for the magnetron has been studied in considerable detail, both experimentally and theoretically. This structure has been incorporated with promising results in a 13-cm f-m magnetron of the reactance-tube type (Model 6), a 14-cm C-W magnetron (Model 7), and an insertion magnetron for use with a tunable external cavity (Model 9). The first two of these have delivered power in the neighborhood of 200 watts at about 50 per cent efficiency. Only two of the last have been built as this report is written. One of them has delivered 900 mw C-W at 15 per cent efficiency.

c. A second new resonator structure has had preliminary tests. This structure is the Model 8, double-anode, rectangular-cavity magnetron. Two interdigital-anode sets have been operated singly or simultaneously in the same cavity. It has been demonstrated that twice the power of a one-anode set is produced by the two-anode sets working together.

d. A new tube for study of the space charge by exploring with a beam sent axially through the interaction space has been designed and constructed. The first model, called the trajectron, will not give the desired results, but enough data have been obtained to indicate the changes which should be made.

e. The study of r-f properties of the magnetron space charge has been extended to include effects not considered in the treatment of Technical Report No. 1 (they were pointed out in Technical Report No. 4). The work is not quite complete as this report is written. A comprehensive report on this phase of the activity will be issued this spring.

f. Laboratory facilities have been improved primarily by equipment acquired with funds supplied by the University. Construction techniques have also improved, primarily due to increased experience, so that time required from conception and design to completed tube has been greatly reduced.

22. Proposed Future Activity (H. W. Welch, Jr.)

The main emphasis in this laboratory in the past has been on obtaining an improved basic understanding of the theory of the magnetron and of magnetron modulation. The assignment made last March by the Signal Corps was in keeping with this emphasis in that an increased understanding of the low-Q type of operation was desired so that it might be possible to achieve such operation at shorter wavelengths, 3000 to 4000 megacycles. As a result of these studies, several tubes have been conceived and started in development. This development has suffered, however, because of the emphasis just mentioned.

In the future this emphasis will be changed in the following way. Three tube geometries which look most promising will be studied carefully in an attempt to produce from them usable designs which can be frequency modulated. Two approaches will be tried in each of the three models. These are voltage tuning and reactance-tube modulation.

Theoretical study will be carried on at a somewhat lower level of activity. This work should not be neglected because the results form the backlog of future activity.

Specifically, the objectives are as follows:

a. The Model 9 insertion magnetron will be developed for operation in the 3000 - 4000-megacycle range with emphasis on voltage tuning. Reactance-tube and mechanical tuning will be studied as a sideline. This work will initially be the immediate problem of Mr. J. S. Needle.

b. The Model 6 coaxial-resonator f-m magnetron will be developed for operation in the 2000 - 2400-megacycle range with emphasis on reactance-tube modulation. As a secondary acitivity, the basic oscillator geometry of this tube (Model 7) may be used in an attempt to obtain high-power low-Q operation (i.e., greater than 100 watts) with voltage tuning. This work will be the problem of Mr. H. W. Welch, Jr.

c. The Model 8 reactangular-cavity magnetron will be developed for operation in the 2000 - 2400-megacycle range. At present this basic geometry has possibilities for reactance-tube tuning, voltage tuning or high-power operation with several anode sets. This work will initially be the responsibility of Mr. J. R. Black.

d. Theoretical and experimental study of voltage tuning and maximum-current boundary will be continued to supplement information given in Technical Report No. 5. This work will be carried on by Mr. H. W. Welch, Jr.

e. Certain fundamental aspects of magnetron space-charge behavior will be studied. Particularly, knowledge of the effect of the cathode on this behavior is desired; it is quite important to the understanding of voltage tuning. This work will involve statistical theories of the space charge and initially will be the direct responsibility of Mr. G. Hok.

f. The study of r-f properties of the space charge will be brought to completion by the latter part of March or early April. During the time between now and then a very small portion of the project budget will be used in this study. The work will be done by Mr. G. R. Brewer.

g. As a long-term project, the study of the space charge with the trajectron will be continued by Mr. W. Peterson.

The persons named in the above program will not be limited to work on the particular activity with which they are associated. The priority of the activity, as it is presently rated, is approximately in the order that they are listed. Every effort will be made to produce a design for a useful tube and prototypes of the Model 9 as soon as possible. (Program described in part a.)

APPENDIX A

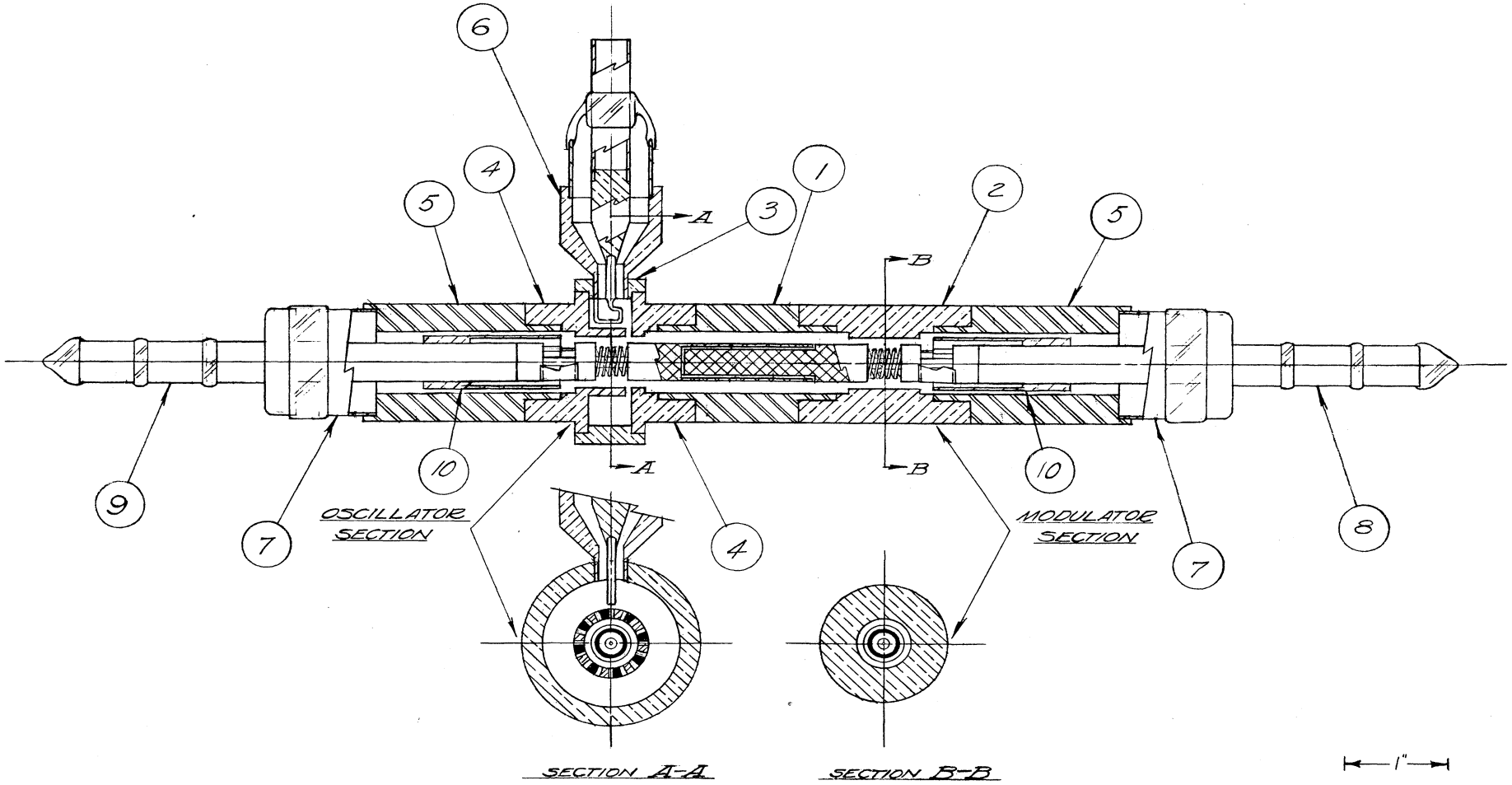

ALL DIMENSIONS UNLESS OTHERWISE SPECIFIED MUST BE HELD TO A TOLERANCE - FRACTIONAL ± 1/64," DECIMAL ± .005," ANGULAR ± ½°

ISSUE	DATE	
3	12/20/44	
2	12/8/44	
1	4/14/48	

DEPARTMENT OF ENGINEERING RESEARCH
UNIVERSITY OF MICHIGAN
ANN ARBOR MICHIGAN

PROJECT M-694

CLASSIFICATION

DESIGNED BY [illegible] APPROVED BY [illegible]
DRAWN BY [illegible] SCALE FULL SIZE
CHECKED BY [illegible] DATE 4/14/48

TITLE FM MAGNETRON

DWG. NO. B-10,005

DWG. NO. B-10,005

DWG. NO. B 10,006A

ALL DIMENSIONS UNLESS OTHERWISE SPECIFIED MUST BE HELD TO A TOLERANCE - FRACTIONAL ± 1/64," DECIMAL ± .005," ANGULAR ± 1/2°

ISSUE	DATE
1	2-20-59

ENGINEERING RESEARCH INSTITUTE
UNIVERSITY OF MICHIGAN
ANN ARBOR MICHIGAN

PROJECT M-762

CLASSIFICATION

DESIGNED BY
DRAWN BY CHW
CHECKED BY
APPROVED BY
SCALE FULL SIZE
DATE 2-20-59

TITLE FW MAGNETRON
MODEL #62

DWG. NO. B-10,006A

DWG. NO. B

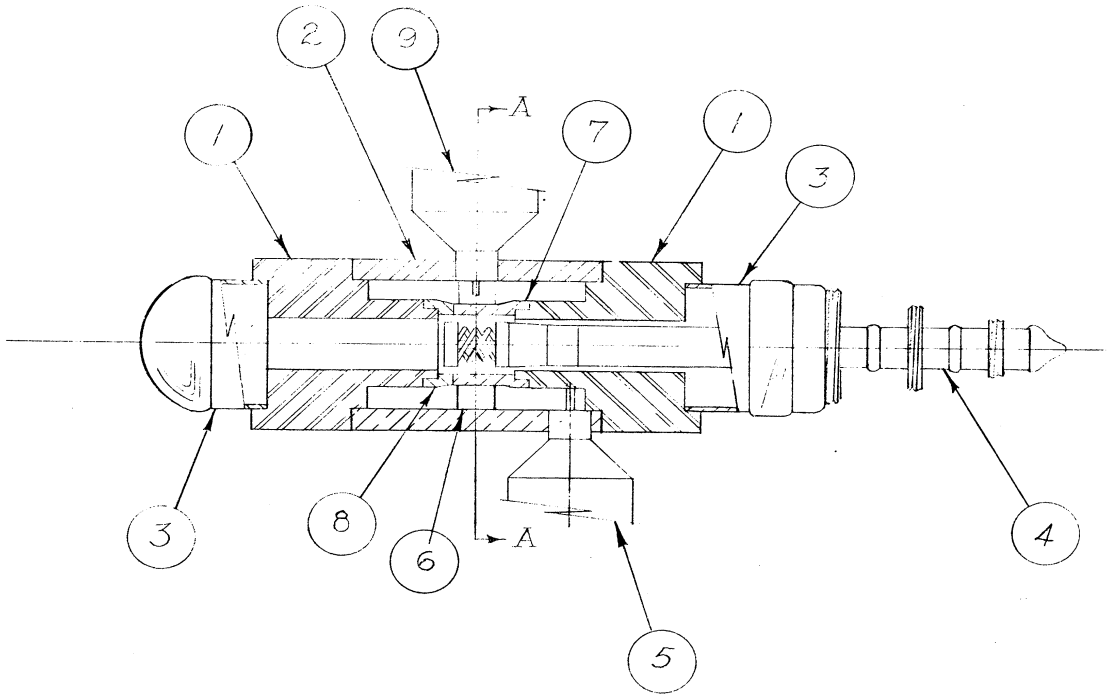

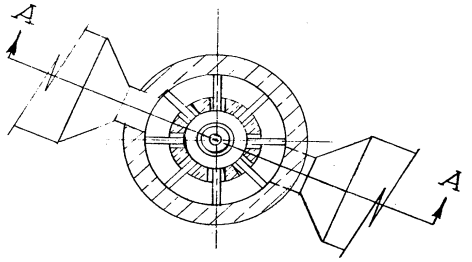

SECTION A-A

1"

ALL DIMENSIONS UNLESS OTHERWISE SPECIFIED MUST BE HELD TO A TOLERANCE - FRACTIONAL ± 1/64" DECIMAL ± .005" ANGULAR ± ½°

		ENGINEERING RESEARCH INSTITUTE UNIVERSITY OF MICHIGAN ANN ARBOR MICHIGAN	DESIGNED BY H.W.W.	APPROVED BY
			DRAWN BY M.M.	SCALE FULL
			CHECKED BY R.E.S.	DATE
		PROJECT M-762	TITLE CO-AXIAL MAGNETRON MODEL 7A	
1	7-[illegible]5	CLASSIFICATION	DWG. NO. B- 10,007A	
ISSUE	DATE			

DWG. NO. B

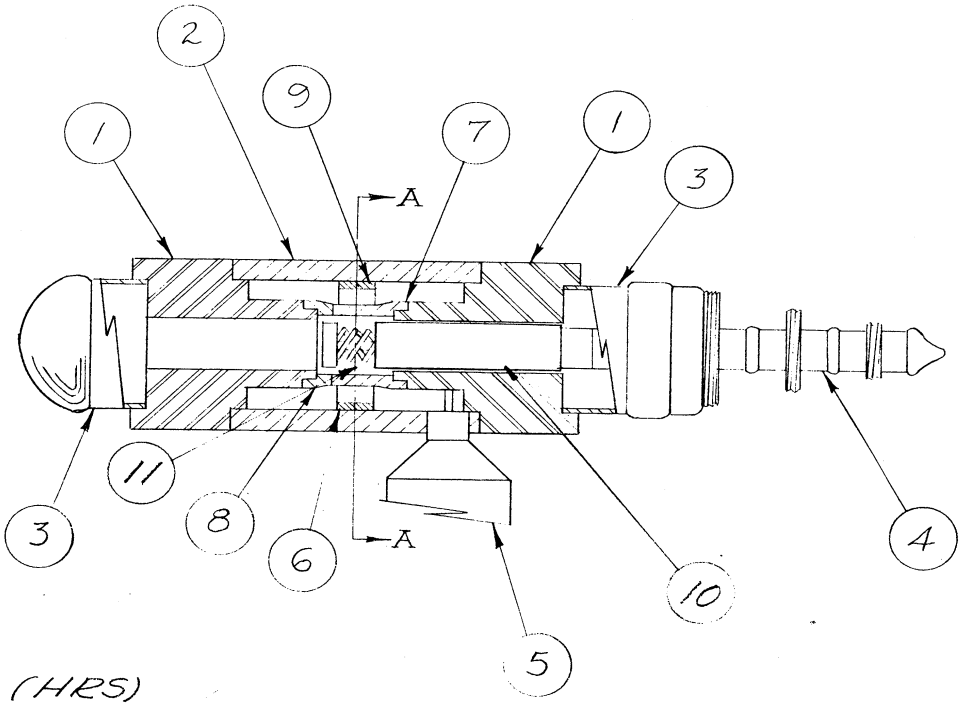

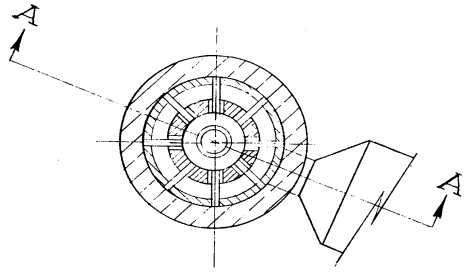

SECTION A-A

1- POLE PIECE (HRS)
2- CAVITY SHELL (Cu)
4- CATHODE CONNECTIONS
5- OUTPUT PIPE
6- FILLER RING (FOR MODE SEPARATION)
7- CAVITY CENTER CONDUCTOR
10- CATHODE LINE BY-PASS
11- INTERACTION SPACE

1"

ALL DIMENSIONS UNLESS OTHERWISE SPECIFIED MUST BE HELD TO A TOLERANCE - FRACTIONAL ± 1/64." DECIMAL ± .005." ANGULAR ± 1/2°

ISSUE	DATE			
		ENGINEERING RESEARCH INSTITUTE UNIVERSITY OF MICHIGAN ANN ARBOR MICHIGAN	DESIGNED BY H.W.W.	APPROVED BY
			DRAWN BY [illegible]	SCALE FULL
			CHECKED BY [illegible]	DATE 10-24-50
		PROJECT M-762	TITLE CO-AXIAL MAGNETRON MODEL 7B	
		CLASSIFICATION	DWG. NO. B- 10,007B	

DWG. NO. B

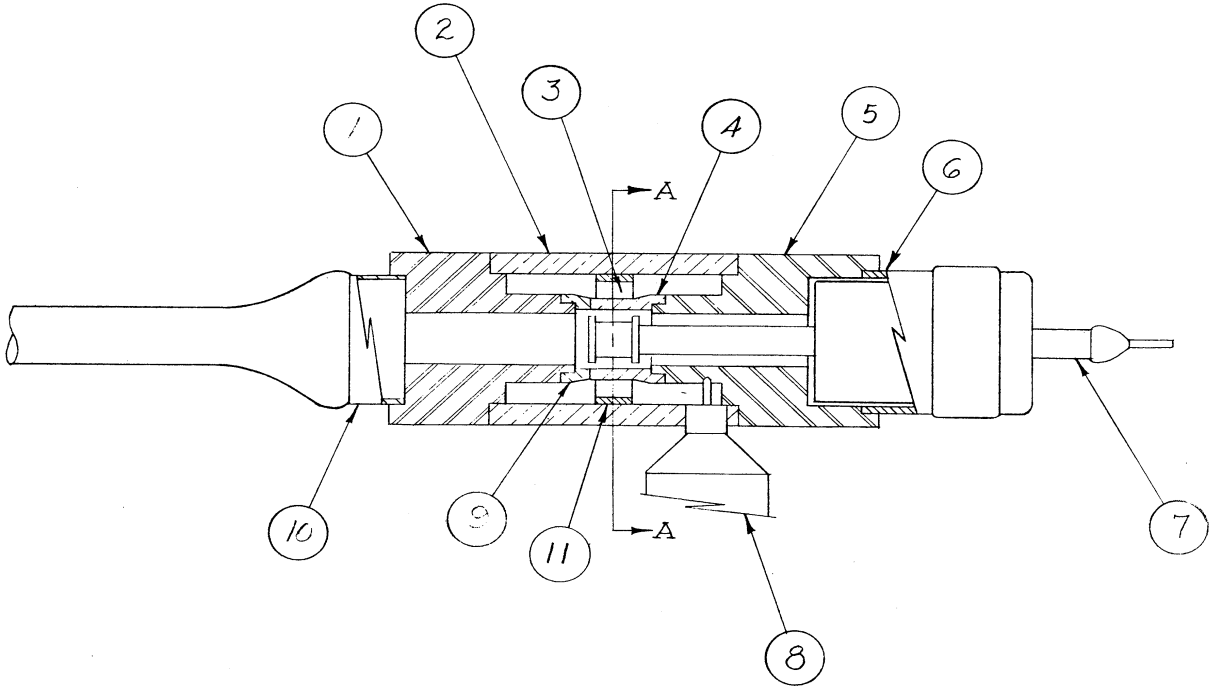

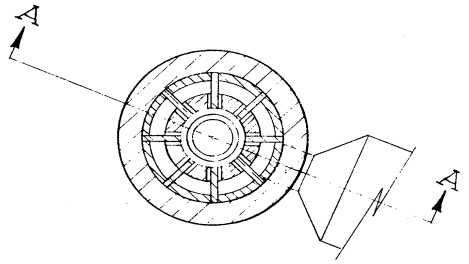

SECTION A-A

1"

ALL DIMENSIONS UNLESS OTHERWISE SPECIFIED MUST BE HELD TO A TOLERANCE - FRACTIONAL ± 1/64" DECIMAL ± .005" ANGULAR ± 1/2°

		ENGINEERING RESEARCH INSTITUTE UNIVERSITY OF MICHIGAN ANN ARBOR MICHIGAN	DESIGNED BY	APPROVED BY
			DRAWN BY JJ PJ	SCALE FULL
			CHECKED BY	DATE 11-13-50
		PROJECT M-762	TITLE CO-AXIAL MAGNETRON MODEL 7C	
ISSUE	DATE	CLASSIFICATION	DWG. NO. B-10,007C	

DWG. NO. B

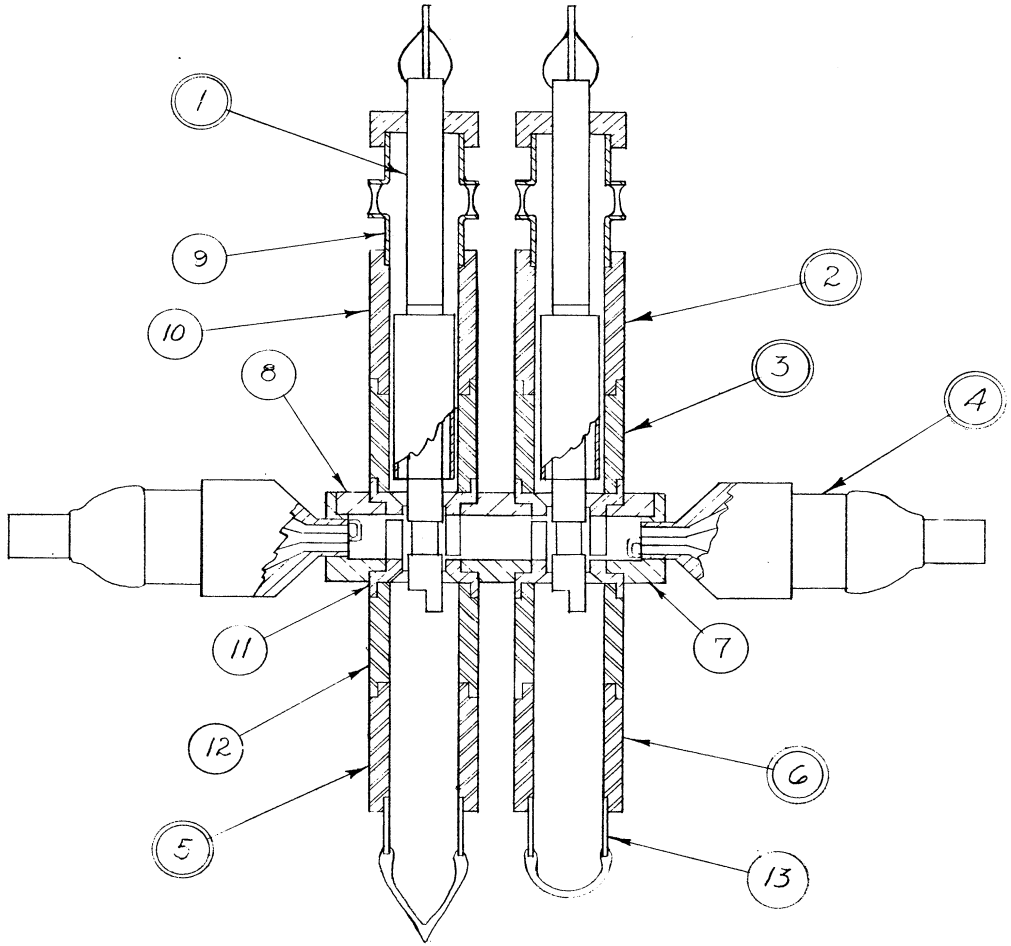

1"

ALL DIMENSIONS UNLESS OTHERWISE SPECIFIED MUST BE HELD TO A TOLERANCE - FRACTIONAL ± 1/64," DECIMAL ± .005," ANGULAR ± 1/2°

		ENGINEERING RESEARCH INSTITUTE UNIVERSITY OF MICHIGAN ANN ARBOR MICHIGAN	DESIGNED BY J.K.E., H.W.(W) / APPROVED BY
			DRAWN BY M.M. / SCALE FULL
			CHECKED BY H.W.W. / DATE 9-15-50
		PROJECT M-762	TITLE DOUBLE ANODE MAGNETRON
ISSUE	DATE	CLASSIFICATION	DWG. NO. B- 10.008

DWG. NO. B

SYM	CHANGES

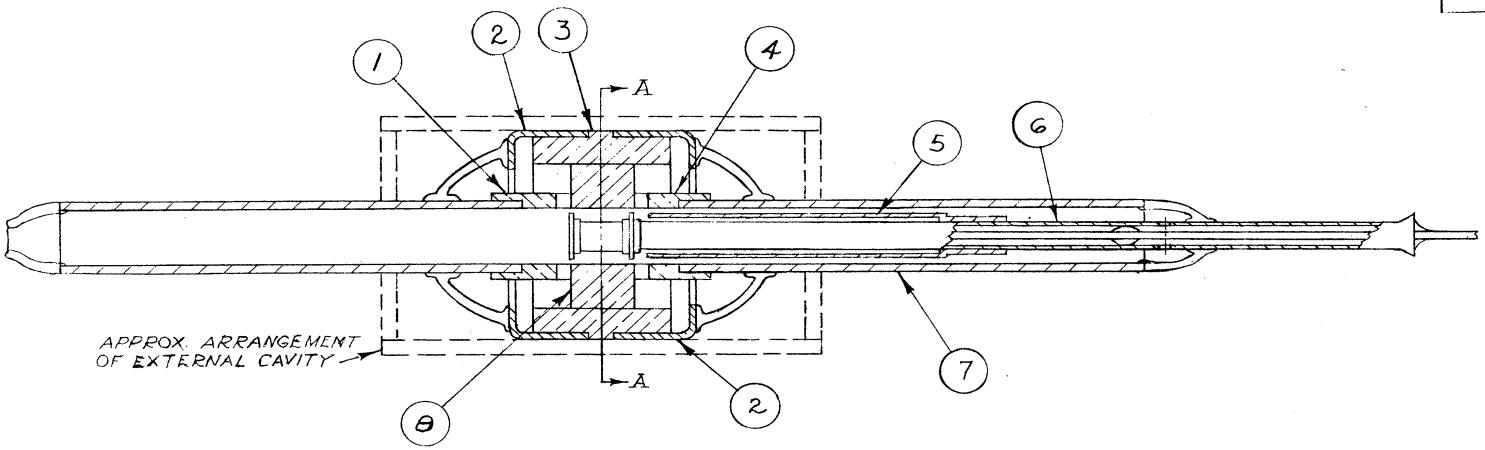

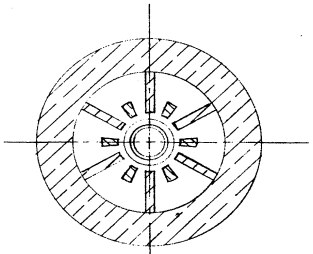

SECTION AA

2"

ALL DIMENSIONS UNLESS OTHERWISE SPECIFIED MUST BE HELD TO A TOLERANCE - FRACTIONAL ± 1/64." DECIMAL ± .005," ANGULAR ± ½°

ISSUE	DATE

ENGINEERING RESEARCH INSTITUTE
UNIVERSITY OF MICHIGAN
ANN ARBOR MICHIGAN

PROJECT
M-762

CLASSIFICATION

DESIGNED BY	APPROVED BY
DRAWN BY NN	SCALE 2X
CHECKED BY	DATE 7-27-50

TITLE
MODEL #9 MAGNETRON

DWG. NO. B- 10,009

DWG. NO. B

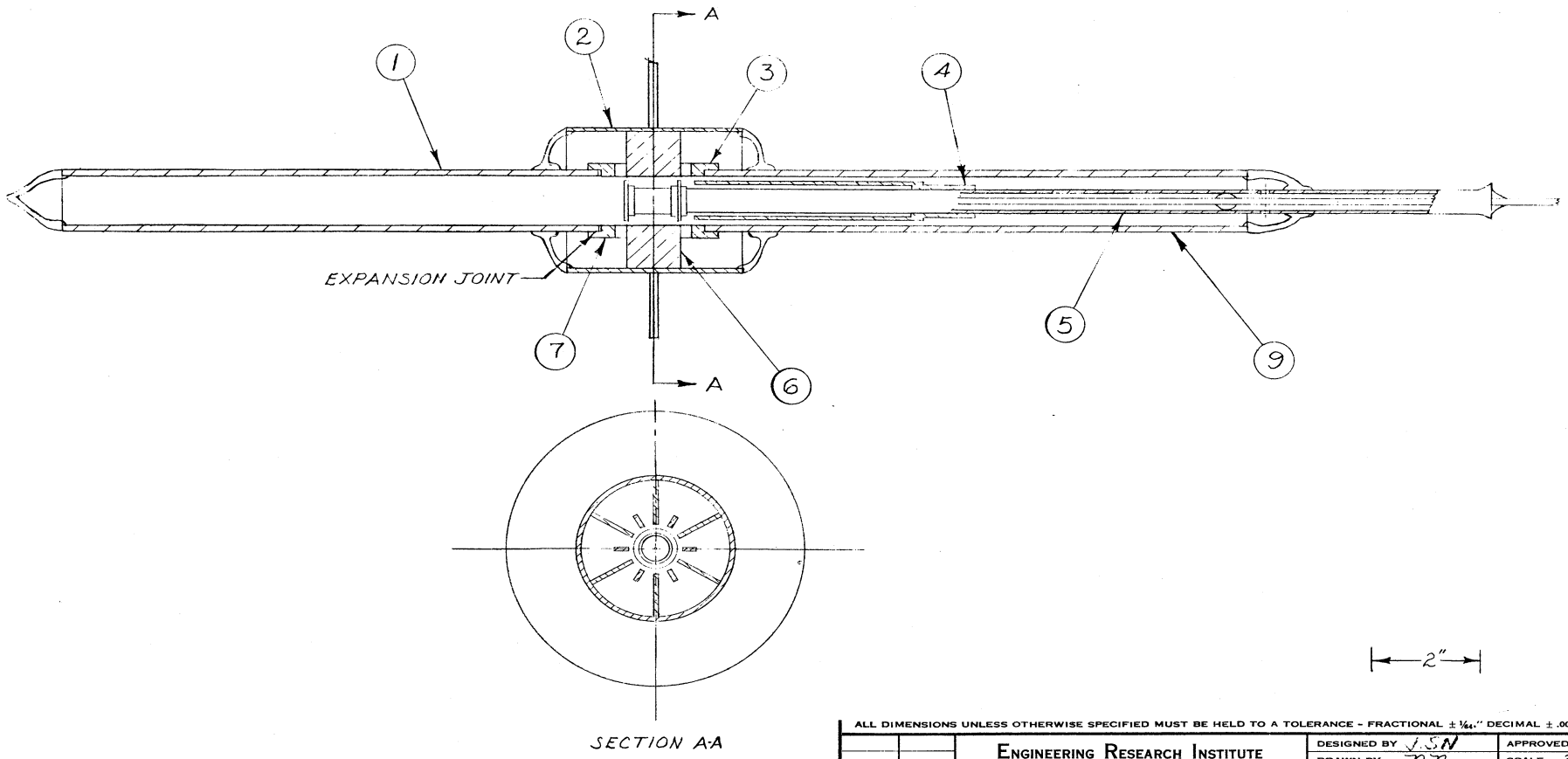

ALL DIMENSIONS UNLESS OTHERWISE SPECIFIED MUST BE HELD TO A TOLERANCE - FRACTIONAL ± 1/64" DECIMAL ± .005" ANGULAR ± ½°

ISSUE	DATE	ENGINEERING RESEARCH INSTITUTE UNIVERSITY OF MICHIGAN ANN ARBOR MICHIGAN	DESIGNED BY J.S.N	APPROVED BY
			DRAWN BY M.M.	SCALE 2X
			CHECKED BY R.L.O.H.	DATE 9-18-50
		PROJECT M-762	TITLE LOW POWER MAGNETRON MODEL 9A	
		CLASSIFICATION	DWG. NO. B-10,009A	

DWG. NO. B

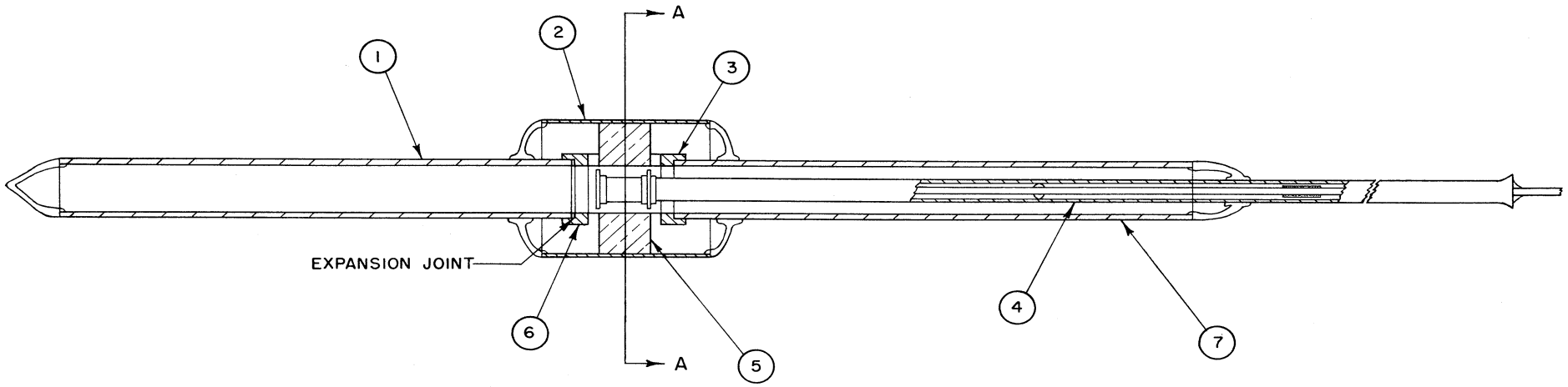

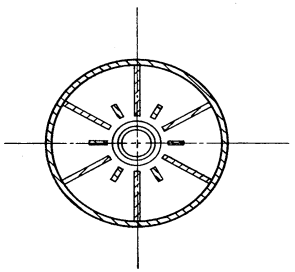

SECTION AA

2"

ALL DIMENSIONS UNLESS OTHERWISE SPECIFIED MUST BE HELD TO A TOLERANCE - FRACTIONAL ± 1/64." DECIMAL ± .005." ANGULAR ± ½°

ISSUE / DATE	ENGINEERING RESEARCH INSTITUTE UNIVERSITY OF MICHIGAN ANN ARBOR MICHIGAN	DESIGNED BY	APPROVED BY
		DRAWN BY NN	SCALE 2X
		CHECKED BY	DATE 1-22-51
	PROJECT M-921	TITLE LOW POWER MAGNETRON MODEL 9B	
	CLASSIFICATION	DWG. NO. B-10,009 B	

DWG. NO. B 11001

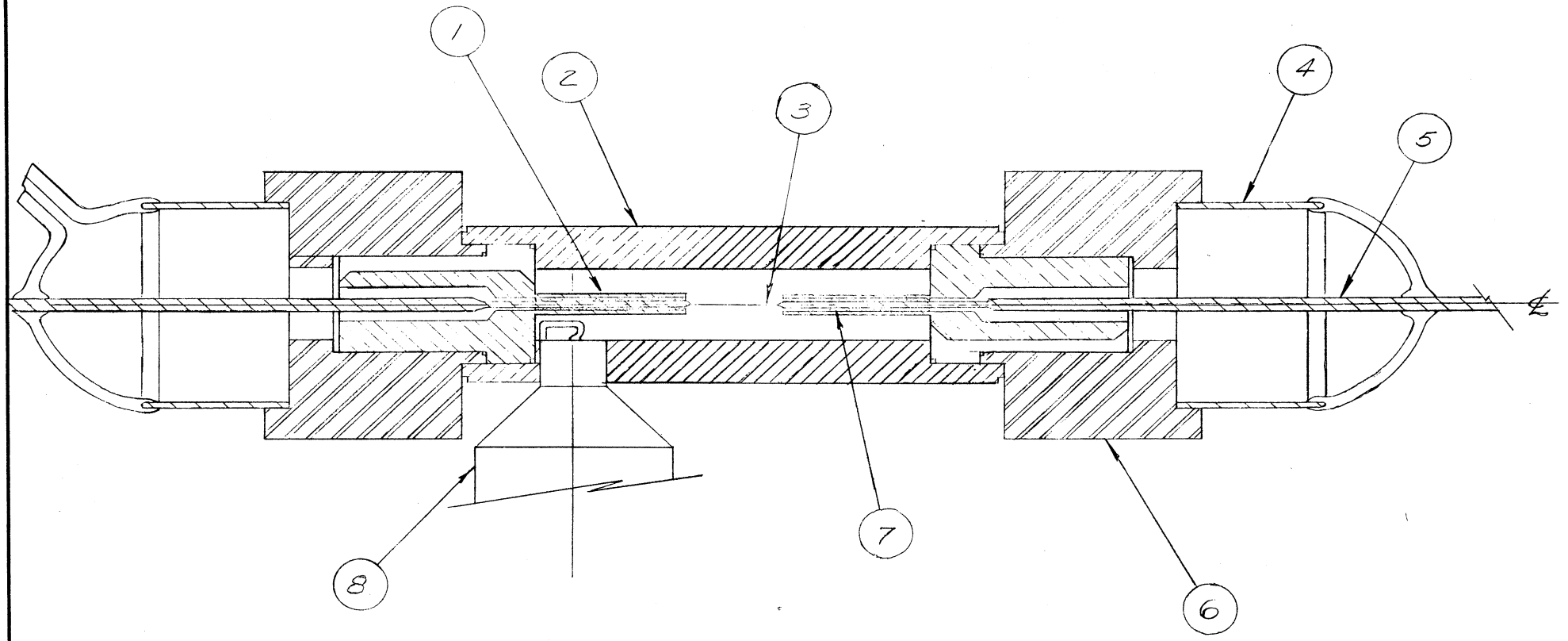

ALL DIMENSIONS UNLESS OTHERWISE SPECIFIED MUST BE HELD TO A TOLERANCE - FRACTIONAL ± 1/64." DECIMAL ± .005," ANGULAR ± ½°

ISSUE	DATE			
		ENGINEERING RESEARCH INSTITUTE UNIVERSITY OF MICHIGAN ANN ARBOR MICHIGAN	DESIGNED BY	APPROVED BY
			DRAWN BY H.	SCALE X 2
			CHECKED BY	DATE 11/11/49
		PROJECT M-762	TITLE 10 CM MAGNETRON DIODE (EXPERIMENTAL)	
1	4/15/53	CLASSIFICATION	DWG. NO. B-11001	

DWG. NO. B

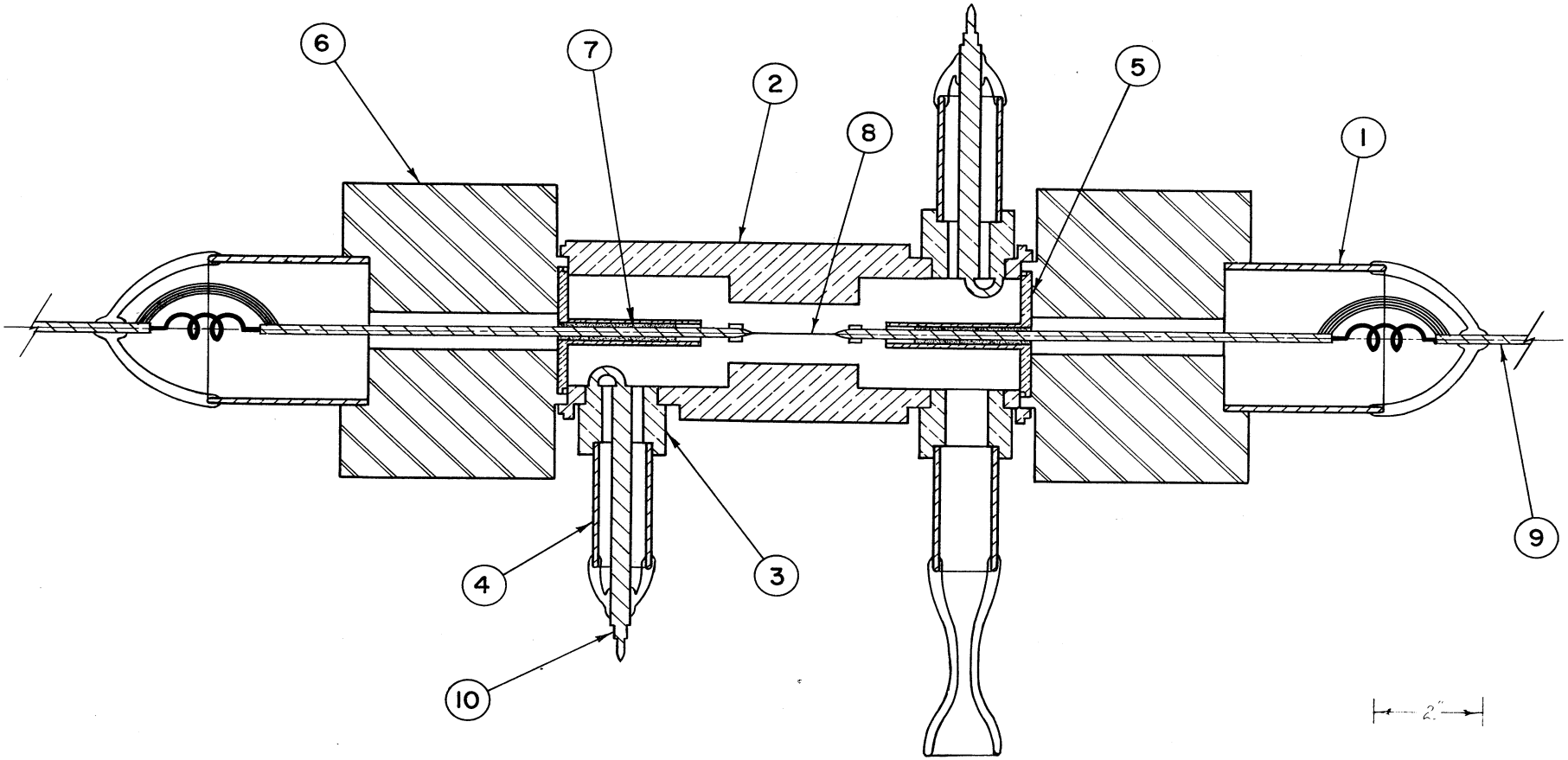

ALL DIMENSIONS UNLESS OTHERWISE SPECIFIED MUST BE HELD TO A TOLERANCE - FRACTIONAL ± 1/64," DECIMAL ± .005," ANGULAR ± 1/2°

ISSUE	DATE	ENGINEERING RESEARCH INSTITUTE UNIVERSITY OF MICHIGAN ANN ARBOR MICHIGAN	DESIGNED BY GRB DRAWN BY NN CHECKED BY VEB APPROVED BY SCALE DATE 4-21-50
		PROJECT M-762	TITLE 10 CM MAGNETRON DIODE (EXPERIMENTAL) MODEL 3
		CLASSIFICATION	DWG. NO. B-11,003

DWG. NO. B

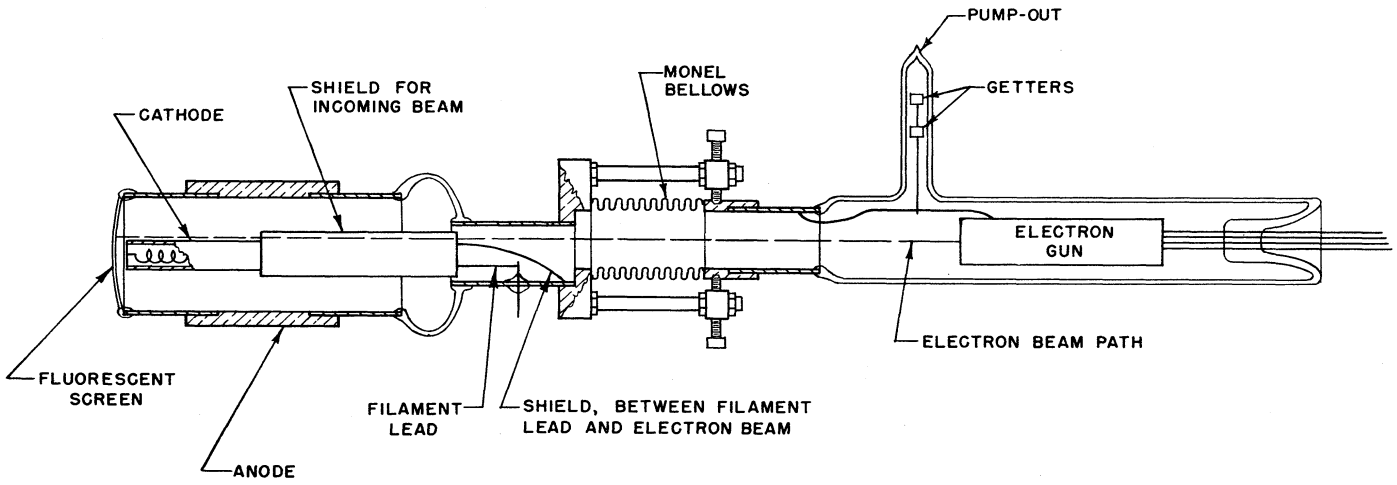

ALL DIMENSIONS UNLESS OTHERWISE SPECIFIED MUST BE HELD TO A TOLERANCE - FRACTIONAL ± 1/64." DECIMAL ± .005." ANGULAR ± 1/2°

		ENGINEERING RESEARCH INSTITUTE UNIVERSITY OF MICHIGAN ANN ARBOR MICHIGAN	DESIGNED BY N.P., H.A.J. / APPROVED BY
			DRAWN BY T.T.T. / SCALE 1/2
			CHECKED BY H.W.W. / DATE 9-20-50
		PROJECT M-762	TITLE TRAJECTRON
ISSUE	DATE	CLASSIFICATION	DWG. NO. B-11,004

DISTRIBUTION LIST

22 copies - Director, Evans Signal Laboratory
Belmar, New Jersey
FOR - Chief, Thermionics Branch

12 copies - Chief, Bureau of Ships
Navy Department
Washington 25, D. C.
ATTENTION: Code 930A

12 copies - Director, Air Materiel Command
Wright Field
Dayton, Ohio
ATTENTION: Electron Tube Section

4 copies - Chief, Engineering and Technical Service
Office of the Chief Signal Officer
Washington 25, D. C.

2 copies - H. W. Welch, Jr., Research Physicist
Electron Tube Laboratory
Engineering Research Institute
University of Michigan
Ann Arbor, Michigan

1 copy - Engineering Research Institute File
University of Michigan
Ann Arbor, Michigan

W. E. Quinsey, Assistant to the Director
Engineering Research Institute
University of Michigan
Ann Arbor, Michigan

W. G. Dow, Professor
Department of Electrical Engineering
University of Michigan
Ann Arbor, Michigan

Gunnar Hok, Research Engineer
Engineering Research Institute
University of Michigan
Ann Arbor, Michigan

J. R. Black, Research Engineer
Engineering Research Institute
University of Michigan
Ann Arbor, Michigan

G. R. Brewer, Research Associate
Engineering Research Institute
University of Michigan
Ann Arbor, Michigan

J. S. Needle, Instructor
Department of Electrical Engineering
University of Michigan
Ann Arbor, Michigan

Department of Electrical Engineering
University of Minnesota
Minneapolis, Minnesota
ATTENTION: Professor W. G. Shepherd

Westinghouse Engineering Laboratories
Bloomfield, New Jersey
ATTENTION: Dr. J. H. Findlay

Columbia Radiation Laboratory
Columbia University
Department of Physics
New York 27, New York

Electron Tube Laboratory
Department of Electrical Engineering
University of Illinois
Urbana, Illinois

Department of Electrical Engineering
Stanford University
Stanford, California
ATTENTION: Dr. Karl Spangenberg

National Bureau of Standards Library
Room 203, Northwest Building
Washington 25, D. C.

Radio Corporation of America
RCA Laboratories Division
Princeton, New Jersey
ATTENTION: Mr. J. S. Donal, Jr.

Department of Electrical Engineering
The Pennsylvania State College
State College, Pennsylvania
ATTENTION: Professor A. H. Waynick

Document Office - Room 20B-221
Research Laboratory of Electronics
Massachusetts Institute of Technology
Cambridge 39, Massachusetts
ATTENTION: John H. Hewitt

Bell Telephone Laboratories
Murray Hill, New Jersey
ATTENTION: S. Millman

Special Development Group
Lancaster Engineering Section
Radio Corporation of America
RCA Victor Division
Lancaster, Pennsylvania
ATTENTION: Hans K. Jenny

Magnetron Development Laboratory
Power Tube Division
Raytheon Manufacturing Company
Waltham 54, Massachusetts
ATTENTION: Edward C. Dench

Vacuum Tube Department
Federal Telecommunication Laboratories, Inc.
500 Washington Avenue
Nutley 10, New Jersey
ATTENTION: A. K. Wing, Jr.

Microwave Research Laboratory
University of California
Berkeley, California
ATTENTION: Professor L. C. Marshall

General Electric Research Laboratory
Schenectady, New York
ATTENTION: P. H. Peters

Cruft Laboratory
Harvard University
Cambridge, Massachusetts
ATTENTION: Professor E. L. Chaffee

Research Laboratory of Electronics
Massachusetts Institute of Technology
Cambridge, Massachusetts
ATTENTION: Professor S. T. Martin

Collins Radio Company
Cedar Rapids, Iowa
ATTENTION: Robert M. Mitchell

Department of Electrical Engineering
University of Kentucky
Lexington, Kentucky
ATTENTION: Professor H. Alexander Romanowitz

Department of Electrical Engineering
Yale University
New Haven, Connecticut
ATTENTION: Dr. H. J. Reich

Department of Physics
Cornell University
Ithaca, New York
ATTENTION: Dr. L. P. Smith

Document Office for Government Research Contracts
Harvard University
Cambridge, Massachusetts
ATTENTION: Mrs. Marjorie L. Cox

Mr. R. E. Harrell
West Engineering Library
University of Michigan
Ann Arbor, Michigan

Mr. C. L. Cuccia
RCA Laboratories Division
Radio Corporation of America
Princeton, New Jersey

Dr. O. S. Duffendack, Director
Phillips Laboratories, Inc.
Irvington-on-Hudson, New York

Air Force Cambridge Research Laboratories
Library of Radiophysics Directorate
230 Albany Street
Cambridge, Massachusetts

Air Force Cambridge Research Laboratories
Library of Geophysics Directorate
230 Albany Street
Cambridge, Massachusetts
ATTENTION: Dr. E. W. Beth

Raytheon Manufacturing Company
Research Division
Waltham 54, Massachusetts
ATTENTION: W. M. Gottschalk

General Electric Research Laboratory
Schenectady, New York
ATTENTION: Dr. A. W. Hull